IMPROVING THE POWER BUS TECHNOLOGY OF A NANOSATELLITE

Bernard Adjei Frimpong

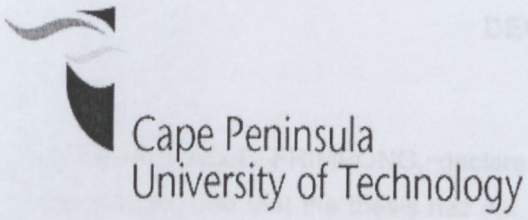

IMPROVING THE POWER BUS TECHNOLOGY OF A NANOSATELLITE

By

BERNARD ADJEI-FRIMPONG

Thesis Submitted in Partial Fulfilment of the Requirements for the degree of

Master Of Technology In Electrical Engineering

In Faculty Of Engineering

AT THE CAPE PENINSULA UNIVERSITY OF TECHNOLOGY

Supervisor: PROF. M.T.E KAHN

Bellville Campus

OCTOBER 2011

DECLARATION

I, BERNARD ADJEI-FRIMPONG, declare that the contents of this thesis represent my own unaided work, and that the thesis has not previously been submitted for academic examination towards any qualification. Furthermore, it represents my own opinions and not necessarily those of the Cape Peninsula University of Technology.

21st November 2011

Signed **Date**

ABSTRACT

The design of nanosatellite power systems plays a major role in micro-sized component development for these spacecrafts. Due to its prospect for future development, industries and universities across the world have accepted them as a teaching tool as well as for conducting space research and development. Since nanosatellite systems have become increasingly popular to commercial companies and research institutions, the need to improve on the power systems has now become a major issue for power system engineers. The power system of a nanosatellite is responsible for the generation and supply of power to the subsystem, as required for a specific mission.

The purpose of this thesis is to highlight on the design and development of a stable and efficient power system to withstand the harsh environmental conditions in order to make satellite missions successful. In working towards achieving this goal, an improved design has been proposed by using a number of current technologies, while literature on a similar subject was reviewed. Current solar cells and battery technologies were extensively discussed and the most efficient method was selected for implementation. Efficient power management architectures to regulate and control power for distribution to the subsystems were also revised. Power subsystem blocks were also reviewed to determine ways of maximizing their performance to enhance effective power supply characteristics for mission operations.

The stability of the system depends on the power distribution bus, which has been developed with efficient mechanisms to eliminate disturbances or unwanted current and voltages to enhance its performance. The stability includes the efficient functioning of power supply units, which involves primary power from solar cells and power storage made up of the batteries and the switching devices, providing a constant supply of power when expose sunlight and eclipse. A maximum power point tracker with a battery bus architecture was used to extract and maximize efficient power for the bus, thus using solid state power controllers to protect the bus system and eliminate faults.

Matlab/Simmulink plots were used to analyse the stable characteristics of the power supply on to the power bus, and a real time simulation was used to demonstrate power system stability implementation in real time operation on a nanosatellite in orbit.

ACKNWOLDGEMENTS

First and foremost, I would like to thank my parents, sisters and brother for providing continuous support and encouragement during difficult times of my study.

I would also like to extend my profound gratitude and appreciation to Prof. M.T.E Kahn for his devotion, consistent and willing desire to direct and instruct me through my research work. Without his frequent encouragement and feedback, this work would not have been completed.

My warmest appreciation goes to the French South African Institute of Technology (FSATI), in collaboration with the National research Foundation (NRF), for granting financial support to aid me through this study. Special thanks go to Prof. Robert Van Zyl and his team at FSATI for their help and support during this course.

My heartfelt thanks also goes to all friends, especially Silas Alfonse Narty, and all my colleagues for their continuous encouragement and support.

DEDICATION

I dedicate this work with humility to Almighty God.

TABLE OF CONTENTS

LIST OF FIGURES

LIST OF TABLES

GLOSSARY

LIST OF ACRONYMS AND ABBREVIATIONS

AC	Alternating current
BCR	Battery charge regulator
BDR	Battery discharge regulator
BOL	Beginning of life
COTS	Commercial off- the- shelf components
DC	Direct current
DET	Direct energy transfer
DOD	Depth of discharge
EOC	End of charge
EOL	End of life
EPS	Electrical power supply
EPU	Electrical power unit
ESA	European Space Agency
ESTEC	European Space Research and Technology Centre
GEO	Geostationary orbit
ISS	International Space Station
LEO	Low earth orbit
MEA	Main Error Amplifier
MEO	Medium earth orbit
MPP	Maximum Power Point

MPPT	Maximum power point Tracker
NASA	National Aeronautics and Space Administration
PBUS	Primary bus
PCM	Power control module
PPT	Peak power tracker
PV	Photo voltaic
SA	Solar arrays
SAB	Solar array bus
SEPIC	Single ended primary inductor converter
SR	Shunt regulator
SSDL	Space System Development Laboratories
SSLT	Surrey Satellite Technology Limited
SSPCs	Solid state power controllers
LU	Latch up

CHAPTER ONE

1 INTRODUCTION

The concept of a nanosatellite was first conceived and developed by Professor Bob Twiggs at Stanford University's space systems development laboratory (SSDL) in 1994 to introduce students to all areas of satellite systems design and operations to enhance their knowledge and practical skills (Obland *et al.*, 2002).

The evolution of nanosatellite systems design currently plays a major role in developing micro-sized components for satellite systems. Due to their prospects for future development, industries and universities across the world have accepted them as a teaching tool, as well as to conduct space research and development.

With nanosatellite systems design becoming increasing popular for commercial companies and research institutions, the need to improve on power systems has become a major issue for power systems engineers because the major causes of failure in mission operations are power systems.

In satellite systems design, the power supply plays a central role to its operation, because it determines how long a mission will last and types of component to use with the kind of payload necessary for the mission. One of the most interesting things about power systems design is how to find the mission geometry.

The power system is basically responsible for power generation, storage, regulation, control and distribution to the subsystems, whose functions are dependent on electrical power consumption (Munteanu, 2009).

The types of orbit of the satellite significantly determine the power requirements of the satellite. For example, the power requirement for a satellite in low earth orbit (LEO) is different from that of medium earth orbit (MEO) or geostationary orbit (GEO) one. These requirements ensure the selection of preferred elements or specific technologies to optimize power sources and the entire distribution system.

The power unit of a nanosatellite is designed to obtain high efficiency and low mass (Tan &Tseng, 2003). It requires choosing a power system topology, which is normally guided by load power requirement, mission length and systems regulation (Moshre, 1999).

However, challenges within the industry have now created conditions on how to develop a cost effective spacecraft. This has shifted power systems design from maximizing performance under technology constraints to minimizing cost under performance constraint (Mosher, 1998).

Due to its distance from the sun, the best method of power generation in nanosatellite systems is by using photovoltaic cells owing to availability, resulting in cost reduction to ensure safety and sustainability. This source of power generated from photovoltaic cells are abundant and uninterruptible within the space environment. Although rechargeable batteries are used for storing energy, they act as backups and a secondary source of power for the satellite during eclipse where there is no sunlight for solar panels to function.

This research focuses on improving the power distribution bus to enable a proper interface between the main components of the power system to ensure an efficient and stable supply of power to the subsystems.

The most difficult part of a satellite power system is the development of a modular power unit, which can be used in all nanosatellite power systems. Most missions a require specific level of power to operate, making the issue of power system development a significant challenge and very difficult to solve (Clark *et al.*, 2010).

1.1 PROBLEM STATEMENT

Nanosatellite communities presently have limitations when it comes to developing and improving power system technologies. The first issue is the selection and implementation of solar cell and battery technologies. Other important parameters to consider in the design include performance and configurations to enhance efficiency.

Secondly, there are limitations imposed on the power systems owing to its size, cost and mass. These limitations are factors that power system engineers consider during their designs and thus form the bases for component selection. These limitations require innovative use of materials which can be miniaturized or yet to be tested on board a mission. It becomes a major cause for consideration when improving the power bus to enhance the systems efficiency. The selection of components to some extent determines the mass and size of the satellite power systems.

The third issue under consideration is the selection of efficient power architecture to manage the power system interfaces. The architecture will integrate specific components and power system topologies flexibly for integration in the power unit. The index performance will take into

consideration the solar cell's efficiency, battery constraints and reliability of the power system technologies.

The final problem which requires critical attention is the distribution bus. The distribution bus allows the power units to communicate with each other. The bus performance is a major concern when stable power is required during distribution to the subsystems or loads onboard a mission.

1.2 OBJECTIVES OF THE PROJECT

This thesis deals with stability of the power system using innovative solutions which are less expensive, in weight and small in size. The main objectives of the thesis are:

- To maximize and improve power efficiency interface between solar cells and the rest of the subsystems to minimize loses.
- To improve upon the power system to protect the satellite from single point failures and also by isolating failure to prevent other systems from failing.
- To operate the system with high efficiency and stability
- The system must be capable of handling the power demand if all electrical subsystems peak simultaneously.
- To integrate sizing and device analysis to enhance the framework for nanosatellite design and optimization.

1.3 STRATEGY TO ACHIEVE OUR AIMS

There are so many objectives when it comes to designing power systems for a nanosatellite. Some of the main objectives are low mass, size, cost and efficiency.

In order to achieve the aims of this project, the entire structure of the power systems will be analyzed to determine the performance analysis of each unit of the subsystem. After the analysis has been performed, the best solution for modelling of the units of the subsystem will be chosen thus considering the importance of developing an efficient bus.

Secondly, a review of various techniques of power management and power optimization methodologies for implementation is discussed, w hich should aid the selection of effective components to reduce mass and size for better performance. The power management system is responsible for allowing the power from the source to be regulated and controlled effectively on the bus.

The third assignment involve the implementation of an efficient protection device and a power conditioning system to aid in bus stability. To achieve this task, a stability circuit is proposed in conjunction with the most efficient protection device to provide a stable power distribution bus. A simulated model of the power distribution bus was developed to evaluate efficiency and performance.

Finally, based on modelling and simulation results, a conclusion for this research was drawn.

1.4 SCOPE OF THE PROJECT

The thesis describes the implementation of a high performance nanosatellite power system. With emphasis on various power components to achieve the required expectations, special attention was p laced on the abilit y to maintain a steady power supply to the subsystems, because the power system is responsible for producing, storing, managing and distributing power to subsystems. Due to major limitations on size, mass and cost, designs were based on commercial off-the-shelf components. To keep the study focused on a particular study area of the power system, the research was narrowed to maintaining stability of power on the bus to enhance survivability and efficiency.

1.5 BACKGROUND OF THE PROJECT

The task of the power system is to supply sufficient power for the spacecraft to accomplish its desired objective during a mission. The power system is responsible for producing continuous regulated and conditioned power, which is distributed to the subsystems. It is also responsible for providing sufficient power to the satellite during peak and average periods of consumption.

However, the backbone of the power system is the power bus, which is responsible for providing a link for all the power components to communicate with each and to supply efficient and stable power.

The basic subunits of the entire power system include the primary power supply made of solar arrays, the power storage made up of batteries, power regulators used for regulation and control and a power distribution system.

The primary source uses photovoltaic (PV) cells to convert solar energy into useful energy by employing traditional silicon array or improved Gallium Arsenide (GaAs) arrays. The power

accumulated produces voltage and current to the entire system. It incorporates a maximum power point tracking system to extract maximum power to the subsystem and loads.

The power storage system is achieved by using batteries, which provide a continuous supply of power to the satellite during eclipse. The batteries used are recharged from the energy which are produced directly from the photovoltaic cells. If the power from the cells are not adequate, the battery bank is automatically switched on to provide power, although it is normally not used when power is produced from the solar cells in the required quantity.

The power regulation and control unit is also responsible for managing power supply from the source to the subsystems.

The distribution system is responsible for shearing power accordingly through the system for subsystems to operate effectively. It includes power converters, protection devices, a cabling harness and the power distribution bus.

The main objective in this research is to improve on the power distribution bus by developing a stable system for a nanosatellite for all conditions during mission operation. This involves proper implementation of innovative commercial off the shelf components into the power system to maintain effective supply and regulation of power for distribution. This will improve the distribution system and the conditions on the bus to enhance system performance.

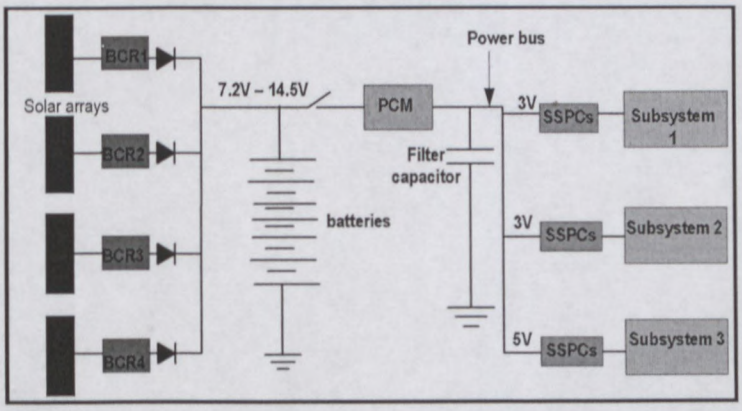

Figure 1.1 Power systems Block with 3V, 5V and the main power bus

1.5.1 DESIGN PARAMETERS

The following parameters are important when considering the design of power systems for all types of spacecraft. Although they are not discussed in detail in this project, they are guiding principles that help power engineers make the right choice when it comes to component selection.

- REQUIREMENTS OF AVERAGE ELECTRICAL POWER
  - Amount of average power EPS must be able to produce;
  - The main effects of power supply and storage capability.
- PEAK POWER REQUIREMENTS
  - The maximum amount of power that should be delivered to the loads; and
  - The effects of the storage system on the distribution.
- MISSION LIFE (End Of Life, EOL)
  - Long mission life requires a redundant design, which includes independent battery charging, larger battery capacity, large power source and an auxiliary bus.
- ORBITAL PARAMETERS
  - This includes the radiation environment, both sunlight and eclipse period and incident solar energy.
- SPACECRAFT CONFIGURATION
  - For a spinning satellite, solar cells must be body mounted; and
  - And for 3-axis stabilized satellite the solar cells are deplorable.

1.6 OUTLINE OF THE REPORT

The chapters in this thesis explain the integrated view behind improving the power bus technology in relation to a nanosatellite. It explains various technologies and the framework for optimal selection of components to enhance the systems configuration.

CHAPTER 1 briefly introduces the area of this research project by listing the objectives. It further gives the background to the study and explains the direction of the project.

Chapter 2 is a general discussion of the related literature on various power technologies in spacecraft power systems.

CHAPTER 3 emphasises implementation of a primary power production system, which conforms to the power requirements of a nanosatellite with focus on solar panels selection, rechargeable battery to store energy, and the efficient interface of the solar panels to the storage device, as well as supplying to load. The means that fault propagation to protect both the solar arrays and the batteries, is also be reviewed.

CHAPTER 4 demonstrates the concept of various power system methodologies, which can be adopted to maximize power from various components of the power systems.

CHAPTER 5 deals with the topologies of the power management architecture, which is necessary for various components of the power system to operate efficiently.

CHAPTER 6 finally deals with the distributions system, focusing on the power distribution bus, where MATLAB/SIMULINK were used as the software for modelling and analyses the bus characteristics, performance or conditions.

CHAPTER 7 formally concludes project and presents recommendations for future work.

CHAPTER 2

2 GENERAL POWER SYSTEMS CONSIDERATIONS

2.1 INTRODUCTION

This chapter provides a general overview of power systems components of a satellite, as is presented in subsequent chapters for a nanosatellite power system. The power system of a satellite is the most critical and important system which is responsible for providing energy to operate all the subsystems. The main duty of the power system is to supply continuous electrical power to the subsystems onboard a satellite. The power system must also be able to related information regarding the health and state of its operations, and offer to protect the loads against faulty conditions that may occur in the system. There are factors, which contribute to the selections of power system components, beginning with the mission and its requirements. Generally, the power system is composed of the primary power source, power storage, power management and distribution. The primary power source produces power generated during active periods of the satellite, while the power storage is made up rechargeable batteries to supply power during eclipse. Regulation and control ensure proper power conditioning, while the distribution system is responsible for transporting power from the sources to the satellites loads. These power components are the support unit that contribute to the power bus technology. With spacecraft now on a nanosatellite scale, the design challenges make the task even more difficult owing to size limitation, which requires an efficient and robust system.

The focus here is on the characteristics of spacecraft power generation and energy storage systems, power management and power distribution units, as described for general spacecraft systems.

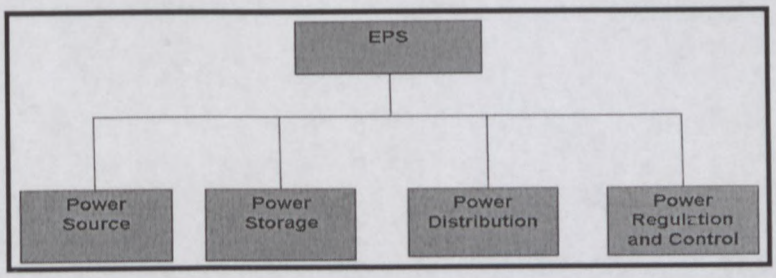

Figure 2.1 Power systems component

2.2 PRIMARY POWER SOURCE

The primary power source of a spacecraft is responsible for converting energy from a given source into an electrical power to maintain the spacecraft and its subsystems. The common sources of primary power generation on board spacecrafts are mainly from nuclear, chemical or solar cell technologies. One of the key factors, which determine selection of a power generation source includes how long the mission will last (Patel, 2005). In LEO where mission period is mostly short, power generation depends on chemical systems such as primary batteries, fuel cells and dynamic chemical conversions. Long missions depend on solar arrays or nuclear systems. Presently spacecraft use solar array to generate its primary power.

The solar arrays are made of photovoltaic cells, which are arranged in series and parallel to obtain the desired voltage and current characteristics. Power is generated by using photovoltaic cells to convert incident solar radiation directly from the sun to electrical energy (Ebale, 2005).

These photovoltaic cells are simply made up of two semiconductor layers, namely the p-type and the n-type. These semiconductors are sandwiched to form a p-n junction. The p-type semiconductor material is silicon (Si) doped with relatively positive impurities such as aluminium boron or gallium. The n-type semiconductor has impurities made of antimony phosphorus or antimony. The p-type conducts positive charges while the n-type conducts negative charges or electrons. In semiconductors the positive charges are called holes, while the negative charges are called electrons.

Electric field in the junction is induced by the p-n junction. The semiconductor then absorbs photons and transfers the resulting energy produced across the material.

The electrons and holes in the cells close to the p-n junction are swept in the opposite direction of the electric field, and it diffuses towards the junction to replace them. The separation charges induce voltage across the device by connecting it to an external circuit where the electrons flow (Caicedo *et al.*, 2008).

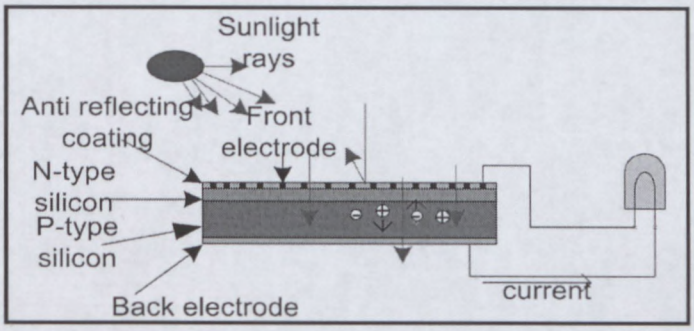

Figure 2.2 Power generation from PV cells (Adapted from *Caicedo et al.*,2003)

Generally, PV cells used in space application are developed from pn-type semiconductors with n-layer placed on top owing to p-layer sensitivity to radiation damage. PV cells have multiple junctions, which can be joined to different bandwidths to increase net efficiency across a broad spectrum (Krishnmurthy, 2008).

These sources are the most common among spacecraft systems today because of the abundance of solar radiation and energy emitted by the sun. Incident photons energy is normally converted to a DC current, which flows through the load connected to it. PV is idealized as a constant current source in parallel with a diode and a shunt resistance, as shown below.

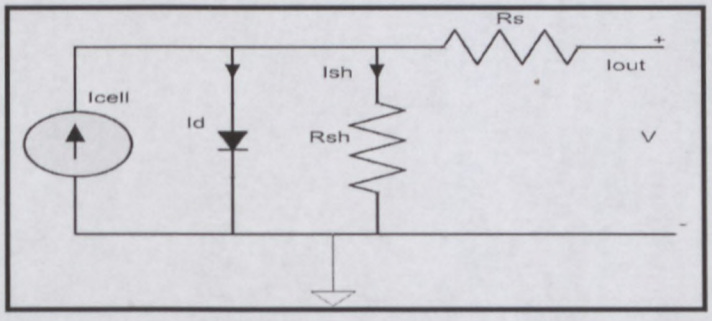

Figure 2.3 Equivalent solar cell circuit (Adapted from Patel, 2005)

Figure 2.3 shows that the current output of the PV cells at the point of load I_{OUT} is the parasitic sums through the diode and shunt. $I_{OUT} = I_{CELL} - (I_d + I_{sh})$. Where I_{CELL} is the photo generated current caused by incident radiation. Cell current may now be driven across by the voltage to the

output voltage and voltage across the developed equivalent series resistance $I_{OUT}R_S$ (Goldsmith *et al.*, 1976). With respect to the diode equation, the current directed through the diode will be given by:

$$I_d = I_{SAT}\left[e^{\frac{q(V+I_{OUT}R_S}{nKT}-1}\right].....1$$

- I_{SAT} is the diode saturation current;
- q is the elementary charge;
- k is the Boltzmann constant;
- n is the diode I deal factor; and
- T is the absolute temperature.

The diode is then calculated from

$$I_{SAT} = qA\left(\frac{D_p p}{L_p} + \frac{D_n n}{L_n}\right) \qquad (1.1)$$

Where A is the total of the diode, D_p is the coefficient of diffusion for hole in n region, D_n is the diffusion coefficient of electrons in p region, p is the equilibrium concentration of holes in the n region, n is the equilibrium of concentration of electrons in the p region and L_p L_n are holes and electron diffusion lengths, respectively (Bonin, 2002).

The shunt current can be written by using ohm's law $I_{sh} = \frac{(V - I_{out}R_S)}{R_{sh}}$ (1.2)

Evaluating from equation 0, $I_{OUT} = I_{CELL} - I_{SAT}\left[e^{\frac{q(V+I_{OUT}R_S)}{nKT}-1}\right] - \frac{(V + I_{OUT}R_S)}{R_{Sh}}$ (1.3)

In order to understand the low- level characteristics of solar cells, a higher model for spacecraft design utility is represented by $I_{OUT} = I = I_{SC} + A(1 - e^{BV})$ (1.4)

where A and B in the equation are constants and are measured to account for inherent degradation during manufacture and assembly. From equation (1.4) it can be deduced that the output current of the solar cells will vary with regard to applied voltage from short circuit current I_{SC} at zero voltage to zero current at the open circuit voltage V_{OC}.

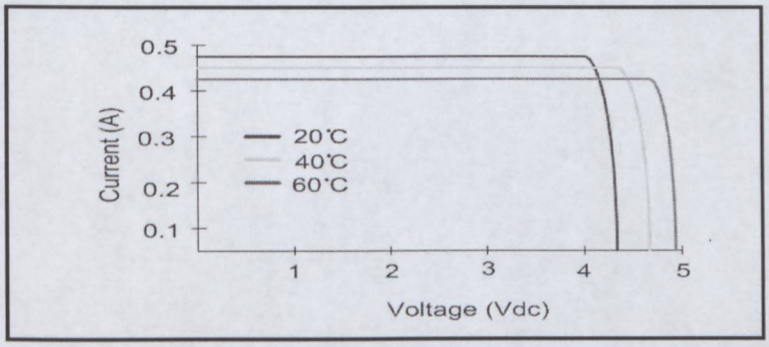

Figure 2.4 Typical solar cells I/V characteristics of constant temperature

(Adapted from Tan &Tseng, 2003)

2.3 POWER STORAGE

Power storage is an important integral part of the power system for storing energy, which is generated from photovoltaic or solar thermal dynamics. Energy storage typically occurs in batteries although flywheels and fuel cells have been considered for various spacecraft.

A battery is normally made of individual cells that are connected in series. The number of cells determines the bus voltage. The energy stored in the battery is recorded in ampere-hour capacity or watt- hour capacity. These batteries can be connected in series or parallel to increase voltage or current output by watt-hour capacity (Fortescue *et al.*, 2003).

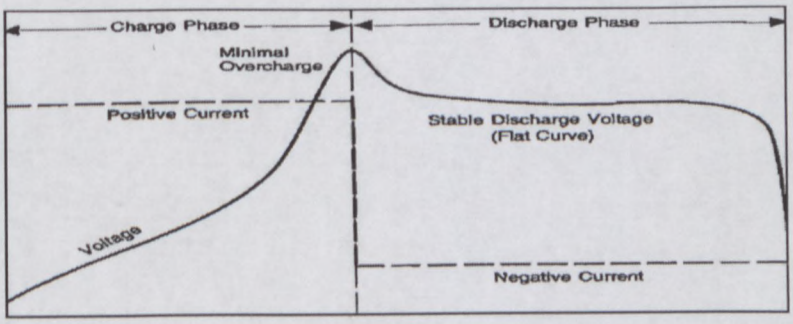

Figure 2.5 Charge –discharge characteristics of the storage system

(Adapted from Larson and Wertz, 2003)

An overcharge and a flat discharge curve, which extends through most of the capacity are needed. Most batteries easily become degraded by overcharging; therefore, it is good to match the characteristic of the battery cells with charging inconsistencies. When the batteries experience stress and degradation, the life span of the power system reduces. Since the batteries are rechargeable, it can be used for a longer duration, say more than a year.

However, it can be used as primary sources for short durations, which normally last for hours or a day. The rechargeable batteries are used as energy storage by converting chemical energy to electrical during discharge, and electrical into chemical energy during charge. This process is recycled for a number of times. The most common batteries available for energy storage in spacecraft power systems are NiCd, NiH_2 and the lithium ion (Jappesen and Thomsen, 2002).

Energy storage is basically responsible for power supply during eclipse and the primary power from photovoltaic arrays is useful in sunlight to level the loads. Charging and discharging occur during sunlight and eclipse while orbital parameters of the spacecraft determines the charge and discharge cycles which are needed by the battery to maintain the mission.

Geo-stationary satellite stores energy for two 45-day eclipse periods per year. The longest eclipse period is 72 minutes each day. Geostationary orbits require few charge and discharge cycles during eclipse, allowing about 50% Depth of Discharge (DOD). Satellite missions in LEO undergo at least 15 eclipses per day with a maximum shadowing of approximately 36minutes. Hence the batteries are charged and discharged about 5000 times each day. The life cycle of a battery determines how many times it can charge or discharge before the battery permanently loses its ability to store energy. Hence the life cycle is measured by the performing cycles of a complete charge and discharge (Larson and Wertz, 1999).

Table 2.1 battery status and densities

(Adapted from Jeppesen and Thomsen,2002)

Secondary Batteries	Specific Energy Density (W-hr/kg)	Status
Nickel-Cadmium	25-30	Space- qualified, extensive database
Nickel-Hydrogen (Individual pressure vessel design)	35-43	Space-qualified, good data base
Nickel –hydrogen (common pressure vessel design)	40-56	Space-qualified for GEO and planetary
Nickel – Hydrogen (single pressure vessel design)	43-57	Space- qualified
Lithium –ion (family)	70-110	Space-qualified for LEO
Sodium-Sulfur	140-210	underdevelopment

The depth of discharge is a parameter related to the life of the battery. When the battery becomes fully discharged and recharged, the cycle life of DOD goes to 100%.

When the battery is discharged to half of its capacity, that is 50% and is recharged again a number of times, the battery's discharged and charged level rises to more than double. Typical data for a number of cycles verses DOD are available for NiCd Li-ion and NiH_2 as shown below in Figure 2.6

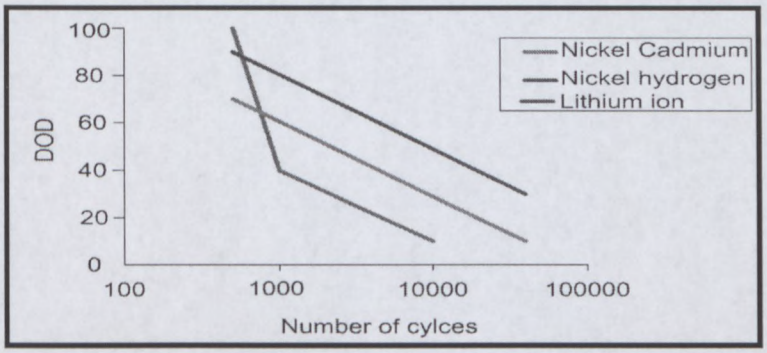

Figure 2.6 DOD characteristics of NiCd, NiH and Lithium ion batteries

(Adapted from Jeppesen and Thomsen, 2002)

NiCd is the most common and widely used energy storage system for many spacecraft applications. It has been qualified and is extensively data based for any type of missions. A 28Vdc aerospace NiCd battery normally consists of 22 - 23 series connected cells. Typical capacity for NiCd battery is around 5-100A/hr.

NH_2 in recent times enjoyed its presence in space application, specifically where higher energies and long life is an important factor. It has three design configurations, namely individual pressure vessel, common pressure vessel and single pressure vessel. The individual pressure vessels were the first NH_2 used in space application. It has only has a single electrochemical cell within the pressure vessel, and normally with a terminal voltage of 1.22V-1.25V dc depending on the discharged loads. Typical individual pressure vessel battery designs include multiple cells connected in series to obtain the correct battery voltage. The cell diameter is between 9-12 cm with a capacity of around 20-300 A/hr.

The common pressure vessel is similar to individual pressure vessels, except that internal wiring of electrode stacks are different. Individual pressure vessels allow electrode stacks to be connected in parallel. The common pressure vessels have two sets of electrode stacks connected series to produce a terminal voltage of 2.44V-2.50V dc. The common pressure vessel has a configuration between 6 - 9cm with a battery capacity of 12 – 20 A/hr. The single pressure vessel is designed with a common hydrogen supply used by three or more series connected cells with a single pressure vessel. Each cells stack here has it own electrolyte supply isolated within individual cell stacks container.

The key operating characteristic of this design is to allow free movement of hydrogen within the cell stacks while maintaining cell stack electrolyte isolation. These batteries are presently available in a 12.5cm or 25cm diameter design (Fortescue *et al.*, 2003:325-367).

Lithium ion battery technologies now offer an improved energy density advantage and a much wider operating temperature range over NiCd and NH_2 batteries. Typical constituents of the lithium ion cell are lithium thionyl chloride, lithium sulphur dioxide, and lithium carbon monofloride. Nominal voltage for lithium ion is around 3.6V - 3.9V dc. These allow for the reduction of cell number to about one- third when compared to NiCd and NH_2 cells. Lithium ion has 65% volume advantage and 50% mass advantage for the fast growing space systems industry. The lithium ion battery technologies have now been qualified for planetary, GEO and mostly LEO applications (Jeppesen and Thomsen, 2002).

2.4 POWER MANAGEMENT

In order to regulate and control power on the spacecraft, various sources of power should be determined. The three modes in which power regulation and control can be achieved is by:

- Solar array control;
- Bus voltage regulation; and
- Battery charging.

In solar array control, peak power tracker (PPT) and direct energy transfer (DET) systems are used to eliminate overcharging and undesirable heating in the power unit. PPT is used to extract power at the array's peak power because it is non dissipative. The DET is dissipative and the dissipation is done on the solar arrays or through external banks of shunt resistors to avoid internal heating. DET uses shunt regulation to maintain bus voltage at a predetermined level. Below are figures which represents the basic types of DET topologies available.

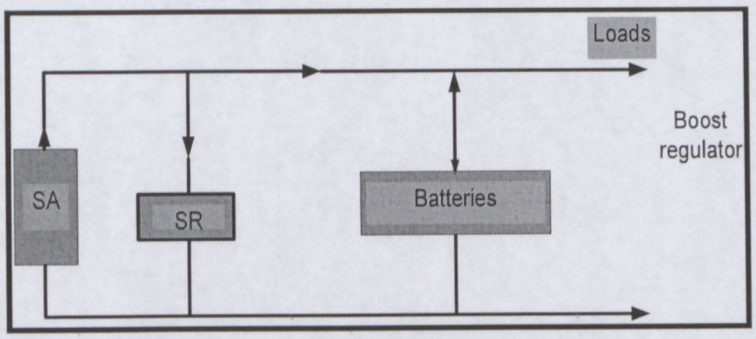

Figure 2.7 DET unregulated bus using parallel batteries

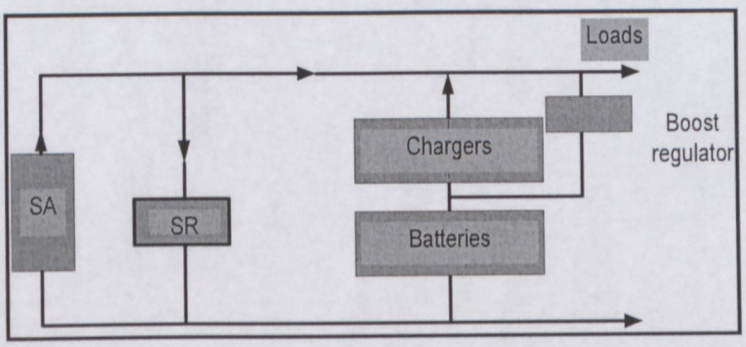

Figure 2.8 DET fully regulated bus system

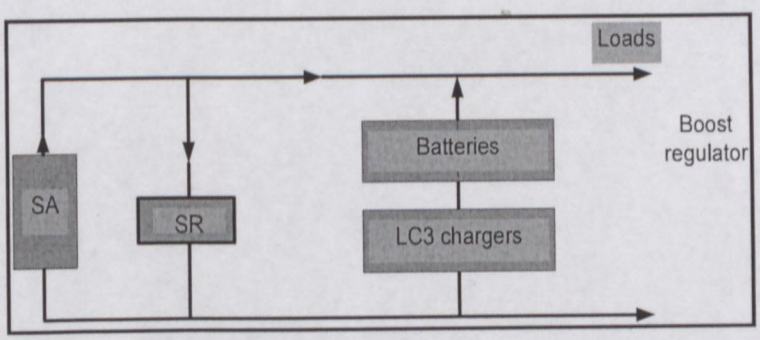

Figure 2.9 DET unregulated bus using linear charge

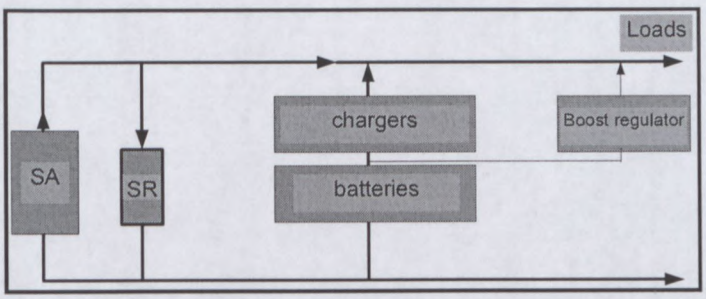

Figure 2.10 DET using fully regulated bus

The PPT is a dc-dc converter place in series with solar arrays to change the source array voltage and to track the peak power when energy demands become higher than the peak power. The array voltage is allowed to rise to its maximum power point by changing the converter input to an equivalent output power at different currents and voltages. Large amounts of power is obtained when solar arrays are cold owing to array-source characteristics at the beginning of life. A peak power tracker replaces the shunt regulation in operation by backing off the peak power point of the arrays towards the end of the battery's charging period. Because the PPT is in series with the array, it uses 4-7% of the total power. Figures 2.11, 2.12, 2.13 and 2.14 represent the basic types of PPT regulators that are available. A PPT has advantages for missions less than 5 years old that require more power at BOL than at EOL.

DET places a shunt regulator in parallel to the array and the shunt array current away from the subsystem when the load or battery that is charging does not need power. Shunt regulation is quite efficient with little dissipation by simply shunting excess power through shunt resistor banks or on the arrays. The shunt regulators have low mass, fewer parts, and a higher efficiency at EOL.

There are also three techniques which are used to control bus voltage, namely unregulated, quasi-regulated and fully regulated bus systems.

Unregulated bus systems have voltages that vary significantly. The bus voltage regulation derives from battery regulation which varies about 20% from charge to discharge. In an unregulated subsystem the load bus voltage is the voltage from the batteries.

In a quasi-regulated bus system, regulations occur during battery charge and it places battery charger in series with each battery or group of parallel batteries. The bus voltage is kept high above the battery voltage during the charge period. The drop across the charger decreases as

the battery nears its full charge with the bus voltage constantly regulated. It switches to unregulated mode when at discharge, while the diode drop lower than the batteries and decreases as the battery discharges.

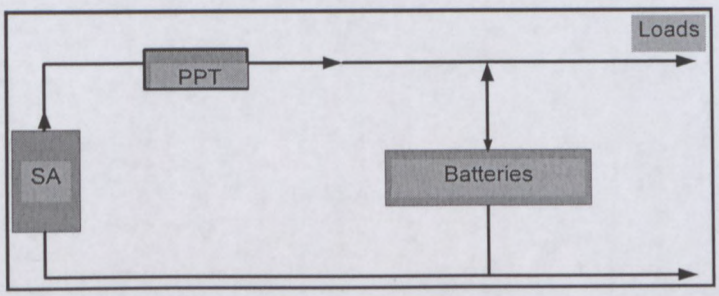

Figure 2.11 PPT unregulated bus using parallel batteries

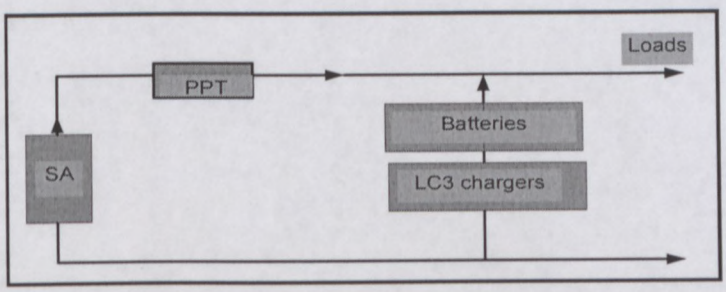

Figure 2.12 PPT unregulated bus series using a bus linear control

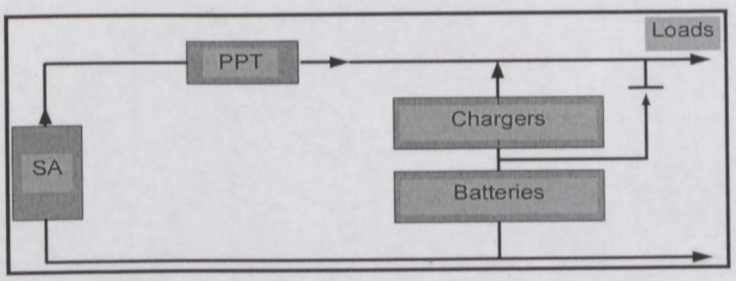

Figure 2.13 PPT quasi regulated bus with constant current charger

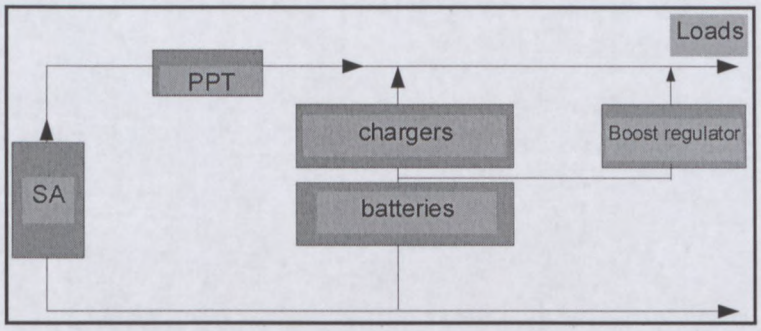

Figure 2.14 PPT system using fully regulated bus

Quasi-regulated bus has low efficiency and a high electromagnetic interference when used with peak power tracker.

The fully regulated bus system is inefficient, but works efficiently on spacecrafts where low power is fully regulated on the bus. It employs charge and discharge regulators. Both linear and switching converter technology can be used for this charge and discharge regulators. But efficient switching converters should be used in both conditions. Design integration is very because it behaves as low impedance power when connected to loads. It is also one of the most complicated systems with extremely low efficiency and high electromagnetic interference when used with PPT or a boost converter (Fortescue *et al.*, 2003:325-367).

2.5 POWER DISTRIBUTION

The distribution systems include the power bus, cabling systems, protection and switching devices. The distribution system is an important feature within the power system as it determines individual loads power switching requirements for the spacecraft. When it comes to developing a distribution system for various power systems, factors to consider are the source characteristics, load requirements and subsystems operations. Choosing a particular type of distribution system requires the following considerations, power losses and mass at minimum whilst paying attention to survivability, cost, reliability and power quality.

The power switching devices used for protection and switching are normally developed from mechanical relays owing to their proven historical record in flight activities, reliability and low power dissipation. Field effect transistors made from metal-oxides semiconductor are based on power technologies, and can be designed from solid state devices (Larson and Wertz, 1999:407-426).

The power bus is a single channel to transport a variety of voltages and currents to meet the needs of the subsystems. The European space agency (ESA) generally uses a regulated bus, typically 28V, 50V. However, the generation of a meteosat system has a bus voltage of $28.2V \pm 1\%$ and artemis has $42.5 \pm 0.5V$ made of a regulated bus in Europe.

However, United States spacecraft systems have adopted the unregulated bus system. Hence NASA standards provide variable voltages between 21V-35V dc. Recent designs have high bus voltages around 100V to 150V dc to reduce resistive losses and to harness mass. In both regulated and unregulated bus topologies, dc-dc converters are applied to convert input to required output voltages. The switching helps the spacecraft to vary its power consumption. Transient conditions that occur generate noise, which can easily be transferred to load through the bus. The converters in the system are used to eliminate the noise from the bus and to regulate the power connected to the load against disturbance from the bus. They also protect the bus from load failure by switching ON and OFF power to the desired load.

Any dc-dc converter connected to the bus must dampen its electromagnetic-interference filter to keep step loads from causing excessive ringing. The demand for low power leads to the 28V bus standardization, since demand for power is increasing; the 28V will result in losses in cabling and mass limitation. The cables, which are used to connect the power systems include a large part of the system's mass. Therefore, the cables must be kept short to avoid voltage drops and to regulate bus voltage. Below is a typical graph plot between cable mass and current.

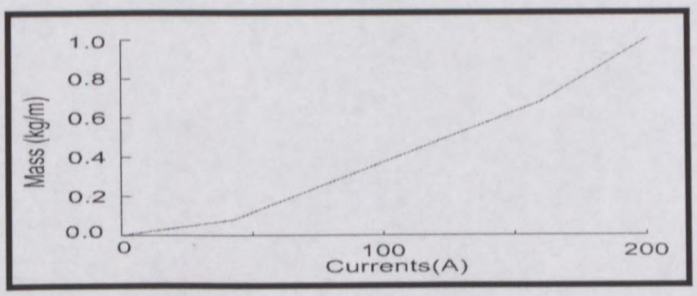

Figure 2.15 Cable vs. mass current

Spacecraft distributing systems have predominantly been dc because of dc power production. Converting dc to ac requires extra electronics and mass, which can impact heavily on the weight of power systems. AC distribution bus is most required in spacecraft where high power is

needed, for example, the international space station (ISS) where there are many electrical loads with different duty cycles (Fortescue *et al.*, 2003:325-367).

The distribution system can also be centralized or decentralized based on where the converter is located. A decentralized system places converters at each load separately. While the centralized system distributes power within the main bus. A decentralized distribution system uses the unregulated bus system, but the regulated bus has power converters at the load interface owing to different voltage requirements ($\pm$ 5V, $\pm$ 12V dc). One advantage of the centralized system is that, there are no redesign for different application. In most cases the decentralized distribution systems are used in large spacecrafts with the unregulated bus (Larson and Wertz, 1999).

2.6 RELATED WORK

Quite a substantial amount of work has been done in power systems by trying to develop an efficient power bus for large and small satellites. Although nanosatellite systems have a young history, there have been many launches over the decade which have over the years brought to the notice of engineers that the main causes of mission failure is the power system. The reseacher reviews some power buses developed in different satellites, although they might not directly or easily be applicable to nanosatellite systems owing to size, mass and cost involved in the design and development. The systems in consideration are "A 100 volts power bus more-than a higher voltage" and "A non-sequential power bus for leo application".

2.6.1 A 100 VOLTS POWER BUS- MORE THAN A HIGHER VOLTAGE

According to Olsson (1998), ESTEC has been responsible in the past 20 years for promoting the development of a high quality power bus. These bus systems have been adopted by commercial communication satellites companies to supply efficient and reliable power to the subsystems.

This satellite uses deplorable solar cells on a three axis stabilization to produce more than 5KW of power. The preferred choice of voltage regulation is based on a fully regulated bus system.

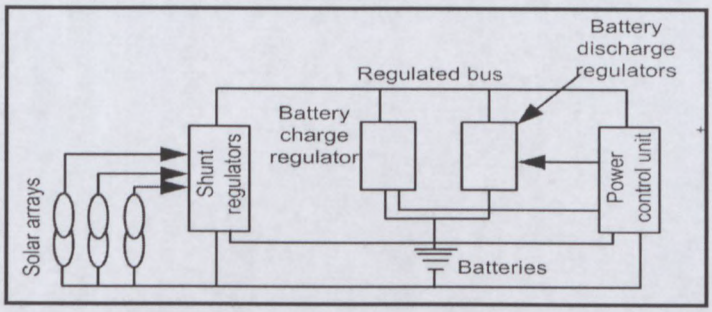

Figure 2.16 Architecture of regulated bus

(Adapted from Olsson, 1998)

The input voltage regulation is based on three core factors, namely the bus voltage reference, bus impedance and distribution impendence.

2.6.1.1 BUS VOLTAGE REFERENCE

A very high precision ICs or zener diodes with a typical long term drift of 15-25 ppm per 1000 hours, correspondingly to 0.3% in long period of years is normally confirmed by a radiation environment.

2.6.1.2 BUS IMPEDANCE

The bus impedance is one of the core factors, which can be manipulated by design to achieve a good result. The significance of producing low bus impedance is to increase the main capacitor bus bank.

2.6.1.3 DISTRIBUTION IMPEDANCE

The graph below displays a typical characteristic of bus impedances. The impedance comes from the wiring inductance seen by users for frequencies above few KHz.

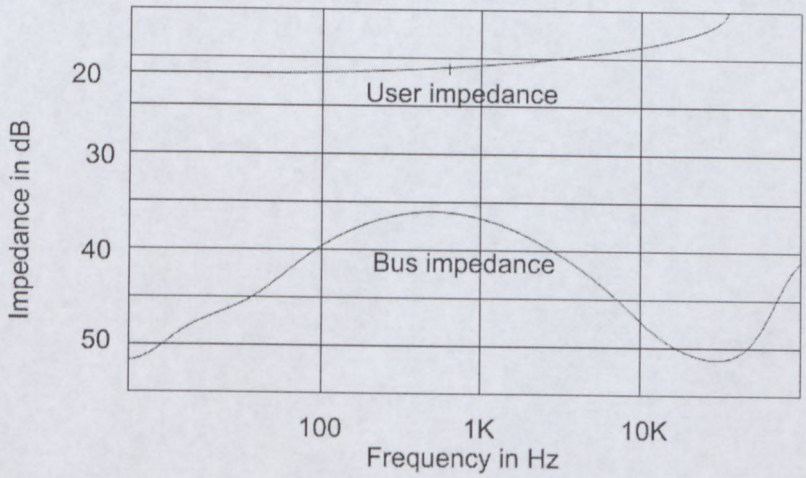

Figure 2.17 Bus impedance at regulation point and user

The system's entire performance is based on the quality dc power bus regulation, transient response, distribution impedance and sometimes the reduction of noise generated by the converter of the solar array regulator.

The power produce is uninterruptible owing to the introduction of solid state power controllers. The standards for the bus impedance are:

$$R_{BUS} = \frac{0.02 \times V^2}{P}$$

Where V represents the bus voltage, P is the maximum bus power and R_{BUS} resistance of the bus. The bus capacitance can also be deduced from the following

$$C_{BUS} = \frac{1}{2 \times \pi \times R_{BUS} \times f_{BW}}$$

Where f_{BW} represents the bandwidth.

This power bus maintains a high level of power stability because the voltage is fully regulated at the generation point. If the impedance designed is very low, switching between the devices can be eliminated, which makes the interface simpler and cheaper.

With the application of SSPCs the system eliminates all forms noise and ensures quality delivery of power. The inverters normally used in this topology is the half or full bridge type, because either of them limits maximum voltage on the bus. Although push-pull in its operation will multiply the input voltage to obtain twice the output.

2.6.2 A NON- SEQUENTIAL POWER BUS FOR LEO APPLICATION

Alcindor and Clarke (2005) explain in this design that power is produced for the bus through traditional means of mounting solar arrays on the sides of the satellite and by deploying the rest of the arrays to obtain a wider surface area for power generation. An EOL voltage produce is a little above the main bus voltage. The solar arrays are divided into strings and are connected in series and parallel to produce equal current size. They are connected to the body of the spacecraft by solar array drive mechanism (SADM), which has bearings and power transfer assembly (BAPTA). Power produced from the solar cells in orbit is almost equal to the transconductance gain (Gm) of the sunlight power system. The gain is normally altered by seasonal changes of the sun. The mode of regulation is based on sunlight regulated bus method.

Main Error Amplifier (MEA) is used to divide the solar arrays parts to the power bus, as shown below.

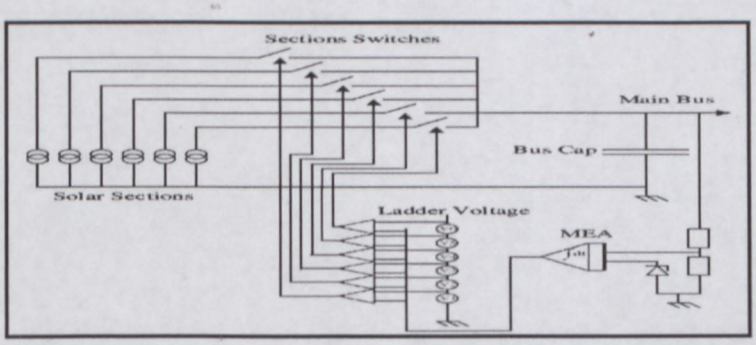

Figure 2.18 Architecture of sun regulated mode with MEA

The potential divider ratio (β) is represented at the gain stage, the gain proportion for MEA (K_{MEA}), the total array current ($6 \times I_{SECTION}$) and the ladder voltage (V_{LADDER}).

$$Gm = \beta \times K_{MEA} \times \frac{n \times I_{SECTION}}{V_{LADDER}}$$

When the bus voltage is maintained at 2%, the voltage regulation of load change has 50% of maximum power by the fixed values of (β), K_{MEA} and V_{LADDER} since $I_{SECTION}$, which can be considered as constant.

In general terms, power systems of small satellites generate power from body mounted and deplorable solar arrays made of GaAs single junction solar cells for effective and steady supply to the subsystems.

MPPT is used in this design to maximize power from the source to the power bus when the satellite is in sunlight by efficiently regulating the currents and voltages. The sequential switching was introduced because the sun sometimes has different fluxes and operates at different temperatures.

BCR is used at the dedicated section of solar panels to extract the maximum power to the bus, which is why centralized MEA will not function properly because it will need power from the BCR just like the sequential system. The BCR is made up of a buck dc-dc converter to step down voltage from the arrays to the bus voltage.

The storage device is made of NiCd battery cells to maintain bus voltage and to provide the necessary power during eclipse. In an event where battery voltage is equal to the temperature compensated voltage reference of PWM IC, the output error amplifier is low and the width of the PWM is zero. Therefore, increases in battery temperature give negative temperature coefficient of the thermistor, which reduces the resistance and thus lowers the EOC voltage reference.

A series of redundant power switches that are implemented are normally used to activate the battery voltage monitor, and if BCR malfunctions or EOC interface fails causing battery overcharge beyond EOC voltage, the voltage protection will be activated and the load equivalent charge connected across the battery.

2.6.2.1 BUS IMPEDANCE

Bus impedance is always dominated by the battery because it is always in the circuit. Load switching characteristics are monitored by the distribution system where every non-essential load is fed by the current limiting power switch. With low battery impedance a better power response will be established.

The power conditioning in this system is used to maintain system stability and to improve the flow of power. In worst case conditions where there is failure, the system's redundancy will act as protection by using a protection circuit to restore the system.

2.7 SUMMARY

This chapter focused on a general overview of spacecraft power systems and related work on the power bus for small and large satellite systems. Each unit of the power system of a spacecraft was review. This theoretical foundation is the same for all spacecraft power systems.

It is on this basis that the concept of a nanosatellite power systems was developed, which guides towards subsequent chapters in this project

CHAPTER 3

3 POWER SUPPLY

3.1 INTRODUCTION

This chapter is discusses power from solar panels and the storage of energy in batteries to ensure that adequate power is produced and maintained for effective distribution to the subsystems.

Photovoltaic cells basically provide load power and battery charge current during sunlight. The battery storage is responsible for supplying all the power for the spacecraft during eclipse and sometimes supplement extra power in case of high load activities. Not even both the solar arrays and the batteries operate under constant voltages. Unloaded voltages from solar arrays will generally appear quite higher in cold conditions such as in eclipse and at the beginning-of-life (BOL) prior to experiencing any environmental degradation. The battery output voltages vary largely with a lot of factors and a lower voltage during discharge as opposed to battery charge or open-circuit conditions. There are some regulating methods, which are used to obtain useful and stable power from the photovoltaic cells and batteries.

The goal here is to implement a primary power production system, which conforms to the power requirement of a nanosatellite. The power generation unit will offer scalability, reliability and flexibility with a focus on solar cells selection, rechargeable batteries to store energy, and an efficient interface of the solar panels to the storage device, as well as supplying to load. The means of fault propagation to protect both the solar arrays and the batteries are also discussed. Approaches of this design architecture have are outlined in this chapter.

3.2 PRIMARY POWER GENERATION

Power generation in nanosatellite systems basically consist of solar arrays, normally arranged in series and parallel combinations to obtain the desired voltage and current characteristics. The energy generated is converted into dc current and transported through the bus to the loads.

Generally, PV cells can be idealized as a constant current source in parallel with a diode and a shunt resistance (Bonin *et al.*, 2009).

In satellite systems operation, the critical point of receiving power from solar cells is always the single point of failure.

Therefore, power production from each solar array must be isolated as much as possible to minimize single point failures. Due to limited area for power generation, the main aim of producing primary power is to extract maximum power, ensure high efficiency, reduce mass, minimize cost and optimization of the total area of solar cells coverage (Alan, 2004).

In a nanosatellite power system, non-deplorable solar cells are always the best option for power production, owing to simplicity and ruggedness. It is also because stability of the satellite is based on two passive axis, which cannot direct deplorable solar cells towards the sun. In order to use deplorable solar array, the stability of the satellite must be redesigned for three axis stabilization which may lead to an increase in the mass of the satellite. However, fixed solar arrays allow the system overall mass to be kept at minimum (Obland *et al.*, 2002).

Harsh environmental conditions cause solar cell degradations in space, which require temperature changes and radiation level considerations to avoid a decrease in efficiency over time. The mission life of a nanosatellite is expected to last for a maximum of two years with solar array degradation of about 10%. Due to limited power production from the solar arrays mounted on the body of satellite, an extremely efficient power bus is required. The amount of solar radiation from the sun per unit area is known as the solar constant and it is a determining factor in primary power design, because it shows the amount of energy for the satellite which needs to be calculated (Polaschegg,2005).

According to Sharps *et al.*, solar cells in space posses size, weight and reliability constraints than manufacturing cost. This has prompted the desire to develop highly efficient solar cells for space application. New technologies that are developed target a wider portion of the incident spectrum and added efficiency of about 30% excess. These promote the emergence of nano-materials which holds a future for this prospect. The typical voltage-current relationship equation for solar arrays is given by $I = I_{PHOTO} - I_O \bullet \left(\exp\left[\frac{q}{AKT} \bullet \left(V + I \bullet R_{SERIES} \right) \right] - 1 \right) - \frac{V}{R_{SHUNT}}$ where I_{PHOTO} is the current photon generated due to isolation, I_O is the reverse saturation current of the semiconductor material, R_{SERIES} represents the series ohmic resistance of the cell, R_{SHUNT} accounts for current leakage, K is Boltzmann's constant, T represents ab solute operating temperature, while q is the charge of a single electron, and A is an ideality factor of the p-n junction.

Semiconductors are the most important part of solar cells with different suitable materials to make their layers. Each material has its own benefits and drawbacks with no ideal material for all forms of available designs. Solar cells are placed on top of a metallic grid for collecting electrons from the semiconductors and to transfer it to the external load with a back contact layer to close the circuit. A glass with an anti-reflective coating is covered on top to trap the sun's rays rather than reflecting it back. One of the simplest ways of maximizing efficiency in solar cells is to reduce reflection of light to increase absorption. An anti-reflective coating and geometry are methods that are used to trap light within cells and the two represents the main optical methods to minimize reflection. The anti-reflection coating absorbs more light for cells to increase its efficiency (Markvart, 1994).

The materials commonly used to develop solar cell technology are silicon and gallium Arsenide.

Silicon: Is the most common and the most widely used material for solar cell technology in space applications owing to its abundance. In order to optimize silicon material to achieve an optimum result in solar cells design, it must be purified to almost 100%.

PV cells are produced when silicon is doped with impurities or semiconductor material to obtain an n-type and a p-type structure. The molecular structure of single-crystal silicon is uniform owing to the growth of an entire structure on the same crystal. This uniformity is ideal for transferring electrons through the material with semi-crystalline silicon made up of small particles of crystals across boundaries. These boundaries drastically reduce the movement of electrons and allow them to regroup with holes thereby reducing the power output of the cells. Semi-crystalline silicon is cheaper to develop than single-crystalline silicon. These create opportunities for scientist to develop new technologies to minimize the effect of grain boundaries (Spectrolab,1984).

Gallium Arsenide: is a compound semiconductor material made from two or more elements typically gallium and arsenic. It is a by-product of typical elements such molten aluminium and zinc which are rarer than gold. Thus arsenic is a poisonous element. The development of solar cells from Gallium-Arsenide (GaAs) technology has gained popularity after it was initially used in light-emitting diode, lasers and other optoelectronic devices. GaAs is particularly desired for developing multi-junction and high-efficiency solar cells because the energy band gap is 1.43eV and very ideal for single-junction solar cells. The cells need only few microns to absorb sunlight owing to its high absorptive nature. Unlike silicon cells, gallium-arsenide (GaAs) cells are not affected by heat.

Alloys produced from GaAs using phosphorus, aluminium, antimony or indium have characteristics that are similar to that of gallium-arsenide, which ensure flexibility in cells design. Gallium-arsenide is highly resistive to radiation and has prolonged life with increased efficiency, making it most desirable for spacecraft application (Wijesinghe, 2003).

In recent times, multi-junction solar cell technology has been space qualified and used to actually maximize power production from solar cells, with efficiency around 25% and more. Compared to previous designs, the triple junction solar cells convert a large portion of solar spectrum into useful power at about 35% increase for the same solar panel area thus reducing the cost per watt at 15-20% . Table 3.1 is a brief comparison of solar cell technologies with their advantages and disadvantages .

Table 3.1 Comparison of Solar cell technologies

MATERIALS	THICKNESS	EFFICIENCY	ADVANTAGES	DISADVANTAGES
Monocristalline (Si)	0.3mm	15 - 18 %	Best researched solar cell, high power/area ratio	
Polycrystalline (Si)	0.3mm	13-15 %	Highly used	Lengthier Production procedure
Edge defined Film Fed Growth(EFG)	0.28mm	14%	Significant decrease in production costs Possible in future	Costly at the moment
Amorphous silicon	0,0001mm + 1 To 3mm Substrate	5 – 8%	Designated for future low cost applications	Low efficiency and lifespan
Cadmium Telluride (CdTe)	0.008mm +3mm glass Substrate	6 – 9 %	Still under development	Poisonous raw material
Hybrid Silicon (HIT)	0.02mm	18 %	Higher efficiency between temperature Coefficient and lower thickness	Limited use of this production procedure
Gallium Arsenide (GaAs)	0.03mm	18 – 20 %	High efficiency, better radiation tolerance	More expensive than Si cells
Multi-junction GaAs	0.03mm	24 -35 %	High efficiency, better radiation tolerance	Still expensive than Si cells
Tandem GaInP/ GaAs	3.5mm +1 to 3 mm Substrate	29.5 %	Highly efficient, cost effective	Very expensive
Tandem GaInAsN/ GaAs/ GaAlAs	3.5 mm + 1 to 3 mm Substrate	38 %	Highly efficient	Very expensive

The mode of extracting power becomes inefficient when photovoltaic cells are directly connected to the load (Polaschegg, 2005).

The arrangement of photovoltaic cells in series may not provide the required power, because series modules couple the same current.

The differences between temperature insolation and the quality of the cells cause individual cells to produce different I/V curve, which have a different MPP. The cells become reversed biased and the power produced is dissipated as heat when the cells supply less current. This process will result in a highly poor performance and cause damage to the cells.

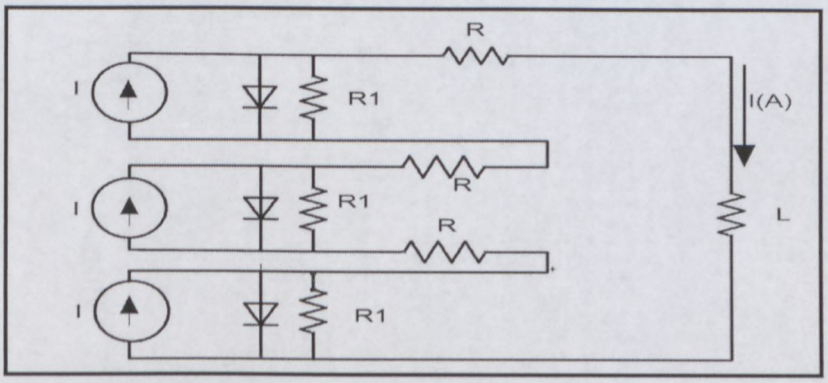

Figure 3.1 Equivalent resistance and reverse biased conditions of PV cells in series

Therefore, a bypass diode is placed parallel with each photovoltaic cell to avoid reverse biase by weak cells from more than one diode drop of (~0.7V). It now has the process of protecting the cells and minimizing power losses. This still leaves the system without any contribution from weak cells.

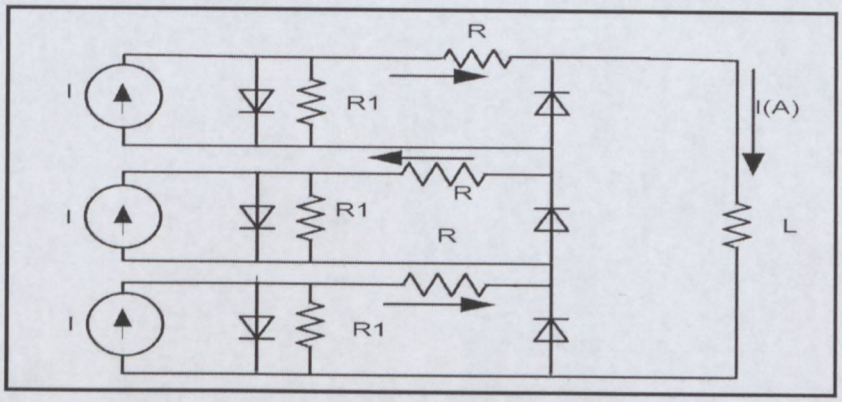

Figure 3.2 Series connected bypass diode and equivalent load to increase power to load

When cells are parallelly connected they display a similar problem as in series connections, but this time in the voltage mode. In this case, instead of the same current in series connection, it is the same voltage in parallel connection.

Due to differences in temperature, cell quality and insolation of the cells have different MPPs. Optimal power could be extracted from one or more modules, because they are made to operate at the same voltages. If any of the cells are operating significantly lower than the other cells, it will sink the current by loading down the others, which would have provided it with power.

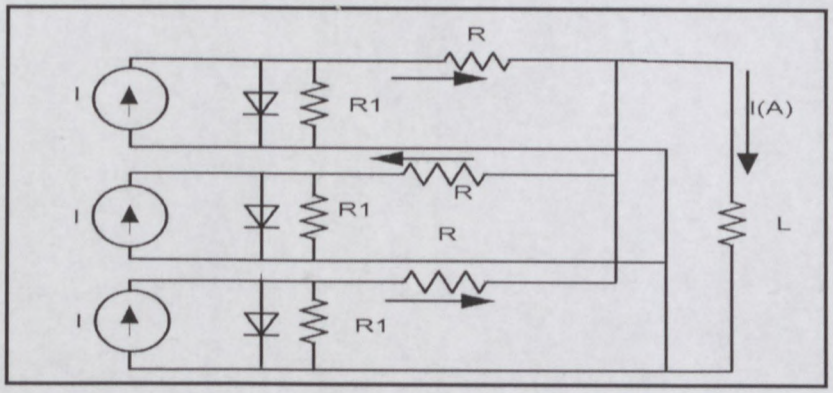

Figure 3.3 Parallel connection PV cells across equivalent load shows sinking behaviour when cells do not have equal insolation

Power losses in parallel connection are considered negligible, but the PV cells are susceptible to degradation owing to power dissipation in the shaded cells. Blocking diodes are placed in series with the cells to keep current away from weak cells. The new arrangement prevents shaded modules from damage and it becomes permanently sunk with respect to the rest of the arrays, although it introduces more losses to all the operating cells.

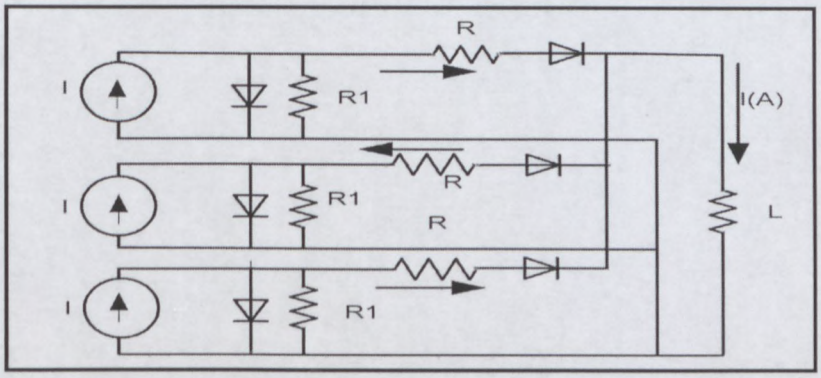

Figure 3.4 Parallel connected PV cells with diode, to prevent current from sinking

The introduction of switch mode converters at the output of each PV cell resolves mismatch that occurs in series and parallel connection of PV cells, because they sometimes behave like transformers to set V/I characteristics of the load until each cell operates at its MPP. Figure 3.5 displays the characteristics performance of solar arrays in different operating conditions. Output current of the arrays decreases with terminal voltage increase (Cooper, 2008). Each of the curves has a point where it delivers the maximum power. This point is the operating optimal point where power is efficiently maximized for application by solar arrays.

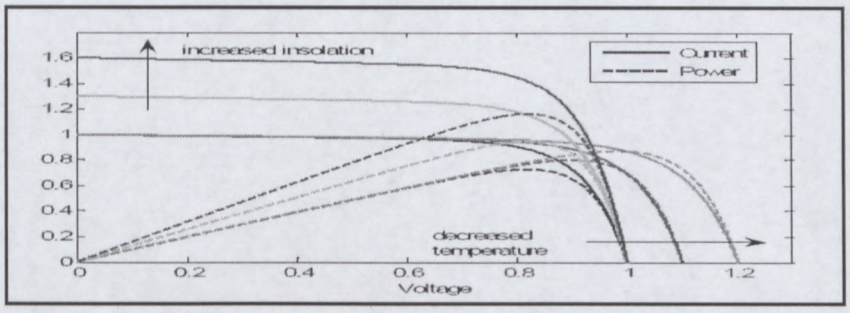

Figure 3.5 Typical -normalized- terminal characteristics of solar arrays

(Adapted from Al-trash, 2007)

The resistance increases of the arrays are negative, thus the output current of the array steadily decreases with increase in terminal voltage. On each curve is the point of maximum power, which is normally called the maximum power point (MPP). This optimal point is where the utilization of solar arrays efficiency is achieved.

On the left hand side (LHS) the arrays look like a current source that supplies increased power with increased voltage. On the right hand side (RHS) also the arrays look like a voltage source that supplies decreased power with increased voltage (Al-trash, 2007).

The terminal characteristics change constantly owing to variations in irradiance, temperature, and other operating conditions.

Photovoltaic cells with an output switch mode converter connected in parallel or in series can still retain stability in its operation. There is less power loss in parallel arrays as compared to series arrays. Parallel arrays at each stage sources power directly to the battery and the loads. Series arrays transfer power to the battery or loads through other stages in the arrays. The losses at output stages of each switch mode converter are compounded in series arrays. High voltage series arrays are the most suitable. Hence parasitic losses prevent the switch mode converter from operating at the required output voltage without losses (Jeppesen and Thomsen, 2002).

Brown (2002) reveals that, photovoltaic arrays use cells that are grouped in series to increase voltage to a desired level. This group of cells are called strings, and the strings are either connected in parallel and series to obtain the required current levels. However, the most important parameter to determine a fault is to consider voltage and current states by connecting the solar cells in series and parallel to obtain the desired power level.

With increasing demand for efficiency and low mass as the prerequisite for nanosatellite power supply, the most efficient and space qualified solar cell technology based on commercial off the shelf component was used. Hence with improved solar cell technology, GaAs multi-junction cells from Clyde space, a company specialized in producing COTS based in Scotland was selected because it has features such as a low maximum power point voltage (VMPP) temperature coefficient and a higher cell voltage with a superior radiation tolerance. The higher VMPP cell voltage for the multi-junction GaAs is twice that of silicon with temperature co-efficiency around -6mV/C and the expected temperature range between -40 to +70. The innovation on this cell technology makes it ideal for power production in nanosatellite systems where size and mass are critical to the design. The cells are mounted on four panels and placed on the sides of the satellite. Each of the panels is made of six multi-junction GaAs solar arrays in series. The solar arrays were designed to provide voltages between 12V -18V dc and a nominal of 14.5Vdc with a total power level of 5W. Appendix A display solar cells mounted on four sides of a Cubesat.

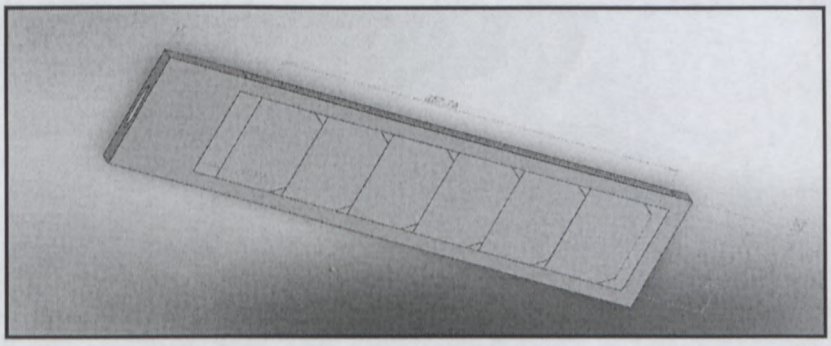

Figure 3.6 six solar array in series on a panel

The diagram in Figure 3.6 above represents an arrangement of solar cells on the panel which was mounted on the sides of the satellite. Figure 3.7 below represents the efficient production of power from the solar arrays configuration of Figure 3.6 at exactly 5W.

The blue colour represents direct incidence in the sun; Red represents the panels directly below, and the green represents the panels directly opposite to panel incidence on the sun. This clearly shows how energy at various times on the panels are produced during sunlight.

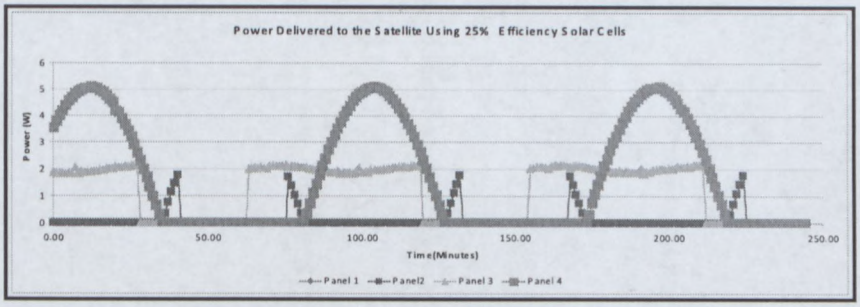

Figure 3.7 Power generated by solar arrays at 25% efficiency

3.2.1 CAUSES OF SOLAR ARRAY FAILURE

3.2.1.1 CORONA EFFECT

When solar arrays experience corona owing to the presence of high radiation from the environment caused by electrostatic charging of arrays surface, it leads to insulation breakdown and arcing, which take place between the sectors or at the end of the block by minimizing the power output for a short period or cause a permanent power failure from the sector or block, though it is less catastrophic to the spacecraft. This effect is minimized by connecting all external surfaces to the structure and possibly coating the array with layers of conducting indium-tin oxide.

3.2.1.2 SOLAR ARRAY PARASITIC CURRENT LOSS

According to some discoveries made by NASA, when solar arrays have a positively biased charge, just like plasma absorbs its own plasma electrons, a parasitic loss to solar arrays occur to the power system. This loss is similar to solar array corona discharge, which causes solar array arcing. *Medley* (1995) also confirms that these losses affect only high voltages in low earth orbits.

3.2.1.3 SOLAR ARRAY ELECTROMAGNETIC INTERFERENCE

The process whereby an electromagnetic action causes interruption, obstruction, degradation or limit the performance of solar array, is known as solar array electromagnetic interference. Whitehead and Johnson (1993) further explain that this interference is usually caused by high current switching devices, and it can be solved by introducing soft start circuits on the loads. The

emissions from the sun-dominated radiation environment produce electromagnetic interference on the arrays and the unlimited emissions from the sun by atmospheric absorption, which cause surface charging of these arrays, which causes in turn discharge and arcing of the areas around solar arrays.

3.2.1.4 SOLAR ARRAY DEGRADATION

Solar degradation is also described by Whitehead and Johnson (1993) as a result of contamination, substandard cells or physical damage to cells by micro- meteoroids impact and space dust. The ultraviolet radiation contaminates the optical surfaces causing less light to reach the solar cells under the substrate, which results in power degradation. Solar array degradation is more likely to occur close to a heavenly body. The arrangement of the solar arrays is to provide power in the worst case conditions when the sun's intensity is least.

3.2.1.5 SOLAR ARRAY SHORT CIRCUIT

Whitehead and Johnson (1993) further illustrate that when one or more solar cells become reversed biased during shadowing, a permanent power loss and localized dust heating will occur. This problem can be eliminated by using shunt diodes.

3.2.1.6 SOLAR ARRAY OPEN CIRCUIT

Open circuit of solar cells occur owing to poor manufacturing and testing which takes place when the cells are interconnected at the assembly plant. This occurrence results in low power production. The entering and existing sunlight by the spacecraft causes expansion and contraction of solar arrays known as thermal cycling.

3.2.1.7 ISOLATION DIODE OPEN AND SHORT

Whitehead and Johnson (1993) reveal that when an isolation diode is opened, the behaviour is similar to the open circuit of solar arrays. The short experience on the diode causes the battery to discharge its power into the solar arrays. This causes loss of battery power and solar array heating, which results in a loss of efficiency.

3.3 POWER STORAGE DEVICES

The power storage system is the secondary source of power supply based on electrochemical battery cells. Its purpose is to store and deliver electrical power during eclipse. A battery is simply made up of cells connected in series or parallel. The main aim of the battery is its ability to provide and store the required energy at a desired voltage level over a period of time.

Paramount to the requirements of nanosatellite storage systems are those of size, mass and cost (Asif, 2008). The batteries can be considered as an ideal voltage source/sink or as an energy reservoir. During sunlight excess energy is stored in the battery. Depending on the circumstances of the satellite, when the load demands increases the battery bank can release extra energy to support the power source. Some batteries require specific charging techniques to optimise performance. High energy density and low or no maintenance together with a long lifetime, are all critical requirements for batteries that are used in spacecraft systems (Al-atrash, 2005). The following requirements are important in battery selection:

- Light weight;
- Size ;
- Structure and vacuum stability;
- Voltage output;
- Internal resistance;
- Voltage stability over temperature range;
- Safe storage over period of time;
- Easy recharging state; and
- Life cycle and availability

The two main dominant batteries in space application are Nickel Cadmium (NiCd) and Nickel hydrogen (NiH_2). NiCd has been the most widely used battery in space application due to its robustness and high life cycle with low energy density. Improved battery technologies have lead to the emergence of Lithium ion batteries which have now become the best choice for space applications and has been highly promoted by the European space agency. Lithium ion batteries are easy to package and are light.

It is important to make a brief comparison of these batteries to determine their advantages within the space community (Polaschegg, 2005).

Nickel Cadmium (NiCd)

- It has enjoyed space dominance because of its reliability in space applications.
- It has low voltage output (1,2V).
- Has low energy density (apprx. 40Wh/kg).
- It suffers from memory effect, that means the battery discharge capacity is reduced when repetitively discharged incompletely and recharged.

Nickel Hydrogen (NiH_2)

- It is also popular in space application.
- It has completely no memory effect.
- It has a higher energy density than NiCd (apprx. 60Wh/kg)
- It has a low output voltage of (1.2V)

Lithium Ion(Li Ion)

- Has higher energy density than NiCd and NiH_2 batteries (above 100Wh/kg)
- Battery voltage is three times the rechargeable NiCd or NiH_2 batteries (3.7V)
- Absolutely no effect on memory.
- It has an extremely flat discharge profile.
- Battery temperature ranges of performance is wider than NiCd and NiH_2.
- But when it suffers from overcharging the battery will explode.
- It has also has a flexible geometry.
- It is very durable and easy to manufacture (Delft University of Technology ,2010)

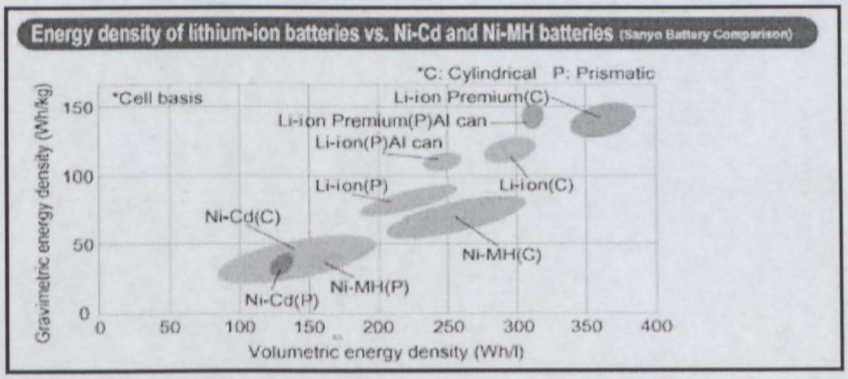

Figure 3.8 Energy density battery technologies

(Adapted from Akagi,2006)

Lithium ion polymer battery is an improved technology that emerged from the lithium ion family. It is versatile because it covers a wide range of cell chemistries (Polaschegg, 2005). The technology puts together a life cycle advantages of safe battery chemistry with flexible geometry. In addition to using solid polymer electrolyte, Li ion polymer has a covered object based on $LiMO_2$ as an active cathode material and a graphite carbon as the active anode material. Lithium ion polymer can easily be made from different level of coating techniques which uses composite anode, cathode and electrolytic polymers (Macklin *et al.*, 1998).

Table 3.2 Types of battery parameters (Macklin et al.,1998)

Battery technology	Cell nominal voltage (v)	Cell average discharge voltage (V)	Cell- specific energy (W-hr/kg)	Cell specific power (W/kg)	Operating Temperature ($^{\circ}c$)
NiCd	1.45	1.25	40-50	150-200	-20-50
NiH2	1.55	1.25	45-65	150-200	-10-50
Li-ion	4.1	3.5	90-150	200-220	10-45

Lithium ion polymer battery has also experienced massive development and innovations over the years and has been selected for integration as the power storage components for this design. This will enhance an effective storage system, which required for energy supply during eclipse. The innovative development of this lithium ion polymer has led to the production of a compatible battery which operates with minimum solar array voltage that is produced. This compatibility allows the selection of two batteries in series to obtain 7.2V dc and current of 2A, which is required to charge the battery. This means that each of the cells using strings provide a minimum BOL capacity of $2 \times 3.6V = 7.2V$. This selection makes the storage facility scalable. This design has an integrated battery heater with a thermostat, battery cell voltage, an effective terminal voltage, current and temperature monitor on the battery. The battery is equipped with protective devices against over-voltage, overcharge and discharge conditions (Clarke & Simon, 2007).

Figure 3.9 shows a typical reaction inside a lithium ion polymer battery at various temperatures. The Top curve represents the maximum capacity at which the battery has been charged, while the line below represents the charged state of the battery, which is seen as discharged.

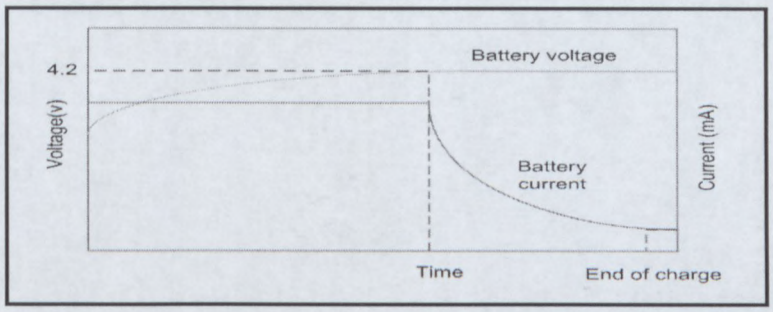

Figure 3.9 Battery charging characteristics for lithium ion polymer

(Adapted from Jappesen and Thomsen, 2002)

3.3.1 BATTERY OVERVOLTAGE

The continuous flow of current to the battery when it is fully charged leads to over–voltage conditions. Over-voltage conditions in lithium ion batteries is normally around 4.2V, and it also has a charging circuit, which isolates the battery from excess charging current for protection. Others such as Ni-NH do not show over-voltage conditions when over-charged; they rather use zero dV/dt, negative dV/dt, dT/dt and a time control to determine the end of charge.

3.3.2 BATTERY UNDER-VOLTAGE

An under-voltage state is a problem for the lithium ion family of batteries. In cases where the voltage drop is significant, the batteries can be permanently damaged. When Ni-MH batteries are discharged with their terminals shorting, there is no danger of any permanent damage. The lithium ion polymer battery protection circuit, however detects low voltage conditions and isolates the battery from discharge.

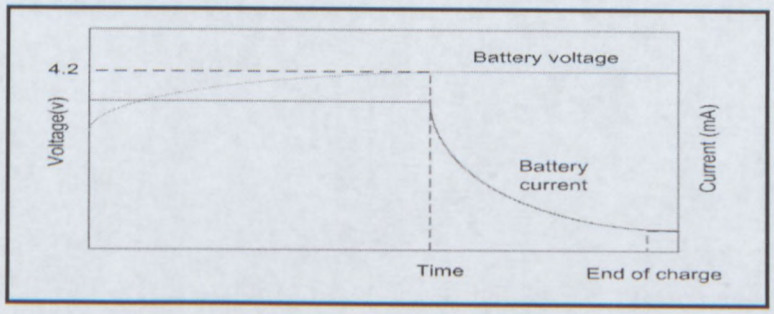

Figure 3.9 Battery charging characteristics for lithium ion polymer

(Adapted from Jappesen and Thomsen, 2002)

3.3.1 BATTERY OVERVOLTAGE

The continuous flow of current to the battery when it is fully charged leads to over–voltage conditions. Over-voltage conditions in lithium ion batteries is normally around 4.2V, and it also has a charging circuit, which isolates the battery from excess charging current for protection. Others such as Ni-NH do not show over-voltage conditions when over-charged; they rather use zero dV/dt, negative dV/dt, dT/dt and a time control to determine the end of charge.

3.3.2 BATTERY UNDER-VOLTAGE

An under-voltage state is a problem for the lithium ion family of batteries. In cases where the voltage drop is significant, the batteries can be permanently damaged. When Ni-MH batteries are discharged with their terminals shorting, there is no danger of any permanent damage. The lithium ion polymer battery protection circuit, however detects low voltage conditions and isolates the battery from discharge.

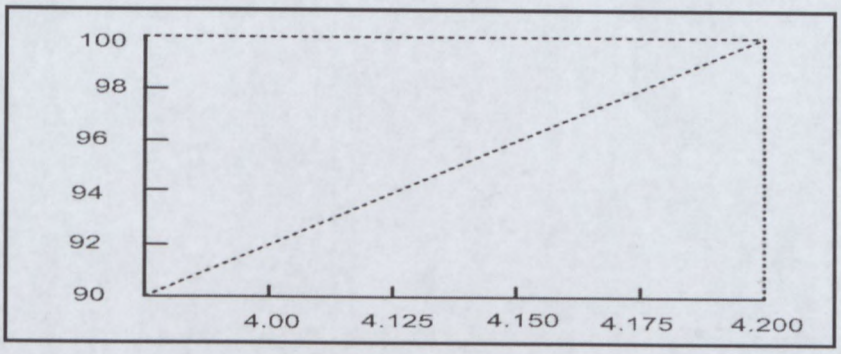

Figure 3.10 Effect of under voltage on lithium polymer where battery voltage is 4.2V

(Adapted from Alan, 2008)

3.3.3 BATTERY FAILURE AND PROTECTION

The failure rates of batteries are normally high compared to some electronic components. It is always good to minimise failure rate and provide redundancy to increase the life span of the storage system. The battery is reduced as the Depth of Discharge (DOD) per cycle increases. The DOD of lithium ion polymer at 40% is important because it prolongs battery life.

3.3.3.1 BATTERY CHARGE CONTROLLERS

The charge controllers are used to monitor transfer of power between the battery, solar modules and the load. The function of the battery charge regulator is to ensure that batteries operate within that charge limit to avoid damage. If the battery charge levels fall below the required level, a low voltage disconnects or cuts the current to the load to prevent continuous damage, while in the event of overcharging, the supply is again disconnected.

3.3.3.2 SHORT CIRCUIT

Short circuits occur because low resistance between conductors where current builds up, which can lead to destruction of the power source. This is a common problem, which is normally seen in batteries where temperature plays a role, and it reduces the voltage considerably.

3.3.3.3 CAPACITY DEGRADATION

When the effectiveness of battery reduces with time, it is said to be degrading. It is normally predictable and caused by temperature and depressed voltage. However, a low voltage cut is added to the battery to prevent loss of power.

3.3.3.4 ENERGY STORAGE FAILURE

According to Whitehead and Johnson (1993), failure occurs when an increase in temperature reduce the battery's ability to charge.

3.4 FAULT TOLERANCE

In order to maintain power system survivability and improve quality power supply, the system must be protected against over-current or must be able to withstand short circuit downstream of the power module. Since most of the components that were used are off-the-shelf, it is difficult to determine, which buses of the power system will run off. Given that the nanosatellite power system have a single string without any redundancy; the protection circuit provided will try to reconnect to the bus in the event of over-current.

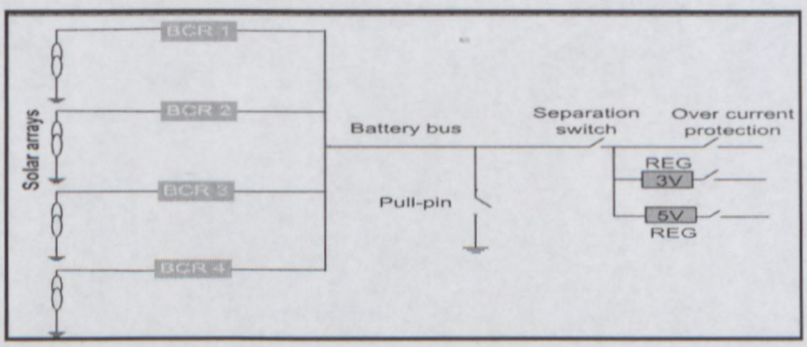

Figure 3.11 Power systems with over-current protection

(Adapted from Clark, 2008)

3.5 POWER DISSIPATION

Power generated from photovoltaic cells is supplied to the loads and to recharge the batteries on board the satellite. When excess power is generated, shunt devices are placed in the system to eliminate this power.

These devices are mainly resistors that are also used as a heater to control temperature in the system. The On Board computer (OBC) can also activate the shunt resistor to warm any unit that needs heat, while the amount of energy dissipation in the shunt is based on the amount of power on the bus. The main power, which will be dissipated on the shunt is from the solar arrays, if it is not used anywhere. The system can also as like a voltage protection system on the bus and limit the amount of current drawn to avoid system collapse.

3.6 LATCH-UP PROTECTION

Latch-up occurs when parasitic SCR made by a couple of CMOS devices are turned on by surge voltage or high energy particles, which induce little current. The result is a self-holding current flow, which causes high power dissipation and result in device disruption. Latch up free circuit can be designed by avoiding a CMOS device and instead adopt radiation hardened devices. Since nanosatellite systems development depend heavily on Commercial off the Shelf components (COTS), the use of CMOS devices cannot be avoided. This calls for a specific protection circuit to protect the CMOS device from latch up. The main idea behind the protection is to constantly measure current and turn off power immediately before anomalous absorption detection occurs. Normal operation will be restored once the transient event is over. Each supply path must have its own protection circuit, which should by itself be latch up free. Below is a latch up circuit block diagram, which includes:

i. A currents sensing differential amplifier;
ii. Monostable circuit; and
iii. Isolating and current-steering switches.

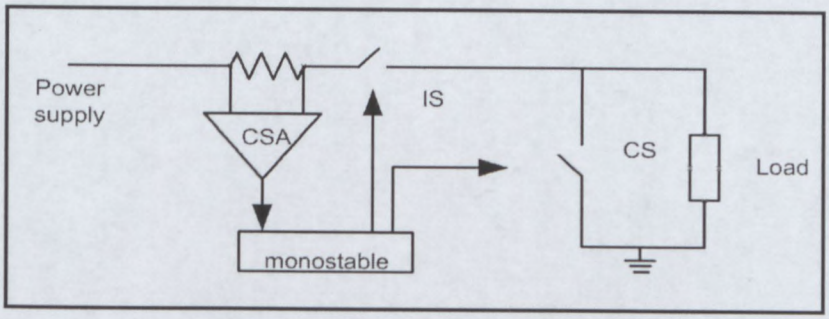

Figure 3.12 block diagram of LU circuit

(Adapted from Speretta et al., 2007)

When the current exceeds the limit set for anti-latch up intervention, the monostable is triggered and isolates the load from the power source for about 100ms. The shunt keeps residual current away from the load to fully neutralize the LU. Stabilizing the LU current threshold with current limit of power supply has always been a difficult task for protection design to control LU. When the regulator current limit is not enabled before the LU, the current will be limited but not reduced to 0, and LU will function for an unspecified period (Speretta *et al.*, 2007).

3.7 SUMMARY

This chapter focussed on the power supply unit, which comprised of power generation and the storage system. The power supply is the point where the primary and secondary power is generated. The various technologies used for power generation and storage were based on solar cells and batteries. The process of interfacing the components allow maximization of energy and an efficient protection system for the unit. These components of the power supply unit serves as a basis for the next chapter to develop methodologies to achieve reliability, reduction in mass and size, and optimization of the components.

CHAPTER 4

4 POWER OPTIMIZATION METHODOLOGY

4.1 INTRODUCTION

This chapter lists the basic power system blocks and the methodologies, which can be used to optimize energy, and reduce mass and size.

These basic nanosatellite power system blocks which c onsidered for power optimization include solar arrays, solar array bus (SAB), satellites primary power bus (PBUS), batteries, power converters, battery discharge regulator, and a power switching device.

These blocks provide power system engineers with opportunities to modify their designs to maximize power from the components during their operation.

In power system design, sizing is used to access the performance of solar cells and array technology, battery design and the voltage bus. This model is used to determine the mass and size of solar arrays, battery capacity (Ah) and battery mass based on the technology of solar arrays, battery cells, solar cells and the configurations used.

Power system components and orbital parameters such as altitude in orbit, sun angle in the worst case and a maximized beta angle can also be used as input. The orbital parameters are used to determine sunlight orbit and eclipse time. Based on the current power system on related technologies the power system block will also be analyzed to check its characteristics to maximize power.

This chapter reviews ways to enhance performance and minimizing size to optimize power from the components of the spacecraft.

4.2 SOLAR ARRAYS (SA)

The choice currently used for nanosatellite primary power generation is to continue to use body mounted solar cells. However, deployed arrays are only necessary if extra power is required. In order to obtain maximum efficiency from the solar array, the solar arrays must be kept pointing towards the sun to be able to produce the required power for the load (Esram, 2007).

4.2.1 SOLAR ARRAY SIZING

The process of solar array sizing can be used to determine the size, mass, cost and for a layout, which can be used in a model analysis. The following factors below are the main inputs to solar array design:

- Sunlight and eclipse duration;
- Spacecraft power profile;
- Array type;
- Solar cell type;
- Solar cell efficiency;
- Temperature coefficients of solar cell;
- Radiation degradation factor;
- Assembly mismatch factor;
- Thermal cycling degradation;
- Packing factor; and
- Bus voltage.

The power of the beginning of life (P_{BOL}) for the solar array is needed to provide the required power by end of life.

There direct energy transfer has system $P_{sa} = \frac{\frac{T_d}{X_d} + \frac{T_e}{X_e}}{T_d} \times P_{avg}$, where P_{Sa} is the solar power is required at the end of mission life.

The power for the b eginning of life is therefore, represented by $P_{BOL} = \frac{P_{sa}}{F_{Loss}}$ w here F_{Loss} represents power loss factor for solar array power due to radiation, temperature, sunlight offset effect along with life time degradation. Together the results are:

$$F_{Loss} = \left[1 - (T_o - 28) \times T_{Coeff}\right] \times P_{Coeff} \times I_d \times |\cos\theta| \times (1 - L_d)^N$$

Where T_{coeff} is temperature factor determined by solar cell, and array, P_{Coeff} is the radiation factor which is determined primarily due to the type of orbit and the lifelong mission with the type of solar arrays and N as mission life in a year

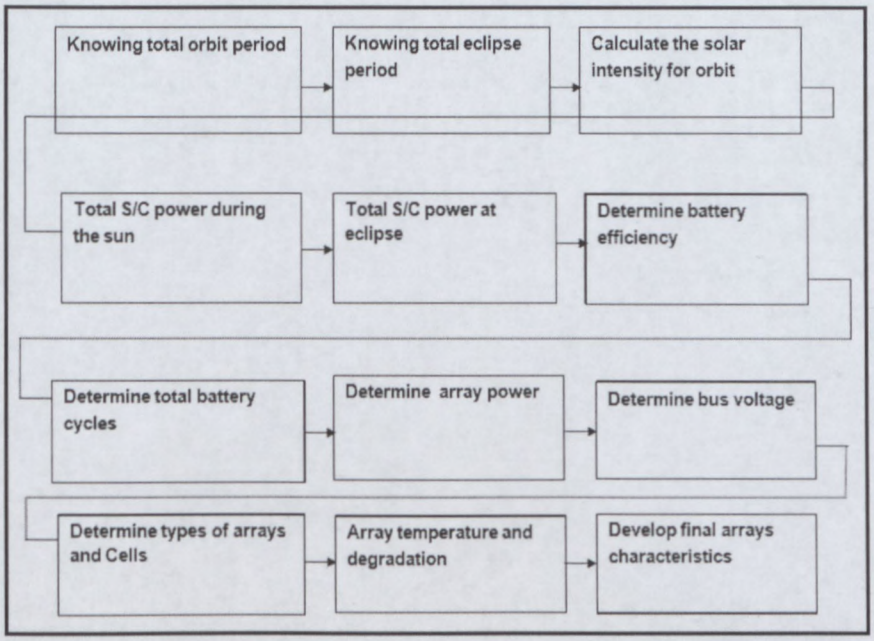

Figure 4.1 Solar array sizing methodology (Adapted from Asif, 2008)

The I_d is an inherent degradation factor owing to design, assembly, cell mismatch and shadowing of solar array. It is a typical value which ranges between 0.49 – 0.88, thus by selecting 0.77. L_d is the degradation performance factor due to thermal cycling, of value 3.75% for silicon and GaAs and 2.75% per year for multi-junction solar cells. The reliability normally added is 5%. Due to array flexibility, additional loss of power must be considered because of the large thermal gradient across the array. It is assumed to be 3% for standard cells such as Si or GaAs and 5% for multi-junction cells. The area of solar cells is determined by calculating the number of cells in series (N_s) and parallel (N_P) which are required to meet the array voltage (V_{sa}) and power specifications.

$$N_s = \frac{V_{sa}}{V_{SCell}} \quad \text{and} \quad N_P = \frac{I_{sa}}{I_{SCell}}$$

V_{SCell} and I_{SCell} represents the operating load voltage and currents at a given temperature with N_s and N_p calculated to their nearest integer value.

The solar cell area ($A_{SCTOTAL}$) is given by: $A_{SCTOTAL} = N_S \times N_P \times A_{SCELL}$

Where A_{SCELL} is the area of individual cells. Some of various sizes are $2 \times 2cm$ and $2 \times 4cm$. Although there are provisions for sizing and analysis tool use to determine the sizes of solar cells of different technologies, the value of 2x4 cm solar cell size can be considered. The total area of solar arrays (A_{sa}) is calculated as:

$$A_{sa} = \frac{A_{SCTOTAL}}{PF}$$

where PF is the solar array packing factor and the value is 0.9 (Larson and Wertz, 1999:325-367)

4.2.2 SOLAR ARRAY BUS (SAB)

The solar arrays output directly supplies the battery charge regulators and the primary bus with voltage. This combined output from the BCR and the bus forms the primary bus (PBUS) voltage. The array voltage is connected to the battery charger while PBUS has regulators, which operate efficiently when the solar arrays draw close to their end of life. These regulators maintain power at the required level to enhance smooth supply of power (Mohammed *et al.*, 1999).

4.2.3 MAXIMIZING SOLAR ARRAY POWER

When a power point tracker (PPT) is placed in series with the solar arrays, maximum power will be produced. The PPT incorporated a dc-dc converter in series to set the arrays output impedance to match the load. The PPT is used to measure the change rate of voltage increase and voltage decay. The control loop maintains stability by detecting changes and reversing the cause. The PPTs work in order to improve power by 10-15 % (Esram, 2007).

4.2.4 PRIMARY BUS (PBUS)

The primary voltage bus is formed by combining solar array output by the PBUS regulator and the battery output. The primary bus voltage must always be slightly higher than the battery voltage. The primary bus voltage is used to charge the battery and is directly supplied to the main bus to feed the spacecraft load. The PBUS voltage can be manipulated to increase the

power to accommodate a high gain transmitter or to decrease the power for low voltage subsystems like the ADCS.

Therefore, efficient regulators and accurate array voltage levels will enhance PBUS performance (Brandhorst *et al.*, 2003).

4.2.5 POWER CONVERTERS

Power converters are used in PPT, battery charged regulators and PBUS regulators. Monolitc ICs and their discrete parts can also be used to build converters with 1-2W at 90-95% efficiency. However, converters that operate at 600 kHz using synchronous rectification are used to reduce losses in switching devices with 85% efficiency, where low power application is more preferred (Kassakian *et al.*, 1991).

4.3 BATTERIES

In order to reduce the number of cells, the battery voltage is selected because a drop in efficiency becomes smaller, but with enough power to perfectly feed the subsystems.

The batteries, which have been considered for implementation was Lithium ion polymer due to its high density, flexible geometry, increased durability and easy production (Akagi, 2006).

4.3.1 BATTERY SIZING

The battery mass and cost can easily be determined by sizing and the requirements for battery sizing depends on required power during eclipse (P_e), eclipse duration (T_e) and the frequency of eclipse.

$$T_e = \frac{T_P}{\pi}\left[\cos^{-1}\left[\frac{\sqrt{1-(\frac{R_e}{R_e+h})^2}}{\cos\beta}\right]\right]$$ where $\frac{R_e}{R_e+h} > \sin\beta$ maximum eclipse duration will occur for a minimum β corresponding to $\beta = 0$.

Before sizing we must determine the energy requirements of the batteries for satellite operation at eclipse. In order to size the battery, we need to select the appropriate electro-chemistry and the number of batteries. The battery characteristics associated with the chemistry and battery are important factosr to consider. The inputs for the battery sizing include:

- Capacity available for each technology;
- Cell average discharge voltage(V_{avg});
- Maximum allowable discharge rate ;and
- Mission life.

The charge-discharge cycle determines mission type and life. In LEO the average discharge cycles are around 5000 cycles per year.

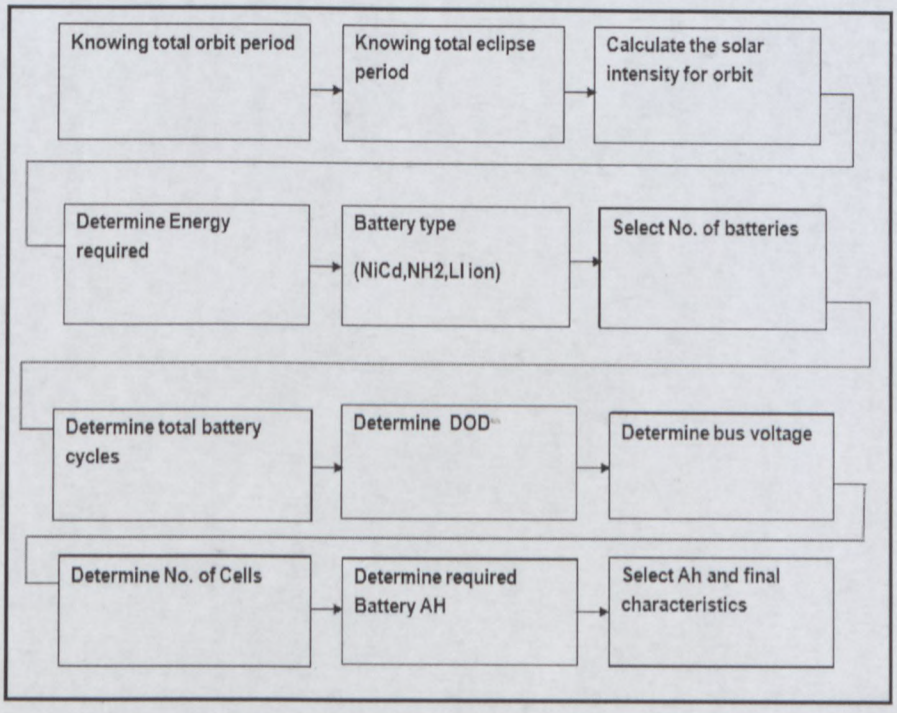

Figure 4.2 battery sizing methodology (Adapted from Asif, 2008)

However, maximum allowable depths of discharge differ with battery type and mission life. It is also used to determine by interpolation of the graphs shown below.

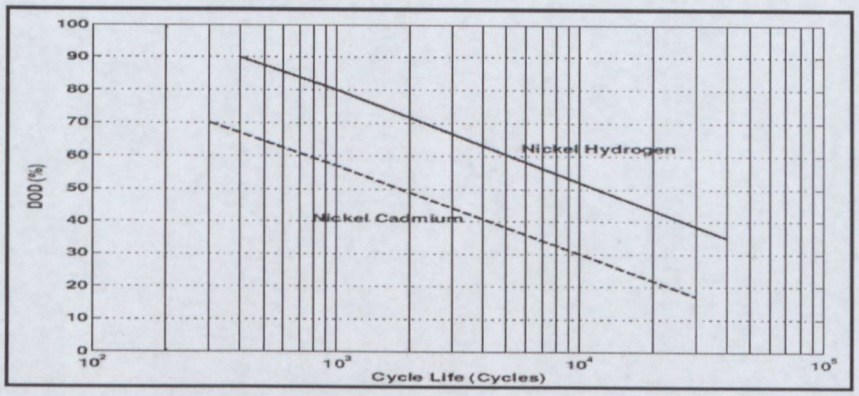

Figure 4.3 Depth of discharge cycle for NiCd and NH2

(Adapted from Macklin *et al.*, 1998)

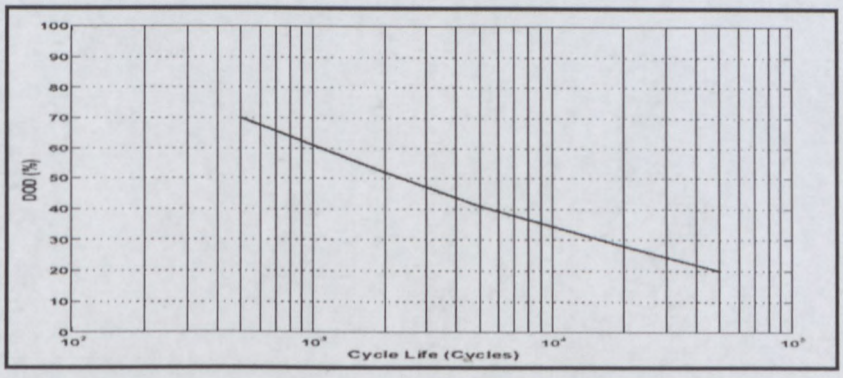

Figure 4.4 DOD vs. life cycles of Li-ion Batteries (Adapted from Macklin *et al.*, 1998)

The number of cells per battery is chosen based on bus voltage. Ampere- hour battery capacity (Ah_{batt}) is calculated based on watt-hour or based maximum steady state power required during eclipse (P_{dis}). The relations for both methods above are:

$$Ah_{Batt} = \frac{P_e T_e}{N_{batt} \times \eta discharge \times \{(N_{cell} - 1) \times V_{avg} - V_d\} \times DOD}$$

$$Ah_{batt} = \frac{P_{dis}}{N_{cell} \times V_{avg} \times C_{rate} \times N_{batt}}$$

where N_{cell} is the number of cells in series, N_{batt} is the number of batteries in parallel, V_d is voltage drop across diode, $\eta_{discharge}$ is battery efficiency during discharge and C_{rate} is the battery discharge rate in terms of battery capacity. The battery with $Ah-capacity$ near the capacity can be picked for further testing to avoid battery constraints on the design. N_{cell} is chosen with the aim of keeping some redundancy in mind (Larson and Wertz,1999:325-367).

4.3.2 BATTERY CHARGE REGULATOR (BCR)

The BCR is a simple hardware, which is used to estimate the maximum power point by sensing solar array substrate temperature by using a thermistor. The array voltage is set to estimate End of Life of maximum power point (MPP) voltage.

The BCR also controls the end of charge (EOC) voltage of the battery by monitoring the temperature using a thermostat. If the battery rises to EOC voltage, the BCR sets the operating point of the solar arrays towards open circuit voltage by providing a trickle charge for the battery. Sometimes additional software is provided to track the MPP of solar arrays accurately (Nugent *et al.*, 2008).

4.4 MASS CALCULATION

The mass of the power system is determined by calculating the mass of the solar arrays, battery and power control unit.

$$M_{eps} = M_{sa} + M_{batt} \times N_{batt} + M_{pcu}$$

where $M_{array}, M_{batt}, M_{pcu}$ represent mass of arrays, battery and power control unit respectively.

Total mass of solar arrays is addition of all the array mass, substrates, deploying mechanisms and interconnections to the units. Mass of solar array values is derived from

$$M_{sa} = (M_{cell} \times A_{sctotal}) + (M_{areal} \times A_{array})$$

Table 4.1 Example of typical bus voltages

BUS VOLTAGE	NORMALIZED MASS	
	BOX	CABLING
28	1	1
50	0.65	0.55
100	0.55	0.25

The battery mass is determined from the battery cell energy density (ρ_{cell}), as the sum of the battery cell and battery structure is taken as 10% of the battery cells. The battery mass is calculated as:

$$M_{batt} = 1.1 \times (Ah_{batt} \times N_{cell} \times V_{avg} \times \rho_{cell})$$

The mass of the power unit is mostly based on indirect estimation and it is calculated as the sum of the masses of both the power management and the distribution unit, which comprise the following distribution bus (DBUS) and switches, which are denoted below by:

M_{DBUS} and $M_{SWITCHES}$. A simple linear relationship assumed for a 28V bus is given as:

$$M_{DBUS} = 0.01 \times P$$

$$M_{SWITCHES} = 0.02 \times P$$

4.5 RELIABILITY

Calculating the relia bility is also a factor, which determines the entire performance of the system. The reliability (R_{eps}) is calculated as:

$$R_{eps} = R_{scell} \times R_{sa} \times R_{batt}$$

Where R_{scell}, R_{sa}, and R_{batt} represents solar cell factor reliability, solar arrays reliability and battery reliability respectively. The reliability factor for each of this technology is based on each component's heritage and current status (Zahran *et al.* 2006).

4.6 SUMMARY

The methodologies presented in this chapter focussed on conditions for optimizing operations of various power components and procedures to reduce mass and size of the systems. Maximum operating conditions of the components helps achieve optimum reliability. These procedures outline ways to minimize component count, component sizing, mass determination and reliability evaluation. These methodologies serve as a platform for selecting various components of power management unit in the next chapter.

CHAPTER 5

5 POWER MANAGEMENT ARCHITECTURE

5.1 INTRODUCTION

The objective of this chapter is to develop an efficient power management system to meet the requirements of a nanosatellite. The power management technique is a process that is used to eliminate power dissipation, whilst maximising the flow of power. Power management involves the process of power regulation and control, where both regulators and controllers are used. This management approach is a sophisticated regulation and control mechanism to produce an efficient and reliable operation. The power management technique uses power converters that are compatible with space systems to regulate and control the power system. These converters are used to minimize noise and to regulate power to the load against interruptions. The configurations of this architecture are flexible and reliable in their operations.

The focus here is on implementation of the most effective and efficient architecture to support an interface between the solar arrays, the storage device and the bus, as well as the loads.

The three modes of power regulation and control, and their associated control mechanisms are also discussed and were implemented. Various switching topologies to enhance the regulator and control devices are extensively discussed, while the most acceptable topology was integrated into the system to enhance performance and to maximize efficiency.

5.2 BUS VOLTAGE REGULATION

Bus regulation involves special techniques used to control voltage on the bus to achieve the required input during operation in sunlight and eclipse. These techniques include unregulated bus, regulated bus and sunlight regulated bus. They serve as a foundation for designing various power architectures to manage the power system interfaces.

5.2.1 UNREGULATED BUS

In an unregulated bus system, solar arrays and batteries are connected directly to the distribution bus which allow the voltage bus to stay between the solar arrays and battery voltages. In sunlight, solar arrays determine the bus voltage, whiles the battery takes responsibility of the bus voltage during eclipse. When solar array power is exceeded during peak power demand hour, the drop in voltage bus is clamped at the voltage of the battery by the forward-biased diode. Maximum power obtained from the solar arrays supply the loads and charges the batteries. There are also effective control devices to determine the battery charge and discharge level. The main disadvantage of an unregulated bus is how to determine the voltage bus by using electrical characteristics of solar arrays and batteries. The solar arrays characteristics vary owing to demands in load, operating temperatures, variations in solar intensity, and degradation from radiation (O'Sullivan, 1994).

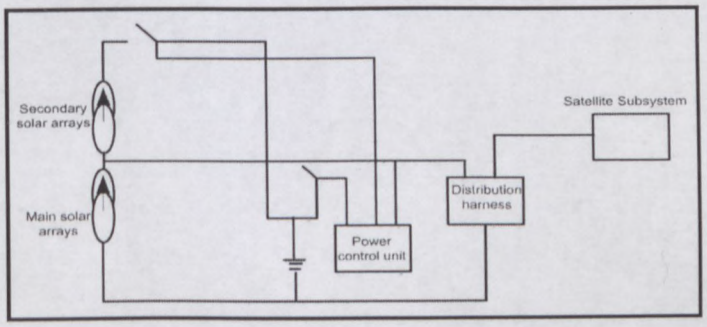

Figure 5.1 Unregulated bus block diagram

(Adapted from Noble, 1990)

Due to these conditions, large variations in voltages do occur on the distribution bus. The topology is most suitable for spacecraft in LEO due to its characteristics of variable input voltages.

5.2.2 REGULATED BUS

In a regulated bus system, the voltage is effectively controlled to obtain the required dc voltage by using a feedback loop. The bus provides a stable voltage during sunlight and eclipse.

The solar array regulator keeps the bus voltage constant in sunlight, while the battery discharge regulator retains constant voltage on the bus during eclipse instead of using switches or discharge diodes.

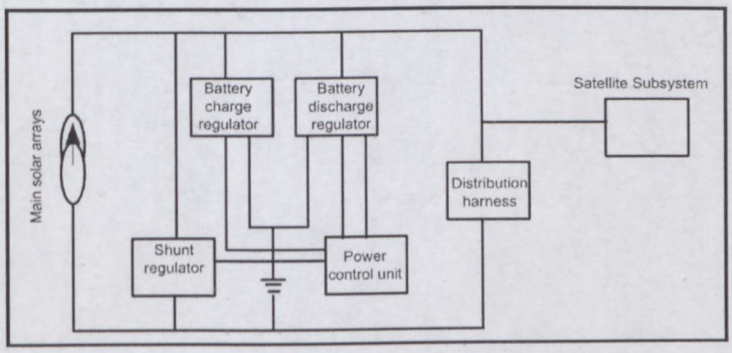

Figure 5.2 Regulated bus block diagram

(Adapted from Noble, 1990)

The disadvantage of using a regulated bus is the increase in hardware ,which normally leads to low efficiency due to battery discharge regulator and a high thermal dissipation.

5.2.3 SUNLIGHT REGULATED BUS

In a sunlight regulated bus system, when the array power that is available is more than the bus load power during insolation the system looks similar to a regulated bus. During eclipse when the load power is more than the solar array power, the system allows the bus to operate as an unregulated bus .The battery charge regulator replaces the switches as seen in Figure 5.3. The solar array regulator maintains the control unit and is dissipated while keeping array voltages at fixed value with the diagram represented below (Sullivan, 1989).

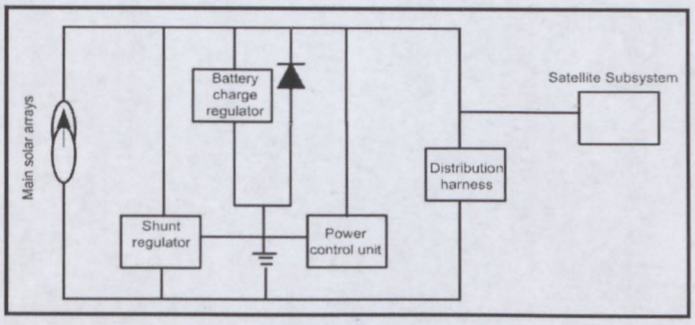

Figure 5.3 Sunlight regulated bus block diagram

(Adapted from Noble, 1990)

When hardware requirements and complexity increase, voltage variations are reduced. The main disadvantage associated with sunlight regulated bus is similar to an unregulated bus where solar array output are clamped to stable conditions, which are less than the optimum.

Considering the merits of all these regulators, the unregulated bus system is the preferred choice for this design because it will makes the power system design simple. It also allows a wide range of voltages to be selected, whilst obtaining better power characteristics (O'Sullivan, 1994).

5.3 DIRECT CONNECTION TOPOLOGY

In direct connection topologies the power bus separates PV sources from the battery pack and the charger stage output. In these systems, maximum power delivered from the PV panels to the power bus is limited by the charger settings. This charge state is found between the PV source and the power bus.

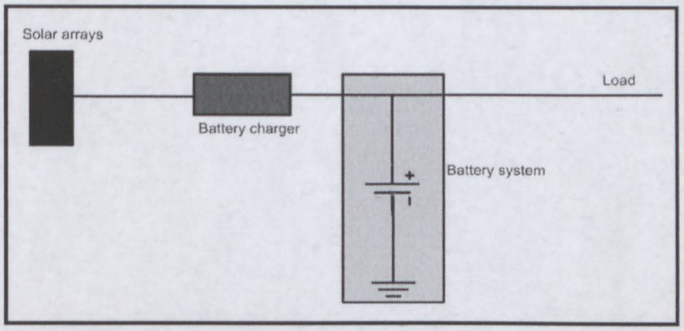

Figure 5.4 Direct connection topology (Adapted from Zhao, 2006)

ADVANTAGE OF DIRECT CONNECTION

- The highest efficiency is obtained in direct connection topologies where the system is powered by the battery all the time due to limitation of switches between battery and the system.
- Direct connection topology is simple and less expensive.
- The overall charge and system currents can be reduced to a desired value by adjusting the charge current limit to a certain value.
- Direct energy topologies are used to reduce the voltage variation of the system.

DISADVANTAGES

- If the current requirements of the system becomes high (but lower than the regulation current), the charging cycle remains constant, he nce the battery is always charged reducing its life time.
- The entire current regulation threshold is fixed because the system always demands some amount of current for which the battery may be fully charged and may lead to a longer charging time.
- If the battery voltage becomes depleted, that is al most dead or becomes short, the system voltage is clamped to the battery and would not be able to function when the PV is present (Zhao, 2006).

5.3.1 DIRECT ENERGY TRANSFER (DET) WITH BATTERY BUS

This topology has a simple power systems configuration due to its mass advantage. The system has a low mass because the solar array regulator interface does not contain an element of switch mode power supply. Although it looks attractive for nanosatellite power systems, economically it

is not desirable because battery coupling and solar arrays voltages directly require a larger solar surface area. This increases the cost in design and mass.

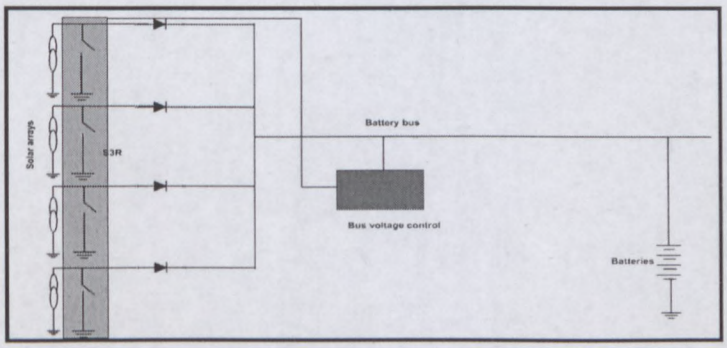

Figure 5.5 Direct energy transfer with battery bus

(Adapted from Clark and Kelvin, 2001)

The problem which is normally associated with this system is how to operate the solar panels to reach their maximum temperature and to fully charge the battery and also allow the solar arrays to maximize its performance. Under this situations the power is mostly not required for any other purpose because the characteristics of solar arrays normally changes with temperature, which is seen on body mounted arrays in Low Earth Orbit (LEO).

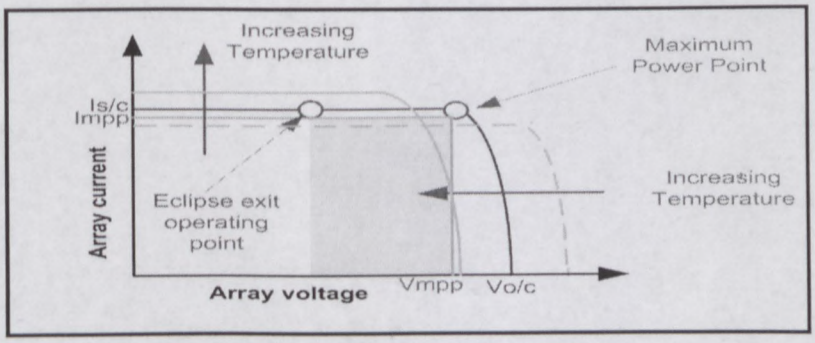

Figure 5.6 Solar characteristics

(Adapted from Clark and Mazarias, 2006).

When maximum power point voltage (VMPP) increases the solar panels cool and increases when it reheated. Conversely the maximum power point current (IMPP) is reduced as panels cool down and become reheated.

The combined effect means that only little of the power is utilized during sunlight. The voltage is clamped to the battery as the spacecraft leaves the eclipse with a cold array and a discharged battery.

The blue paint in the diagram above shows the excess power from the arrays when the battery voltage is low.

This topology displays gains in mass and volume, but these incorrectly produce efficient gains with only a diode drop loss. From the analysis above it is clear that this architecture is not suitable for use in most missions (Clark *et al.*, 2008).

5.3.2 DIRECT ENERGY TRANSFERE WITH REGULATED BUS

The desire of the European Space Agency (ESA) to exert its influence in the space sector has revolutionized one of the most commonly used topologies in spacecraft power systems known as the regulated bus. ESA has favoured its use in different forms over the years.

Below is a typical regulated bus topology, which integrates a sequential switching shunt regulator on the array interface. The topology is suitable in s pacecraft applications where prolonged sunlight is experienced, as well as eclipse (Clark and Mazarias, 2006).

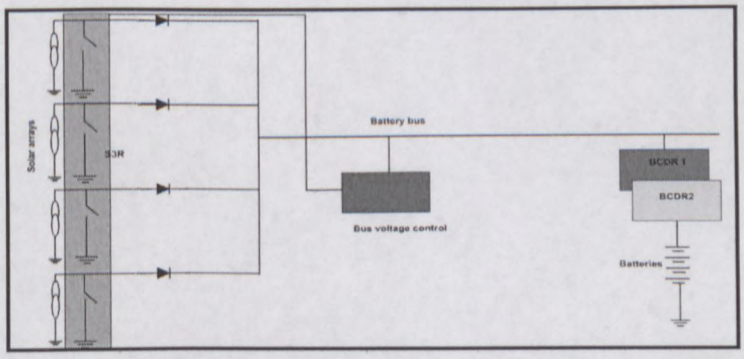

Figure 5.7 DET with regulated bus (Adapted from Clark, 2010)

The power source is directly connected to the bus from the solar arrays via blocking diodes. A typical regulated bus voltage during the sunlight period is between 28V or 50V by the S3R. During maximum power demand hours when power requirements are not met, the battery is made to supply power to the bus at 28V via the battery discharge regulator (BDR) (Clark and Kelvin, 2001).

According to Olsson (1998) the power system is more efficient than energy transfer to the bus in small satellites power systems from the solar arrays. The solar arrays are made to operate at their maximum temperature and close to the end of life for the solar cells to function at their maximum power point for a large part of the spacecraft's operation.

The power from the arrays will not be fully maximized if this system is implemented in LEO because the power system requires larger solar arrays than in the MPPT battery bus, but the solar arrays in GEO can be sized for the equilibrium array temperature so that a reasonable amount of array power is left on the panels.

Some difficulties normally arise when the power system is required to discharge battery through a regulator during eclipse by maintaining a condition where bus voltage is still regulated to fix voltage.

These problems are normally associated with these systems, especially for orbits where prolonged eclipse occurs.

5.3.3 MAXIMUM POWER POINT TRACKER WITH BATTERY BUS

This architecture is responsible for integrating the maximum power point between solar arrays and the battery. According to Denzinger (1995) and Clark (2010), the principle of operation is based on using the power from the solar arrays to charge the batteries and supply the bus during sunlight while adjusting the voltage arrays to maximum power point.

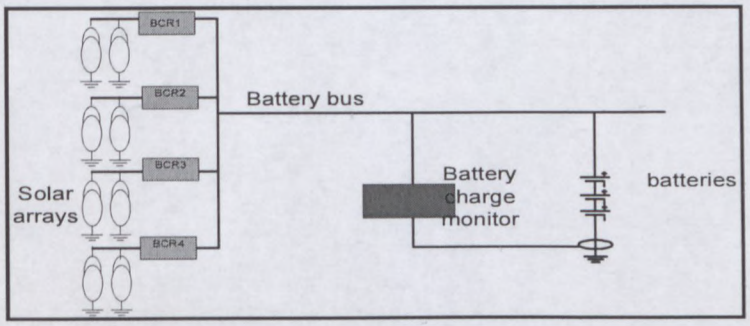

Figure 5.8 MPPT with battery bus (Adapted from Clark ,2010)

If the battery reaches its end of charge state, the MPPT sets the bus voltage at the end of charge voltage and permits current from the battery to automatically taper off to trickle the charge level by backing of the power simultaneously from the solar arrays. It does not require shunt regulator to remove excess power from the solar arrays due to arrays backing off. This process ensures maximization of solar arrays without neglecting inefficiencies, which are associated with MPPT with losses of about 5 -10% of arrays power occurring before it reaches the bus. The occurrence is due to the use of a buck switching converter in MPPT to reduce array voltage to bus voltage by using a control loop to track the maximum power point. The optimal performance of this converter is around 90-95% (Clark and Mazarias,2006).

The MPPT is most utilized in the process where the maximum power point (MPP) of the solar arrays changes considerably over a period of time due to the spacecraft in sunlight. This makes the topology most suitable in LEO where temperature and MPP changes significantly over the sunlight period in orbit. The stored energy at eclipse is transferred directly to the bus from the battery.

This process is very significant for spacecraft that experiences frequent or a long duration of eclipse in orbit (Clark *et al.*, 2008)

5.4 PATH SELECTION TOPOLOGY

In path selection Topology, the input power is split between the charger state and the bus. This is due to the switching network, which creates an independent path for the charger state and the power systems, though the PV is directly connected to the power bus.

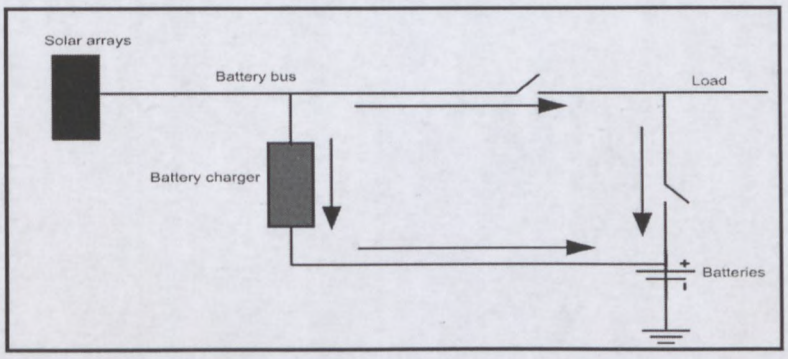

Figure 5.9 Path selection topology (Adapted from Zhao,2006)

Advantages

- It can withstand a high load current from the system.
- The systems load will not affect the operational performance of precharge, constant current fast charge and termination function.
- The systems load does not affect the battery charger because they are independent of each other.
- The battery supplies the systems load current when the input falls below the nominal voltage and the charger is disconnected, because the charger does not cycle between the charging and disconnection.
- This topology is immune to interference, especially low voltage, shorts, dead or depleted systems as long as the input power is on.
- The efficiency is higher than a direct energy transfer connection when the voltage difference between the input and the system exists.

Disadvantages

- This topology is quite complex and very expensive.
- It is less efficient when battery powers the system due to losses on the resistance of the switch that connects the battery and the system.
- It also has a higher system line voltage variation range.

After due considerations, the maximum power point tracker with a battery bus configuration is the preferred choice over all the power architectures due to the following advantages:

- Its flexibility permits different solar cell technologies and length of strings on each panel.
- During sunlight the changing thermal conditions ensure that the maximum power point of each panel is tracked. The panels may have different temperatures, hence different characteristics.
- A graceful degradation is included in the system design with loss of panels or MPPT.
- Maximum efficiency is obtained during eclipse because of the direct connection between the battery and the bus.

- The battery is charged during the sunlight period, hence additional losses through having a switch-mode power supply in series with the arrays, have little impact on the sunlight efficiency of the power system (Zhao, 2006).

5.5 DC-DC CONVERTER TOPOLOGIES

There are various converters that are used in spacecraft power system design to regulate and control voltages and current. These converters are analyzed and compared to determine, which should best be used under the most suitable circumstances. Selection of these converters for power system application has a major impact on both the efficiency and its effectiveness to power regulation and control. The converters are all considered in continuous conduction mode because it is simply to operate and control. The losses in the continuous mode are also very small as compared to discontinuous conduction mode. PSIM software was used as a simulation tool to display the input and output wave forms of various converters in Appendix B.

5.5.1 BUCK CONVERTER

The buck converter is basically used for stepping down high input voltage. This converter steps down voltages to the desired level. It is simply made up of two switches, a transistor, a diode and an inductor.

The diode is placed between the inductor and the transistor switch. A capacitor is then connected across the load in parallel to eliminate low dc output voltage ripples. As the current travels through the converter depending on the application, the converter operates efficiently above 90% due to a few components that are normally used for its design.

In continuous conduction mode, the steady state of a buck converter is represented by

$$V_o = DV_s \qquad (1)$$

where V_o represents voltage output;

V_s Represents the input voltage or source voltage; and

D also represents the duty ration of the system is pulse width modulation

$$\text{but} \Rightarrow (V_s - V_o)t_{on} = V_o(T_s - t_{on}) \quad (2)$$

T_S is the total switching time, t_{on} is the on switching time, t_{off} is the off switching time

With I_o, I_S being the output and input respectively.

$$T_s = t_{on} + t_{off}$$

$$\frac{V_o}{V_s} = \frac{t_{on}}{T_s} = D \quad (3)$$

Neglecting power losses with all circuit the elements, the input power P_s is equal to the out power P_o

$$\therefore P_s = P_o$$

$$V_s I_s = V_o I_o$$

$$V_o = DV_s \quad (4)$$

The corresponding circuit and the waveforms of the steady state operation is displayed below

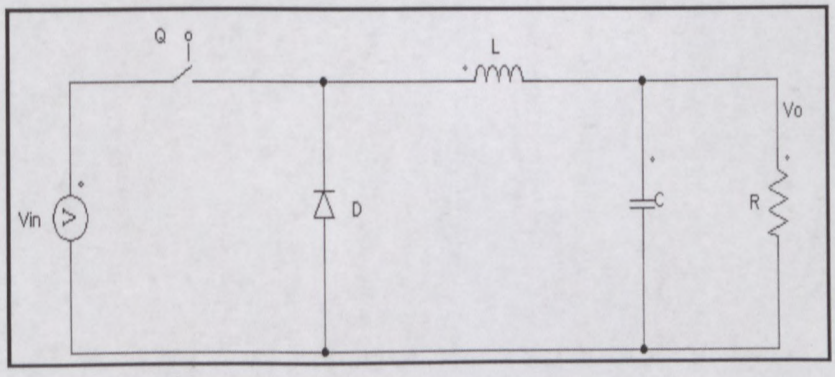

Figure 5.10 Buck converter circuit

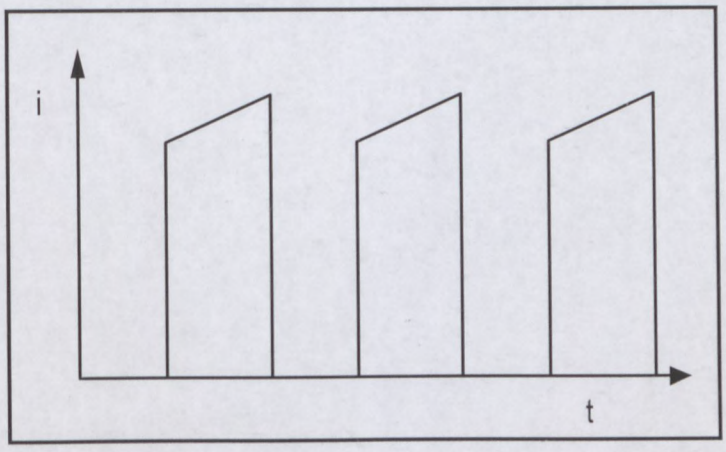

Figure 5.11 Typical buck converter input waveform

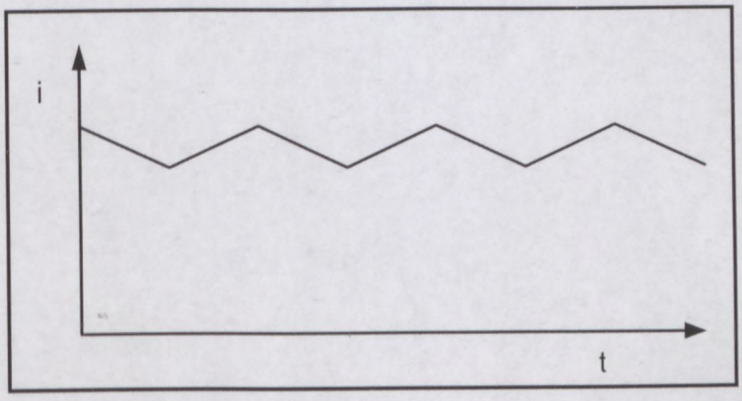

Figure 5.12 Typical buck converter output waveform

The buck converter topology performs efficiently if the output voltage is lower than the source and the photovoltaic arrays are connected in series and parallelly. The PV modules will be inefficient to produce power if these conditions are not meet.

One of the major drawbacks of the buck converter is the pulse input current. Therefore, additional input filtering is required to maintain the PV near MPP, and to eliminate this condition. The input filtering process may also introduce additional losses and stability concerns during the design.

5.5.2 BOOST CONVERTER

The concept of a boost converter is opposite to the buck converter. The components that are used are connected differently in order to step up voltage instead of stepping it down. The boost converter consists of a basic switch, diode, inductor and a capacitor. The boost converter always supplies higher output voltage than the input. In the steady state continuous conduction mode, the equation are represented by:

$$V_s t_{on} + (V_s - V_o) t_{off} = 0 \qquad (5)$$

Dividing through by T_s and rearranging

$$\frac{V_o}{V_s} = \frac{T_s}{t_{off}} = \frac{1}{1-D} \qquad (6)$$

Assuming in the circuit,

$$P_s = P_o$$

$$\therefore V_s I_s = V_o I_o \quad \text{and} \quad I_o = (1-D) I_s$$

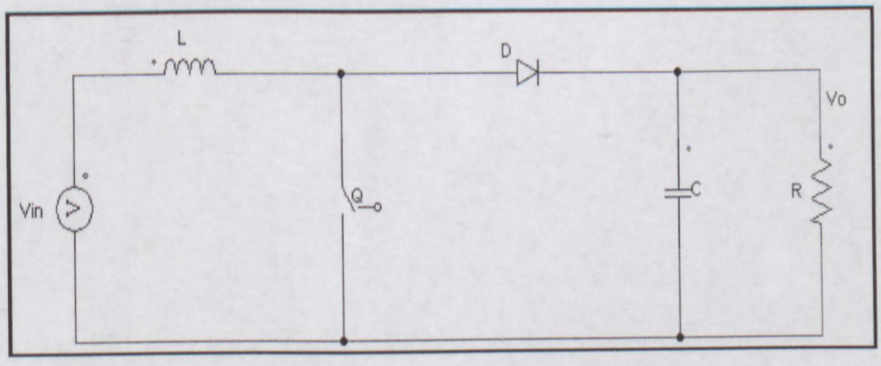

Figure 5.13 A boost converter circuit

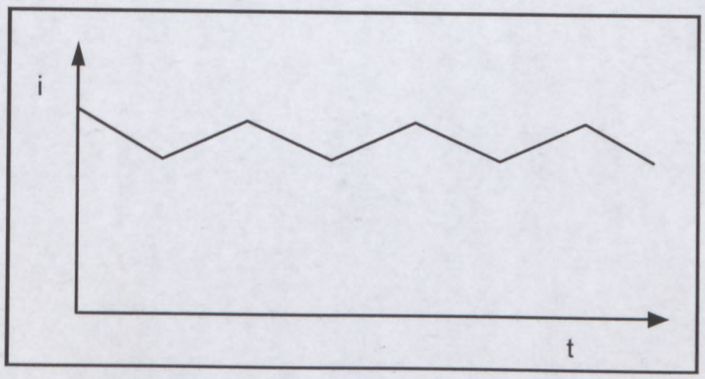

Figure 5.14 Typical boost converter input waveform

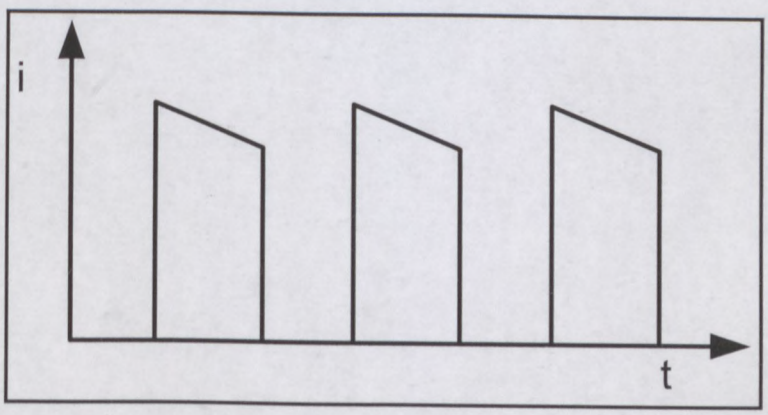

Figure 5.15 Typical boost converter output waveform

The boost converter output is controlled by adjusting the ration of time on/off. Since resistive components are not used here to dissipate extra power, the operating efficiency will range from 80 – 95%. This is good for battery operated devices, because it will maximize the operating time.

The boost converter has a pulse output current and a rippled input current, which reduces all extra input filtering and potentially adds extra requirements of output filtering.

5.5.3 BUCK- BOOST CONVERTER

The buck-boost converter was designed from a hybrid connection of the two main converters, namely the buck and the boost converter. The output voltage is inverted from the input voltage because this voltage can either be made higher or lower than the input voltage. The output voltage has a polarity that is opposite to the input. The cascaded nature of these converters makes it useful in photovoltaic application systems. It allows the converter to extract and maximize power from the PV modules, irrespective of the current level of isolation or battery charge state. In a steady state the output to input voltage conversion ratio of the cascaded converters are:

$$V_s DT_s + (-V_o)(1-D)T_s = 0 \qquad (7)$$

$$\frac{V_o}{V_s} = \frac{D}{1-D}$$

$$\therefore V_o = \frac{DV_S}{1-D} \qquad (8)$$

$$\frac{I_o}{I_s} = \frac{1-D}{D} \qquad (9)$$

Where D is the duty ratio of the converter. (Mohan *et al.*, 2003).

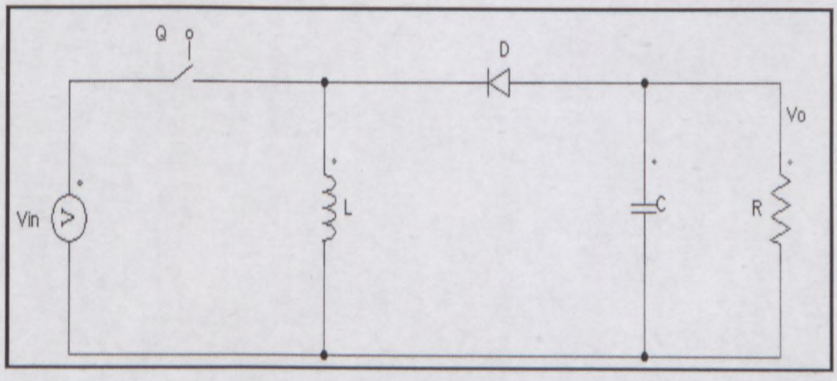

Figure 5.16 Buck-boost converter

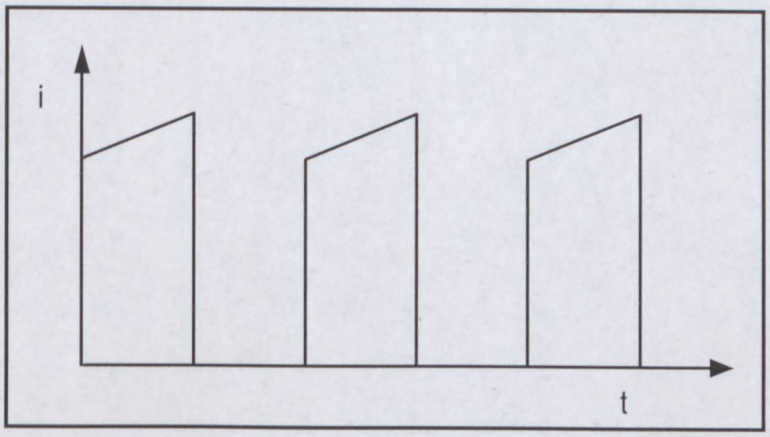

Figure 5.17 Typical buck-boost converter input waveform

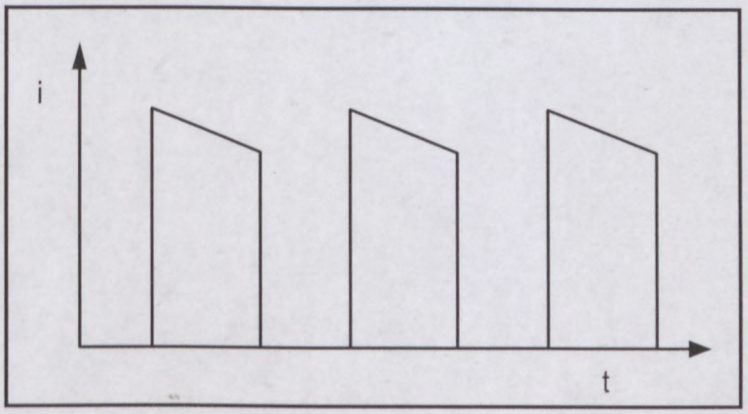

Figure 5.18 Typical buck-boost converter output waveform

The inverted output of this converter has no effect on the input source of PV modules, because they do not have a connection to the ground for effective operations. The negative side of the PV module is connected to the positive terminals of the battery. However, in a high voltage system safety will be an issue and care must be taken against shocks by leading access to the conductive part of PV cells with the voltage. Similarly, the buck–boost converter has a pulse input current like the buck converter. This means additional filtering at both the input and the output.

5.5.4 CUK CONVERTER

The CUK converter was named after Slobodan CUK at the California Institute of Technology. He used the duality principle in a buck-boost converter to manipulate a capacitor to act as a primary energy storage device instead of an inductor. The CUK converter DC transfer function has the same bearing as the buck-boost converter shown in equation 8 similarly as shown in equation 10 below

$$D = \frac{V_O + V_D}{V_S + V_O + V_D} \quad (10)$$

$$V_o = \frac{DV_S}{1-D} \quad (11)$$

$$L = \frac{I}{2} \bullet \frac{V_S D}{\Delta I_L f_S} \quad (12)$$

$$C = \frac{I_o D}{\Delta V f_S} \quad (13)$$

Where , f_S is the switching frequency , ΔV_o output ripple voltage, Δi_L ripple inductor current

L is the inductance and C is the capacitance.

This topology has its pulsing current occurring within the converter. But there are no current pulses at both the input and output of the converter. The use of integrated magnetics neutralizes the input or output current ripple that is normally transferred to the other side of the converter. The CUK converter is more efficient than the filtered buck-boost converter, and its capacitor normally experiences losses that are associated with current pulsing (Middlebrook and CUK, 1976).

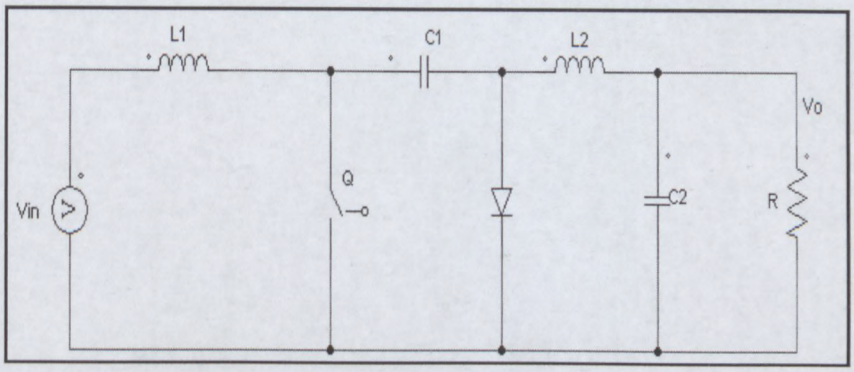

Figure 5.19 The CUK converter circuit diagram

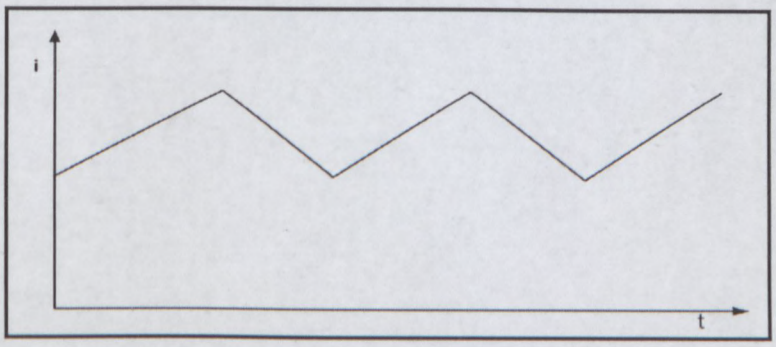

Figure 5.20 Typical CUK converter the input waveform

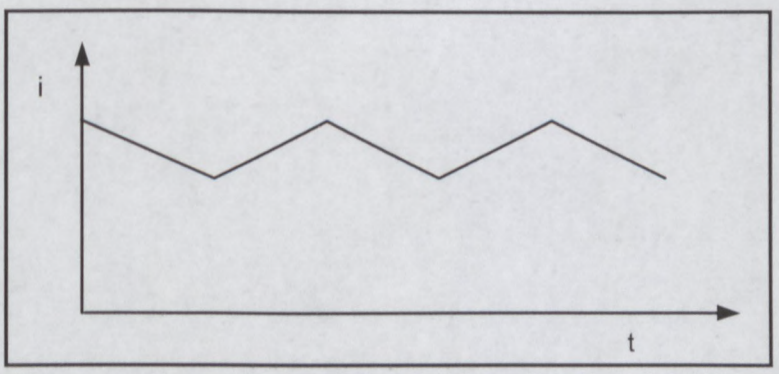

Figure 5.21 Typical CUK converter output waveform

5.5.5 SEPIC CONVERTER

The SEPIC converter is simply known as a Single Ended Primary Inductor Converter and is similar to the CUK converter. But the secondary inductor and the diode are interchanged to make the output polarity the same as the input polarity. It has significant advantages in a chosen application, because the negative input and output terminals of the converter are the same. However difficulties normally arise when reinstating the pulse current on the output (Middlebrook, 1976).

The steady state continuous conduction mode similar to CUK converter is made of the following equations

$$V_o = \frac{DV_S}{1-D} \qquad (14)$$

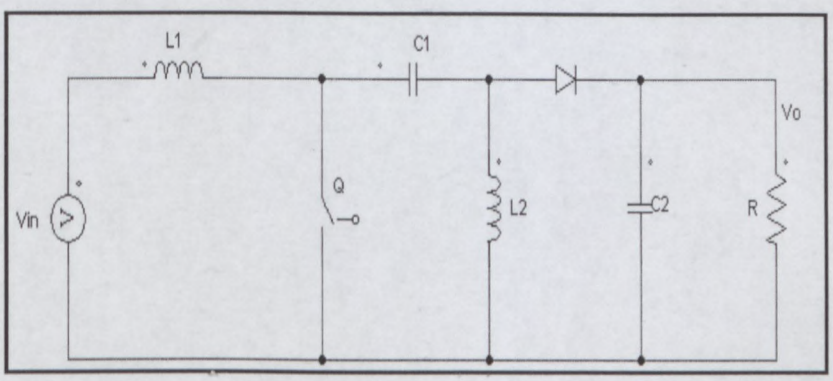

Figure 5.22 SEPIC converter circuit

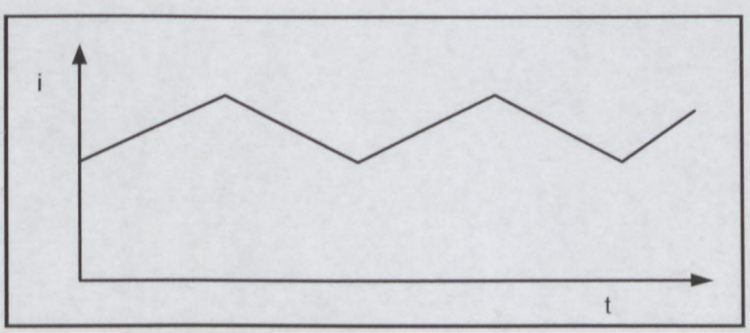

Figure 5.23 SEPIC converter input waveform

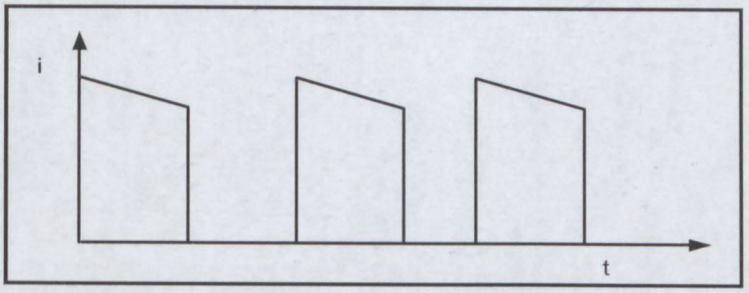

Figure 5.24 SEPIC converter output waveform

5.5.6 ZETA CONVERTER

The Zeta converter is a different version of the CUK converter with an interchanged input inductor and switch with a reversed output diode polarity. It has similar advantages as the SEPIC, but their input currents are pulsed instead of rippled. This topology needs a high side switch. The operational result is excellent when integrated with another converter like the buck-boost to produce negative and positive output rails (Cooper, 2008). In staedy state the Zeta converter with maximum efficiency in continuous conduction mode has the same property as the CUK converter represented by the following equations

$$D = \frac{V_o}{V_s + V_o} \qquad (15)$$

$$\frac{D}{1-D} = \frac{I_s}{I_o} = \frac{V_o}{V_s} \qquad (16)$$

$$\therefore V_o = \frac{DV_S}{1-D} \qquad (17)$$

Where I_s and I_o are the input current and output current respectively.

$$L = \frac{1}{2} \cdot \frac{V_S D}{\Delta I_L f_S} \qquad (18)$$

$$C = \frac{\Delta I \cdot V_S}{8 \Delta V f_S} \qquad (19)$$

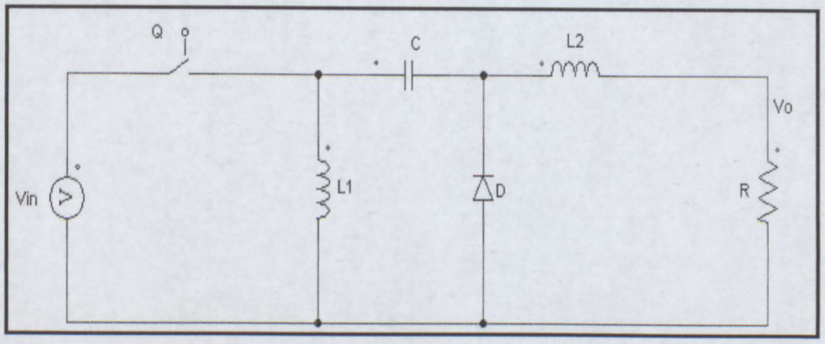

Figure 5.25 Zeta converter circuit

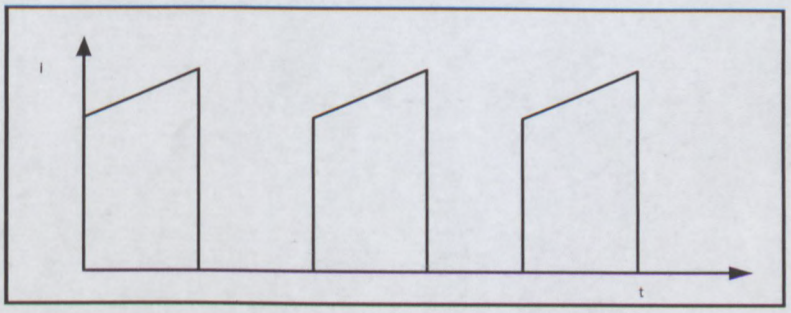

Figure 5.26 Zeta converter input waveform

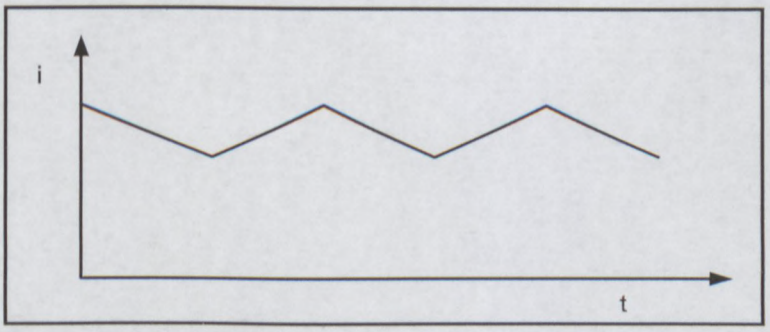

Figure 5.27 Zeta converter output waveform

5.5.7 COMPARISM OF THE CONVERTERS

It is quite perfect if there is an ideal situation where one of the topologies could be used in all applications to replace the others. This is not possible because each topology has its own advantages and disadvantages in a specific application.

The buck converter is considered as the most efficient of all the converter topologies. Since it basically reduces voltage, it becomes inefficient in the application where the source of power is lower than the load whose voltage is greater than the source. For this to be applicable in PV systems, the isolation and PV characteristics of V_{MPP} should be more than the load voltage all the time.

The PV may keep obtaining power as long as the load is smaller than V_{OC} and higher than the sink voltage and is efficient in the utilization of the PV arrays.

Since the objectives of this topology are to maximize efficiency, it is desirable to ensure that PV voltages are much higher than the output storage voltage. An example is when charging a 12V parallel array battery from 28V solar arrays or PV arrays.

The boost converter is also as efficient as the buck converter with some reverse limitations compared to the buck converter, especially when the boost converter output voltage is higher than the input voltage. One of the advantages of a boost converter over a buck converter is that, regardless of whether the operating condition is met, the boost converter will still source power. Again, if pulse current could be received by storage medium, the desire for external filter is not needed to maximize efficiency and controllability.

Buck-boost and zeta topologies can be combined into a single circuit to produce a positive and negative rail. It is not important for optimization reasons drawn from the PV, because it is in design circuits. Both converters can withstand high and low voltage problems that are associated with buck and boost converter topologies. However, they are outperformed by CUK and SEPIC topologies, which are more efficient.

Similarly, the buck-boost and zeta topologies and the CUK and SEPIC topologies can effectively supply power to the loads regardless of how relative the input and output voltages are to each other. These make the topologies ideal when the PV arrays voltage changes or operates near the battery voltage.

The main criteria for choosing between any of the topologies are namely:

1. The SEPIC topology has both the input and output polarity as the same. It is not a technical requirement, but is mostly useful in special situation.
2. The sum of the input and output voltages in the CUK converter is across the primary energy transfer capacitor, but has differences between them in the SEPIC. The specific application determines, which one has value.
3. The SEPIC topology loses the trait of continuous output current due to the reversal polarity of the output component.

This study combined both the SEPIC and the buck converter for various stages of the converter applications as required. Simply because the converters are easy to operate, less expensive and efficient when applied in a specific case where it is required.

5.6 MAXIMUM POWER POINT (MPP)

The battery charge regulator terminals are connected directly to the solar arrays. Low voltage drop protection diodes are placed directly with the power lines from each panel to prevent power from illuminated panels from flowing into non-illuminated panels.

The solar panels used in space are exposed in orbit to a huge temperature variation more than any part of the subsystems (Zhifei *et al.*, 1999).

This means that the maximum power point (MPP) will vary largely over temperature range. Therefore, it is important that the MPP is tracked by the battery charge regulator to extract maximum power for the systems application. The BCR obtains the MPP of the solar panels by the temperature thermistor, which is placed in the holes of the solar panels substrate.

The thermistor is linearized to obtain accurate tracking of the maximum power point and during this process the array voltages are set to the maximum. A low power dc-dc buck converter is used in the battery charge regulator to step down array voltage to bus voltage using a control loop to track the maximum power point. Efficiency of this converter ranges between 90-95 % and its operation is based on the current mode of operation (Clark *et al.*, 2008).

5.7 BATTERY CHARGING

When the battery discharges, it means that the BCR operates in a current mode. In the process, the dc-dc buck converter is used in the BCR once again to track the maximum power point of

the solar arrays and direct it to charging the batteries to meet the power requirements. The BCR is used to indicate the end of charge (EOC) voltage of the battery.

It also insolates the battery from incoming current and maintains a constant voltage which leads to the voltage mode. The BCR constantly limits the incoming current from the battery until a trickle charge state is reached. Due to the progressive charge control, the battery is well protected against overcharge. This method ensures accurate end of charge (EOC) settings, which provide an excellent battery management. The battery's end of charge voltage is not directly proportional to the battery temperature. The BCR units are used to adjust the end of charge level by tracking battery temperature efficiently (Zhifei *et al.*, 1999).

5.8 SUMMARY

This chapter focused on summarizing the power management techniques adopted to analyse the stability conditions which are explained in the next chapter. Considerations were placed on various architecture that interfaces components and manage their functions. Various topologies were also analysed and the appropriate ones under the required conditions were selected for regulation and control of power on the bus. The power management techniques serve as the process to developing power stability on the bus in the next chapter.

CHAPTER 6

6 POWER DISTRIBUTION BUS

6.1 INTRODUCTION

The general function of the distribution unit is to provide a link from the power supply to the loads; eliminating all faults and providing effective protection to the power bus against excessive power demand and overload failures. The distribution system includes the power bus, switches and protection devices. The power bus is responsible for transferring voltages and current to meet various subsystem power requirements. It is considered as the backbone of the power system and the single point for electrical power flow from the generation point to the entire system.

The protection system detect, isolate and fix any fault, which occurs on the bus and the switches employ converters to condition power by switching between voltages and currents on the bus.

The power bus is connected to four main devices which comprise the following:

- The solar arrays responsible for primary power generation;
- Secondary power, which is obtained from batteries;
- Protection devices used to maintain bus voltage and current within specifications; and.
- The loads, which represent the entire subsystems.

The distribution bus is also connected to five designed branches; namely the array bus, battery bus and the three load busses.

There is a power conditioning system placed on the bus to convert the bus voltage to three voltage levels, namely 5V unregulated battery voltage and 3.3V regulated voltages respectively.

This chapter will focuses on using solid state controllers for protection, and the development of techniques to condition power and to evaluate bus characteristics by designing a circuit system to stabilize the bus for effective power supply to the subsystems during mission operations. Simulation and performance analysis is drawn from the behaviour of power on the bus when all the conditions that are proposed are implemented. The innovative aspect of this power bus is the modularity with which the plug and play interconnections of the power modules contribute to enhance its performance.

6.2 SOLID STATE POWER CONTROLLERS

Solid state power controllers comprise of semiconductor devices that are used to control power supplied to the loads. It undertakes supervisory and diagnostic activities to indentify overload conditions and to prevent shorts.

The most common SSPCs controllers that are available are the ac controller used for switching ac voltages, dc controllers responsible for switching dc voltages and ac to dc controllers for switching both ac and dc voltages. Some of the characteristics that are associated with these controllers include dropout voltage, input voltage, load voltage and maximum load current. The dropout voltage is applied to switch the system to the OFF state and the input voltage is applied across the input terminals to maintain the ON state across the output terminals. A set of voltage ranges at which SSPCs operate normally, is called load voltage.

The maximum uninterrupted current across the SSPCs output terminal under specific heat dissipation and ambient temperature is known as the load current. Other parameters include a number of input and output current ranges. The advantages of the SSPCs include analogue switching, high voltage isolation, instant trip protection, noise suppression, over current protection, overvoltage protection or reverse protection. It is immune to electromagnetic interference (EMI) tolerance and radiation hardened. The SSPCs also have in-built heat sink, internal snubbers, soft turn-on, thermal memory, true i^2t protection and visual indicators.

6.3 POWER CONDITIONING

Power conditioning is the process of incorporating SEPIC dc-dc converter to convert the unregulated bus voltage to a 5V and a regulated 3.3V, respectively. This module is equipped with protection features that play a significant role in keeping the satellite from anomalous operational modes (Underhill *et al.*, 1999).

The features are simply used to reduce the output current supply to an acceptable level by limiting the bus current and by protecting the power system from faults. One other feature is to maintain battery under-voltage safety tasks which typically run on the on-board computer (Bekhti and Sweeting, 2008).

The protection system in sunlight will immediately disable the output 5V and 3.3V converters respectively once the battery voltage reaches its minimum acceptable level. The protection system is responsible for turning on the switch, which controls the battery bus and reduces the consumption of power on the 3.3V and 5V buses (Underhill *et al.*, 1999). The built-in hysteresis allows the buses to recover operation if the battery voltage is restored to an acceptable level which prevents the battery from permanent damage. With a 1μF capacitor placed on the bus all the noise produced from the converters on the bus is eliminated.

6.4 POWER BUS CHARACTERISTICS

Due to the application of the unregulated bus system for this design, wide input voltages which vary between 12V–18V were selected. These variable voltages create good conditions for different devices with different output characteristics such as the MPPT which can be modelled as a constant current source or the battery, which can be considered as a constant voltage source. The voltage source was not chosen as a constant source because the rationale was to develop a modular and scalable system. This means that the devices should have the same output voltages which is quite difficult to obtain due to component degradation from radiation, which normally causes variation among the devices. These variations will produce difficult load balances between them because the device with the highest output voltage will supply the highest current. Load shearing becomes simple if we provide a high input and output resistance on every device connected to the bus. This resistance can be equated to a virtual 1Ω resistor to prevent power dissipation. The device can reduce high output current to obtain the lowest output voltage and support any devices that do not supply current to balance the generated power between multiple devices.

Between 13.5V - 14.5V the input and output current practically operates as a zero current source to prevent any of the devices from producing oscillation between the source or sink function due to the small variations in the voltage reference.

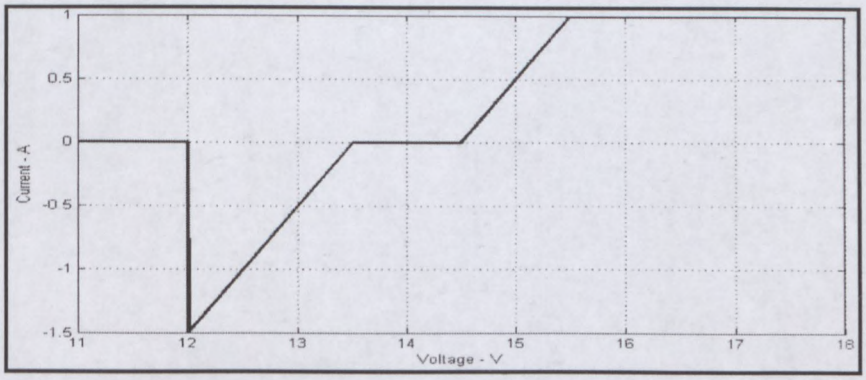

Figure 6.1 Bus characteristics

The bus characteristic in Figure 6.1 above displays the behaviour of current in a positive order when entering the device connected to the bus and in a negative order when leaving the device connected to the bus.

6.5 POWER BUS STABILITY

A system is said to be stable when power flow has been restored to a steady-state after unpredictable disturbances have occurred in the solar arrays, battery or load conditions in all operational states, temperatures, and orbital conditions over a mission design life. The maximum power point is when the controller is tasked to track the required input power from the solar arrays with an output that is normally uncontrolled. If the connected load is weak the voltage increases to maintain constant power output to keep the system stable and when the load is stronger, the voltages reduce which causes the system to draw current, which leads to instability and system collapse. Below in Figure 6.2 is a characteristic graph of an MPPT controller plotted for different power input. The graph shows a constant power curve which is clearly seen on the right side, as it saturates to solar cells maximum current on the left.

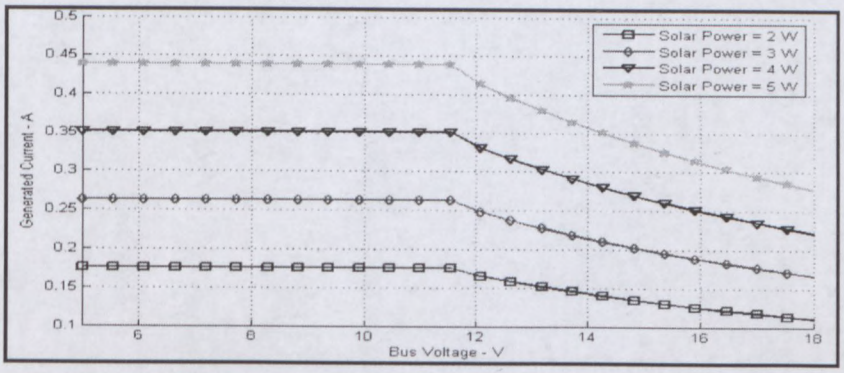

Figure 6.2 Output characteristics of MPPT at different power values

The switching converters connected to the power bus will act as loads, which means that it will possess an input hyperbolic characteristic, and with a coupling MPPT output characteristic can create problems. Figure 6.3 is an equivalent circuit which shows the MPPT output section on the left with its output resistance equivalent and the parasitic inductance and on the right is the DC-DC converter input. This is a second order circuit which represents stability for particular components, but dissipates a lot of power.

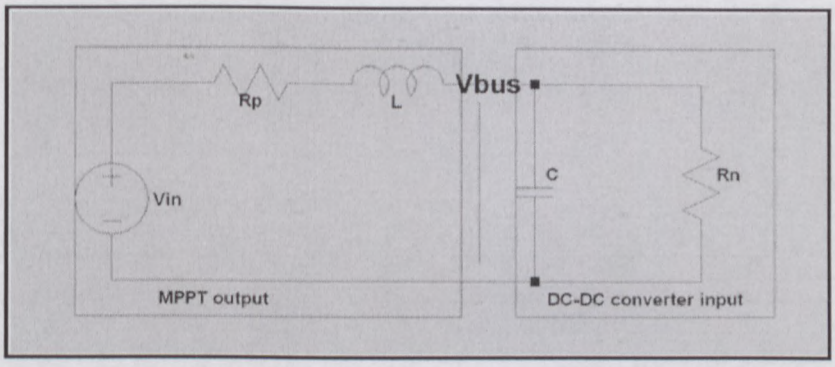

Figure 6.3 Power system stability circuit

The MPPT source to the V_{BUS} voltage is represented by the following transfer function

$$G = \frac{R_P}{s^2 CLR_P + s(CR_n R_P + L) + (R_n + R_P)} \quad (1)$$

where V_{BUS} is the bus voltage, R_N is the negative resistance, R_P is the resistor in series

C is the capacitance and the L is the inductance.

In order to achieve stability we need to arrange the poles on the left side of the complex plane, which requires the poles to be negative and positive.

The root s_1 and s_2 are part of the second order equation with the denominator and its properties being represented as:

$$s_1 s_2 = \frac{R_n + R_P}{CPR_P} > 0 \quad (2)$$

$$s_1 + s_2 = \frac{CR_n R_P + L}{CPR_P} > 0 \quad (3)$$

If we keep both roots positive and negative, the previous inequalities will produce a good result, which means that:

$$R_P < -R_n \quad (4)$$

$$C > -\frac{L}{R_P R_n} \quad (5)$$

In order to attain stability, a proper solution should be formulated. The first condition is to satisfy equation (4) which requires lowering R_P. This will not give us a good result because a lot of power will be required from the large surface area of the solar panel which will result in instability in sunlight conditions. Another way is to increase R_n to a reasonably higher positive state thereby removing any stability requirement.

When the switching converters that are used as loads posses a feed forward input, the output voltage can easily be controlled by using the input voltage, thus ensuring the voltage signal is modified to take information regarding the input current and hence creating a virtual positive input resistance.

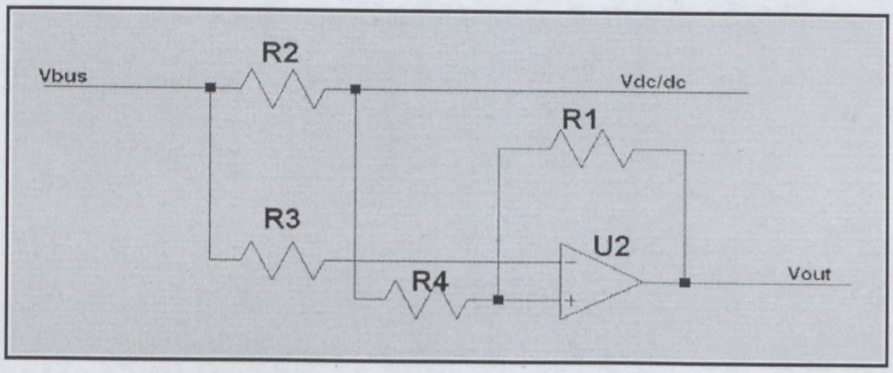

Figure 6.4 DC-DC converter input impedance control circuit

The voltage output has the following representation:

$$V_{OUT} = V_{BUS} - (V_{BUS} - V_{DC/DC}) = (1+k)V_{BUS} - kV_{DC/DC} \quad (6)$$

$$k = \frac{R_1}{R_3} \quad (7)$$

$$R_{eq} = R_2 k \quad (8)$$

$$R_4 = \frac{R_1 R_3}{R_1 + R_3} \quad (9)$$

From Figure 6.4 above R_2 acts as a bus current sensor which senses current to stimulate the input resistance. Due to power dissipation, the resistor must be small with an oper ational amplifier introduced to act as a resistance multiplier with a gain k while R_4 is used to compensate the amplifier bias current. This circuit allows Figure 6.6, which represents the battery charger impedance to rise positively to 15.5V with the negative resistance of bus voltages rising correspondingly. This circuit will not be stable because the input characteristics are resistive starting from 0V to the intersection between the resistive characteristics and the constant power characteristics. However, at 14V the circuit will start to draw current and the solution is to introduce a reference voltage to subtract the output so that the operational amplifier output voltage drops below zero. The temperature and charge status depend on the battery charge current as a result of the transition point.

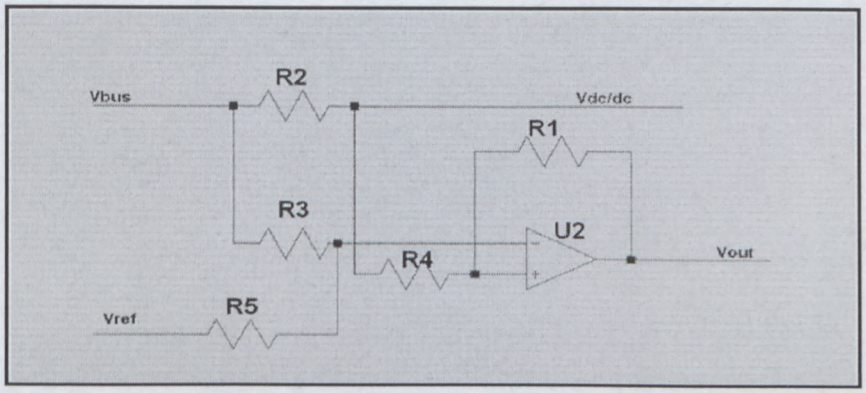

Figure 6.5 Input impedance Control circuit with a reference voltage

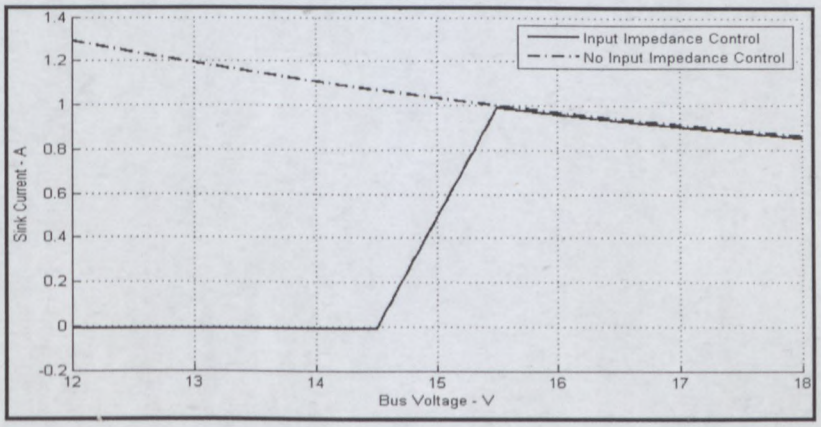

Figure 6.6 Input battery charger with and without input resistance control circuit

In order to improve and manage input impedance, the input current must be decreased with respect to the constant power source because when it is increased, losses are introduced, which is unacceptable. An increase in input resistance value is due to wide ranges of voltages that are selected, which also aids the generation of resistive characteristics with an input resistance of 1Ω which ranges from 14.5V -15.5V and has a maximum input current of 1A, producing a maximum battery charge current of 2A.

The bus stability is achieved when the load side has a positive input resistance for the previous region before the knee point, which depends on the battery charge current as the solar input power.

If the bus voltage passes the knee point, the characteristics is a composition of two hyperbolas, resulting in instability. The solar arrays and the batteries are now modelled as two constant power sources, one producing and the other sinking with a capacitor that models the bus.

In Figure 6.7 the circuit may be used to solve the following equations

$$\frac{dV_{BUS}}{dt} = \frac{I_1 - I_2}{C} \qquad (10)$$

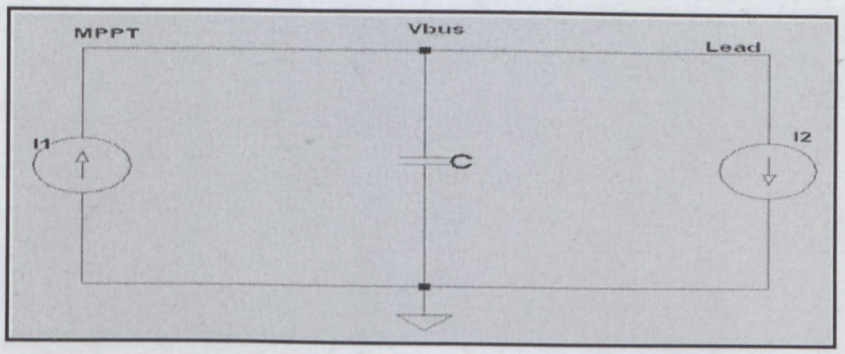

Figure 6.7 Equivalent bus circuit instability modelling region above load point voltages

When input power is greater than load power the voltage tends to rise steadily and falls when the load power is more than the input power. The last mentioned case has an issue regarding stability because voltage drop will retain the system back into a stable region. However, when the load power is more than the input power, the voltage will build up without limit. This can be controlled by using an over-voltage protection circuit with a positive input resistance to act as a load which has a very high intervention, as shown in Figure 6.8.

The bus characteristics have an unstable region between two stable points, resulting in oscillation across these points. This requires complex-conjugate poles within the transfer function, and because it is a first order circuit instability, it will be a regular occurrence.

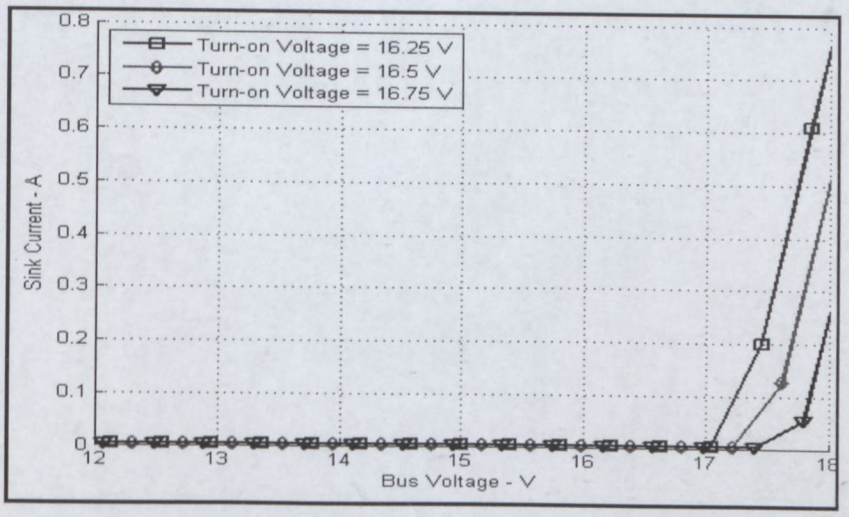

Figure 6.8 Voltages protection characteristics at different interventions

In the discharge mode the batteries become sources of power supply to the bus before feeding the loads and in the charge mode batteries store energy from the sun to maintain an efficient energy level. During the process of power supply the MPPT and the battery charger characteristics indicates that the bus voltage will rise higher than the charging threshold above 14V, resulting in stable current to charge the batteries. If the MPPT and the battery charger characteristics operate in the same way, the desired results will not be achieved and the only process is by modelling the voltage generator with resistors in series. This resistor is normally a virtual 1Ω resistor, which is effective for shearing load among multiple sources because of the low voltage, which means correspondingly high sources of current from other sources activated to supply in support of the loads. A real resistor cannot not be applied because it will cause power dissipation. Since dc-dc converters are responsible for charging and discharging the batteries, a similar principle was used to formulate the characteristic behaviour of a discharge battery circuit, as shown in Figure 6.9 below.

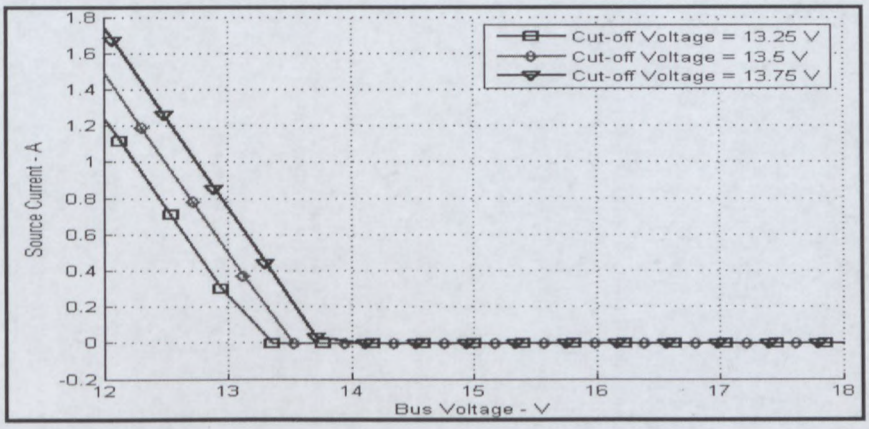

Figure 6.9 Characteristics of battery discharge circuit

Since the primary source of energy obtained from the solar arrays are always connected to the power bus, the input I/V characteristics can easily be obtained by slightly modifying the control loop output filter of the switching power regulators. Since unregulated bus system offers an opportunity for a wide variety of input voltage ranges, the nominal voltage is 14.5V although the operating voltage ranges between 12V -18V.

When nominal bus voltage is exceeded, it means that the solar arrays are receiving energy from sunlight and the sources of power are directly from the solar arrays which are also used to charge the batteries.

When the spacecraft is operating in sunlight, the primary source of power supply is the solar cells which are directly connected to the bus and as the satellite moves away from the sunlight into eclipse, nominal voltage obtained fr om the sun falls below 14V and the batteries are immediately activated as the main source of power supply to the bus. This is why when the bus voltage exceeds the nominal value, the batteries act as a load and recharges from the current that it receives during this process.

In order to reduce degradation and increase performance of the power system the On Board Computer (OBC) is tasked to select which batteries will be used as a power source and, which one should to be charged first on a priority bases.

However, charging and discharging depends on the rate at which bus voltage is maintained over time. The rate at which power flow in and out of the batteries depends on the loads connected to the bus.

The OBC can also be used to manage battery balancing usage, reconfiguration in case of fault and maintenance of battery conditions safety for emergency operations and decisions on which shunt resistors will be activated when needed.

In order to achieve a reliably long operational ability, average power that is generated must be greater than the power that is used. This will ensure that during sunlight the batteries are fully charged while the surpluses are absorbed by the shunt resistors.

Bus voltage has a hysteresis around 14V to avoid continuously turning the battery charger and discharger on and off. This protected area is used to prevent the process where one battery is used to charge another one, which results in power dissipation and increased battery degradation.

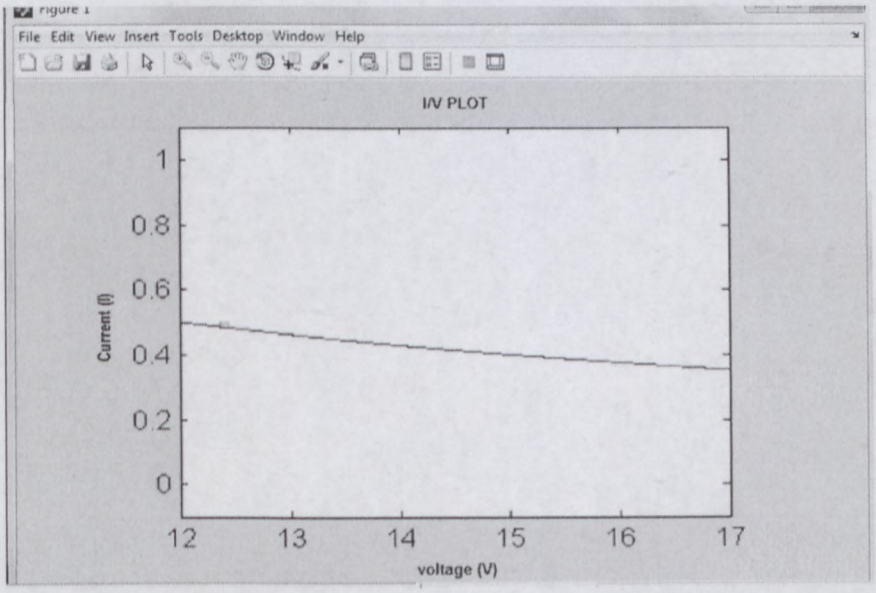

Figure 6.10 I/V characteristics of primary source (solar arrays)

In Figure 6.10 the source of energy from the solar cells produces a constant power characteristics source in sunlight where there is conversion of solar energy to electrical power. This constant power generated during sunlight depends on the level of illumination of the solar cells.

When the voltage that is generated is high the current that is produced is low and a low voltage results in high current output. All loads have their own characteristic and are expected only to sink power with any I/V characteristic or to sink no current when disabled.

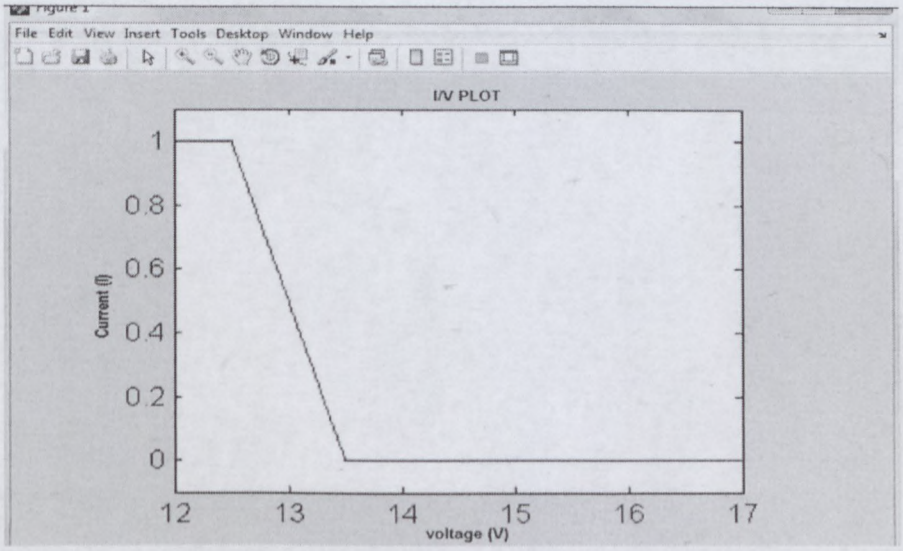

Figure 6.11 I/V characteristics of power storage (Battery sources)

When voltage on the bus falls considerably, the total current used by all active loads is more than the current , which is available from all the primary generation points.

As soon as the threshold reaches 13.5V the battery sources are immediately activated to begin to supply power with I /V characteristics as shown in Figure 6.11. Since the I axis is not absolute to the maximum current it can be sourced by the batteries. If the power that is required by the load rises high, the voltage will drop low, resulting in high current which is normally sourced by the batteries.

Each of the batteries may generate a different amount of current, depending on its capacity, yet all enabled batteries will source the same relative amount of current. Batteries, which have been made inactive or disabled will not source power and will not be operational or discharged.

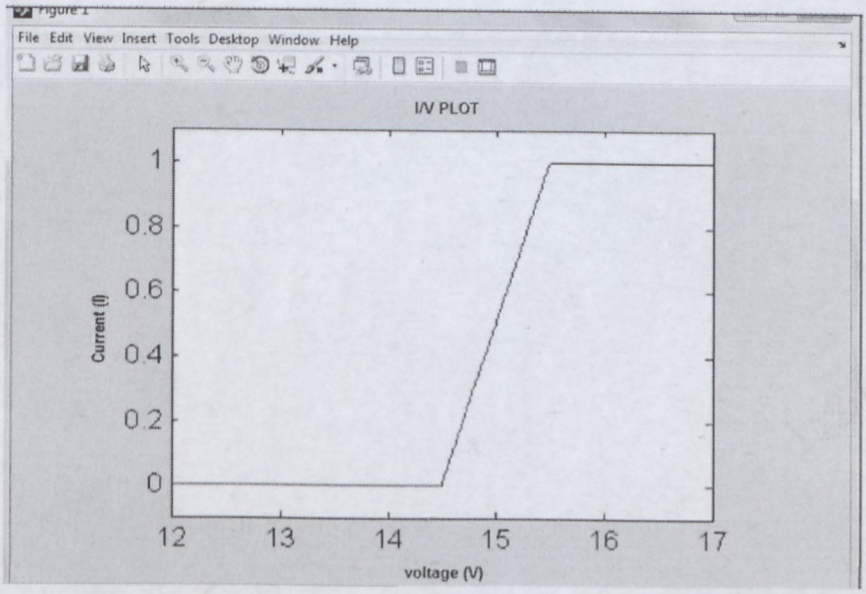

Figure 6.12 I/V characteristics of battery charging

However, if enough power from the primary source is generated than required by all active loads, the bus voltage increases and it reduces the sourced current by the battery to zero. Figure 6.12 shows that when the voltage rises immediately to 14.5V the batteries will be activated or called upon to start sinking current to charge and store energy.

Different amounts of current can be sunk by the battery depending on the charge level and all active batteries will share the same relative amount of current while batteries that are assigned lower priorities will increase the voltage to 15.5V in a way that power will be sunk when all batteries with higher priorities are not needed.

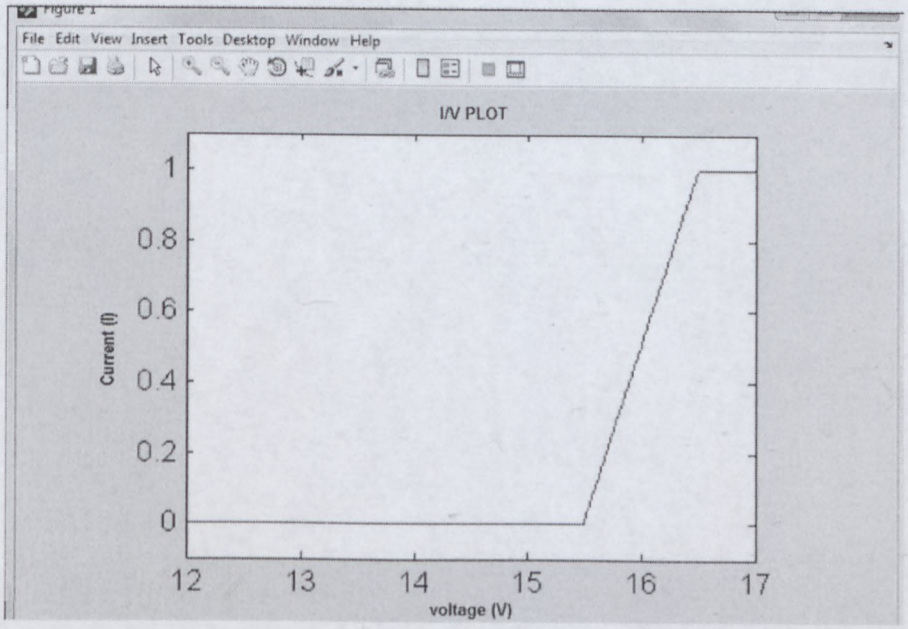

Figure 6.13 I/V characteristics of shunt resistors

The I/V characteristics above in Figure 6.13 show that when the power generated from the primary source has been sufficiently used by the loads and batteries, the excess power left may result in voltage increase. When it causes the voltage to reach 16.5V, shunt resistors are activated to sink the current and the bus voltage will level the power among the shunts. Overvoltage protection circuits are also activated to keep the bus voltage below 18V.

6.6 PERFORMANCE AND RESULTS

This simulation model has been implemented to verify the power bus stability and to evaluate the performance by using simulink model, taking into consideration solar power generated in a spinning satellite with batteries and variable loads. The simulink power bus model and the transient conditions that may occur on the bus due to instability are represented in Appendix A.

The model takes into account the primary power as a constant power source by using energy from the sun during orbit, which simulates the battery charging and discharging and energy storage process.

This system displays a stable condition and an effective response to load transient conditions. It also shows that the system has no critical fault and graceful performance degradation which show that effective fault tolerance techniques are used.

A constant power load and three other loads comprising the on-board computer (OBC), transceiver board and the payload used in the modelling process are summarized in the Table 6.1 below.

Table 6.1 Satellite load average and peak power

LOAD	PEAK POWER(W)	PERIODS(S)	NUMBER OF CYCLES	AVERAGE POWER (w)
1	0.5	4	200	0.036
2	5	5	1000	0.35
3	10	6	2600	0.5
TOTAL	15.5			0.886

Table 6.2 Power consumption in various cases

OPERATIONAL MODE	LOAD 1(W)	LOAD 2(W)	LOAD 3 (W)	TOTAL(W)
1	0.035	0.36	0.5	0.3
2	0.035	0.36	0.5	3.8
3	0.035	0.36	0.5	4.5

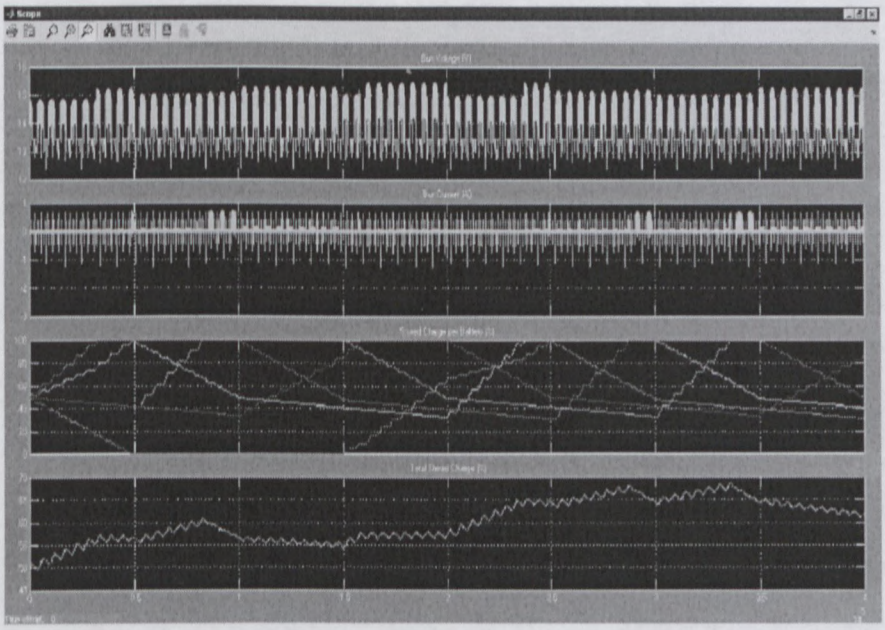

Figure 6.14 Power consumption at 3W

The simulation results in Figures 6.14, 6.15 and 6.16 display the behaviour of bus voltage, bus current, battery charging, battery discharging and the rate of battery storage, respectively on each of the plots. This process occurs when the satellite is in orbit during sunlight where the solar panels are the primary source of power supply and in eclipse where the batteries after storage become the source of supply.

Although stability of the bus is expected at a nominal voltage of 14.5V when the satellite orbits during sunlight, the unregulated bus allows stability at varying input voltages of 13.5V – 15.5V on the bus, which enhances performance of the system. Below 13.5V is considered under voltage and above 15.5V is considered overvoltage. These conditions on the bus will immediately activate the bus protection circuit to isolate the bus for protection until enough voltage is restored for operation.

The stable flow of current shown on the bus corresponds to the voltage stability condition shown above. The trend on the bus displays both negative and positive peaks. The negative peaks represents the load power consumption of the satellite, while the positive peaks shows a stable flow of current from the bus to the loads.

The last two simulations display an interesting observation regarding the battery charge and discharge state and total rate of stored charge.

Two charging trends can be observed from those plots, namely a fast charging trend, which occurs due to one battery charging at a time and another moderate one taking place when two of the batteries are charging at the same time, since a single battery cannot draw all the available power during sunlight.

Discharge conditions of the battery can be seen in the opposite direction to the charging trends as displayed on the plot. In a similar way a fast discharging trend occurs when one of the batteries selected is used to power the electronics, while the moderate discharge trend occurs due to self–discharge by the battery during eclipse.

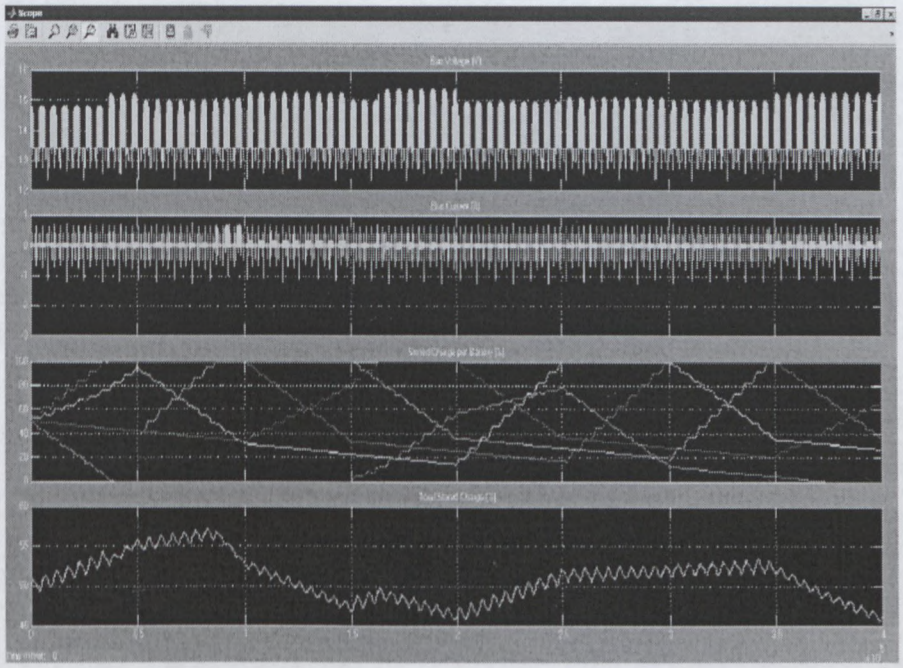

Figure 6.15 Power consumption at 3.8W

The maximum power extracted from the solar panels at input power is 5W, and the power required for normal operations of the satellite is 3W, as shown in Table 6.2 where the satellite operates at the required power range. The internal power consumption consistently stores energy at the required rate. Figure 6.14 displays a steady level at which the storage system stores energy over time to achieve stable performance. It shows that the satellite will operate safely during eclipse where the storage system becomes the source of supply. The total average charge that is stored is not consistent or steady, as expected in Figure 6.15 even though the storage rate still goes above 50%. The power budget in this process is narrow which makes the battery charging and discharging principle quite a complex task because when it comes to battery, efficiency and performance are important to eliminate power dissipation and over charging.

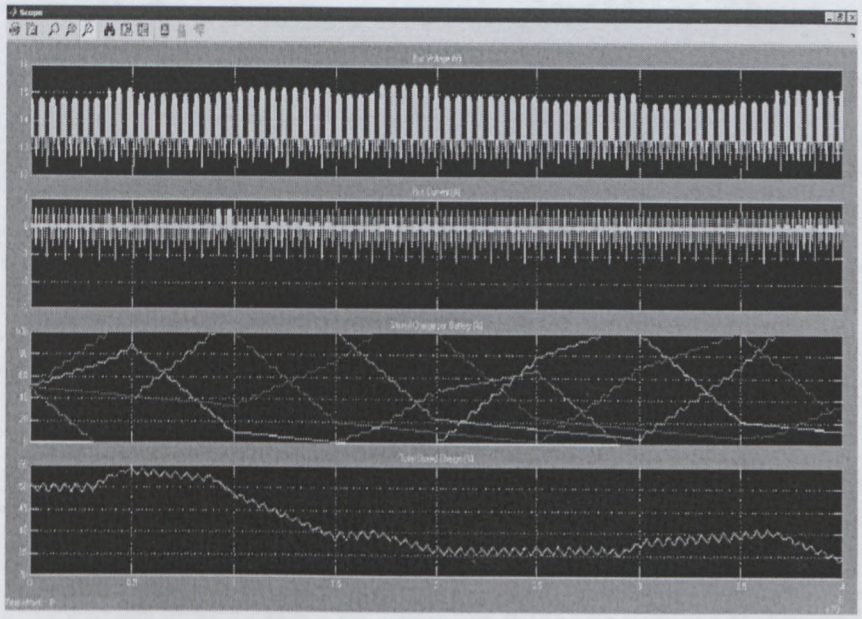

Figure 6.16 Power consumption at 4.5W

In the final stage the storage system looks critical because the power budget ratio has almost the same ratio of 1:1 where it is 4.5W against 5W. The power storage process will gradually degrade itself, and if measures are not established, losses will occure because the safety margin is narrow. The storage process is initially consistent and slowly degrades over a period of time as shown in Figure 6.16.

This simulation shows the safe operational mode of the power system and the stability state of the bus in this worst case scenario.

6.7 SUMMARY

This chapter demonstrated a simple approach to power stability on the bus by using circuit analysis. MATLAB/Simulink software was used to formulate the characteristics of the components, which coordinate to improve the power distribution bus.

The simulation results represent the performance analysis of the modelled system in orbit.

CHAPTER 7

7 CONCLUSION

This research demonstrated a simple and efficient way of maintaining stability of power on the bus in a scalable and flexible nanosatellite power system.

The general overview of satellite power systems set the basis for developing nanosatellite power systems.

Therefore, various technologies for power generation and storage were extensively discussed. The most preferred, reliable and cost effective technologies for power supply during sunlight and eclipse were GaAs multi-junction solar cells and lithium ion polymer batteries. Implementation of these technologies serve as an effective means of power production.

In view of reducing size, mass and optimizing the operations of various power system components to ensure reliability, the basic blocks of the power systems were analyzed to evaluate their performance. The steps to size the components, reduce mass and maintain reliability were also established.

The DET MPPT architecture was proposed to manage the power generated for distribution. In this design it was used to demonstrate that, it out-performs all available DET architectures, which are mostly used in nanosatellite platforms. The architecture has demonstrated its ability to operate effectively in sunlight, maximizing power under illumination conditions and changing illumination intensities during eclipse periods. The architecture promotes the extraction of maximum power from solar arrays, which is used to charge the batteries accordingly during sunlight. Other power management techniques that were implemented were also used to reduce power dissipation and to eliminate component heating for the devices used on the bus. State-of the-art switch mode dc-dc converters were extensively discussed and evaluated, with the most useful one under the given condition selected for implementation.

The reason for using these power system components was to achieve stability on the bus by digitally controlling the power stages with high performance regulation and control of the devices.

Finally, this work presents circuit analysis and modelling of the power distribution bus. The Matlab/Simulink software package was used as a tool to establish stability conditions on the bus and thus displays the characteristics of battery and solar arrays in sunlight. This software was

used to implement models of the subsystems by combining it with all power system units and their interconnectors to the subsystems.

The modelling tool was used successfully to analyse the stability conditions on the power distribution bus. The dynamic power conditioning technique that was implemented was used to effectively maintain a stable power supply between the main supply unit and the entire system. The design proposed has a lot of advantages because it reduces components count, overall mass and size.

7.1 RECOMMENDATIONS

The analysis tools developed in this research can be improved and further developed for application in large satellite power systems. Future nanosatellite power system design considerations may focus on new technologies and their configurations with already existing ones. This will allow power system developers to extend their innovations to maximise efficiency in power systems design. Some of the features that are most difficult to engineers are scenarios where cost and time for design and implementation occur in the shortest possible time.

The system's reliability is based on the component manufacturer and subsystems technology choices. Therefore, reliability measures could be implemented to distinguish effectively between reliable and unreliable ones.

Component protection and stability analysis were measures that were implemented against single point failures based on the systems architecture design. Therefore, a dynamic and rugged redundancy technique can be developed to protect the system from future mission failures.

8 REFERENCES

Abe Seiya, Hirokawa Masahiko, Zaitsu Toshiyuki, and Ninomiya Tamotsu. 2007. Stability Design for On-Board Distributed Power System. Electronics and Communications, Japan, Part 1, 90(7),18 July.

Agrawal, N. Brij. 1986. *Design of Geosynchronous Spacecraft*. Englewood Cliffs: Prentice-Hall.

Akagi, M. Justin. 2006. Power generation and distribution system design for the leonidas cubesat network. University of Hawaii at Manoa Honolulu, HI 96822 [February 2010].

Alfonso, martin manuel, Rueda, Pablo.1998. Limitations fully regulated power buses as specified today & impacts on users power conditioning. *Proceedings of the fifth European space power conference*, Tarragona, Spain, 21-25 September, ESA SP-146.

AL-ATRASH, J. HUSSAM. 2007. integrated topologies and digital control for satellite power management and distribution systems. Master's thesis, University of Central Florida Orlando, Florida [March 2010].

Alcindor Peter and Clark, S. Craig. *2005*. Non-Sequential Power Bus for LEO Applications. *7th European Space Power Conference*, 9- 13 May 2005, Italy.

Anderson, Eric, Dohan, Chris and Sikora, Aaron. 2003. Solar Panel Peak Power Tracking System. Worcester Polytechnic Institute, Worcester, Major Qualifying Project MQP-SJB-1A03, [January 2011].

Asif, Samina. 2008. Evolutionary computation based multi-objective design search and Optimization of spacecraft electrical power subsystems. PhD thesis, University of Glasgow [Online May 2011].

Bekhati, Mohammed and sweeting, M N. 2008. Power system design and in orbit performance of Algeria's first micro satellite Alsat-1. *Electric power systems research*,78:1175-1180, January 31.

Blocke, J. Allen, Litton, Chance, Hall, Jason, and Romano, Marcello. 2008. TINYSCOPE:The Feasibility of a 3–Axis Stabilitzed Earth Imaging Cubesat from LEO. In *AIAA/USU Conference on Small Satellites*, Logan, p.10.

Blocker, J. Allen. 2008. TINYSCOPE: The Feasibility of a Tactically Useful, Three-Axis Stabilized, Earth-Imaging Nano-Satellite. Master's Thesis, Naval Postgraduate School, Monterey, [Accessed May 2010].

Bombardelli, Claudio, Menon, Carlo. 2008. Space power generation with a tether heat engine. *Acta Astronautica*, 63:348-356.

Bonin Robert Grant Raymond. 2009. Power system design, analysis, and power electronics implementation on generic nanosatellite bus (GNB) spacecraft. master's thesis, University of Toronto. [November 2010].

Bonin, G and Sinclair, D. 2009. BCDRv2 design documentation. *Tech. Rep. SFL-GNB-PWR-D004*, UTIAS Space Flight Laboratory.

Bonin, G., Sinclair, D and Zee, R E. 2009. Peak power tracking on a nanosatellite scale: The design and implementation of digital power electronics on the SFL Generic Nanosatellite Bus. *In Proceedings of the AIAA Conference on Small Satellites*, August.

Brandhorst, W. Henry Jr., O'Neill, J. Mark, E skenazi, Mike. 2003. Photovoltaic options for increased satellite power at low cost. *3rd World Conference on Photovoltaic Energy Conversion*, 11-18 May.

Brown, D Charles. 2002. *Element of Spacecraft Design.* AIAA Education Series.

Brogan, W. L.1985. *Modern Control Theory.* 2nd Ed. Englewood Cliffs, N.J :Prentice-Hall.

California Polytechnic State University -San Luis Obispo. 2009. CubeSat Community Web site. http://cubesat.atl.calpoly.edu/media/CDS_rev12.pdf, [April 2011].

California Polytechnic Institute State University of San Luis Obispo. 2009. CubeSat.org. http://www.cubesat.org/,[March 2010].

Capel, A & O'Sullivan, D. 1985. Influence of Bus Regulation on Telecommunication Spacecraft Power System and Distribution. *Proc. Power Electronics Specialist Conference*, ESA SP-230.

Caicedo, Christian, Dhar, Saurav , Ryan, Eamonn, Pertsovsky, Anna .2008. CubeSat Texas Power Subsystem. *Final Report*, The University of Texas at Dallas.

Chobotov, A. Vladimir. 2002. *Orbital Mechanics.* American Institute of Aeronautics and Astronautics, 3rd Ed., Reston: AIAA.

Clark, S. Craig, Hill, D Alan and Day, Martin. 1998. Commercial Nickel Cadmium Batteries for Space Use: A Proven Alternative for LEO Satellite Power Storage. Surrey Satellite Technology Ltd., *European Space Power Conference*, Tarragona, Spain 21-25 August 1998.

Clark ,S. Craig. 2010. An advanced electrical power system for cubesats. *Pestana Conference Centre – Funchal*, Madeira – Portugal 31 May – 4 June.

Clark, S. Craig, Hall, W. Kevin. 2001. Power system design and performance on the world's most advanced in-orbit nanosatellite. Surrey Satellite Technology Limited, Surrey Space Centre, University of Surrey, Guildford, Surrey, GU2 7XH, U.K.

Clark, S. Craig, Mazarias, Lopez Alejandro. 2006. Power system challenges for small satellite missions. Clyde Space Ltd., 6.01 Kelvin Campus, West of Scotland Science Park, Glasgow G20 0SP Scotland.

Clark, S. Craig, Mazarias, Lopez Alejandro, Kobayashi, Chisato, Nakasuka, Shinichi. 2008. The design of a power system for the Petsat modular small spacecraft bus. *Astro-Technology SOHLA Creation-Core 2102*, Aramoto-kita 50-5, Higashi-Osaka, Department of Aeronautics and Astronautics, University of Tokyo, Hongo 7-3-1, Bunkyo, Tokyo,

Clark, S. Craig, Stain, Andrew, Mazarias, Lopez Alejandro. 2008. High performance, very low cost power system for microspacecraft. Clyde Space Ltd, 1 Technology Terrace, Glasgow G20 0XA, Scotland.

Clark, S.Craig and Simon, Evelyn. 2007. Evaluation of Lithium polymer technology for small satellite application. *SSC07-X-9*, Technical paper.

Cloyd, J S.1997. A Status of the United States Air Force's More Electric Aircraft Initiative. *Proceedings of the 32nd Intersociety Energy Conversion Engineering Conference,* 681-686.

Corso, D D, Passerone, C, Reyneri, L M, Sanso`e, C., Borri, M., Speretta, S., and Tranchero M. 2007. Architecture of a Small Low-Cost Satellite. *10th Euromicro Conference on Digital System Design*, August, 428–431.

Cooper, Michael Sean. 2008. Control of a satellite based photovoltaic array for optimum power draw. Master's thesis,Worcester Polytechnic Institute,[March 2010].

Cornell University. 2002. http://www.mae.cornell.edu/cubesat/cube2002.html.[January 2011].

Cubesat Community Website. Available: http://cubesat.calpoly.edu.[March 2010].

Day, Alan Christopher. 2004. The Design of an Efficient, Elegant, and Cubic Pico-Satellite Electronics System. Master's thesis, California Polytechnic State University,[June 2010].

De Mello, F P, and Feltes, J W . 1996. Voltage Oscillatory Instability Caused by Induction Motor Loads. *IEEE Trans.*, PWRS-11, (3):1279-1285, August 1996

DeRusso, M P, Roy, R J and Close, M C.1965. *State Variables for Engineers.* New York: Wiley and Sons

Delft University of Technology, http://dutlsisa.lr.tudelft.nl/sis/index.html, [May, 2011].

Denzinger, W. 1995. Electrical Power Subsystem of Globalstar. *Daimler-Benz Aerospace – Dornier GmbH, Fourth European Space Power Conference*, Poitiers, France, 4-8 September.

Dorn, Jr., Tyrone, Lawrence. 2009. NPS-SCAT: Electrical Power System. Master's Thesis, Naval Postgraduate School, Monterey. [April 2010].

Dorf, R C.1967. *Modern Control Systems.* Addison-Wesley.

Ebale, G., Lamantia A., La bella, M. 2005. Power control system for the agile satellite. *Seventh European space power conference*, stresa, Italy, 9-13 May.

Elbuluk, M. E and Kankam, M. D. 1995. Motor Drive Technologies for the Power-by-Wire (PBW) Program: Options, Trends, and Tradeoffs. *Proceedings of the IEEE National Aerospace and Electronics Conference*, NAECON, 511-522.

Elden L. Edgar.2008. Power management system for a picosatellite. online Project report, Norwegian University of Science and Technology Trondheim,[may 2011].

Esram, T and Chapman, P. 2007. Comparison of photovoltaic array maximum power point tracking techniques. *In IEEE Transactions on Energy Conversion*, 22:439-449, June.

Evju, S. E. 2007. Fundamentals of grid connected photo-voltaic power electronic converter design. Master's Thesis, Norwegian University of Science & Technology, [May 2010].

Fortescue, Peter, Stark, John and Swinerd, Graham. 2003. *Spacecraft systems Engineering.* 3rd Ed. Sussex: John Wiley & Son

Femia, N, Petrone, G, Spagnuolo, Vitelli, M. 2004. Increasing the efficiency of P&O MPPT by converter dynamic matching. *IEEE International Symposium on Industrial Electronics*, 2:1017-1021.

Ghi, Ianzoni L, ESA Hall Effect Current Sensor, ESA Patent No. 186.

Gonzalez, Malberto and Antonio, Melo. 1999. Thermal Design. Photon 1.5 Final Design Report, University of Central Florida.

Hamill, C David and Krein, T Philip. 1999. A Zero Ripple Technique Applicable to Any DC Converter. *IEEE Power Electronics Specialists Conference*, 1165-1171

Hand, F Gregory. 1999. Intermediate Design and Analysis of the PANSAT Electrical Power Subsystem. Master's Thesis, Naval Postgraduate School, Monterey.

Halliday, David , Resnick, Robert and Walker, Jearl.1997. *Fundamentals of Physics*.5th ed. New York: John Wiley & Sons.

Heidt, Hank, Puig-Suari, Jordi, Moore, S Augustus , Nakasuka, Shinichi, and Twiggs, J Robert. 2001. CubeSat: A New Generation of Picosatellite for Education and Industry Low-Cost Space Experimentation. Logan, United States of America: American Institute of Aeronautics and Astronautics / Utah State University.

Hahn, W.1963. *Theory and Application of Liapunov's Direct Method*. Englewood Cliffs, N.J: Prentice-Hall

Hanrahan, Patrick .2009. TINYSCOPE Payload. Master's Thesis, Naval Postgraduate School, Monterey.

Hoyt, Robert, Slostad, Jeffrey, Twiggs, Robert. 2003. The *multi-application survivable tether(mast),* Tethers Unlimited, Inc.

Huynh, P. T and Cho, B. H. 1999. Design and analysis of a regulated peak power tracking system. *In IEEE Transactions on Aerospace and Electronic Systems*, 35 ed. January 1999.1

Hyder, Wiley et al. 2003. *Spacecraft power technologies,* London: Imperial College Press.

IEEE Committee Report. 1982. Proposed Terms and Definitions for Power System Stability. *IEEE Trans.*, PAS- 101(7):1894-1898, July.

Ippolito, Jr. Louis J. 2008. Satellite Communications Systems Engineering. John Wiley & Sons Ltd.

Jang, Sung-Soo, Kim, Sung-Hoon, Lee, Sang-Ryool, and Choi, Jaeho. 2010. Energy Balance and Power Performance Analysis for Satellite in Low Earth Orbit. *Journal of astronomy and space science*, 27(3):253-262.

Jeppesen,Thomas, Thomsen, Michael. 2001. Power supply for DTU's Cubesat. [July 2010].

Jeppesen, Thomas and Thomsen, Michael. 2002. DTU: Design of a Power Supply System for DTUsat, February[January,2011].

Jin Kim et al. 2007. Efficient Tandem Polymer Solar Cells Fabricated by All-Solution Processing.

Johnson et al. 1999. Nanosat Intelligent Power System Development. *Procs. of 2nd International Conference on Integrated Micro-Nanotechnology for Space Applications*, 2:475.

Kapat, Jay and Zhili, Hao. 1999. Photon II Spacecraft – Thermal Subsystem Design. Florida Space Institute.

Kassakian, J. G., Schlecht, M. F., Varghese, G. C. 1991. *Principles of Power Electronics.*New York: Addison-Wesley.

Kekez, D. 2007. Nanosatellite protocol (NSP), version 3. Tech. Rep. SFL-GNB-OBC-D001, UTIAS Space Flight Laboratory, September.

Krishnmurthy, Narayanan. 2008. Dynamic modelling of Cubesat project move. maters Thesis, available online],http://epubl.ltu.se/1653-0187/2008/080/LTU-PB-EX-08080-SE.pdf , [April 2010].

Larson, J. Wiley and Wertz, R. James. 1999. *Space Mission Analysis and Design*. London: Kluwer Academic Publishers.

Lacore, D. 1989. Analysis of Power Bus Topologies used in Telecommunication Satellites. *Proc. European Space Power Conference*, Madrid. ESA SP-294.

Litton, C. Chance. 200 9. TINYSCOPE: The Feasibility of a Tactically Useful Earth-Imaging Nanosatellite and a Prelimiary Design of the Optical Payload. Master's Thesis,Naval Postgraduate School, Monterey.

Levins, Dermot. 1991. Protection Concepts used In Spacecraft Power Systems. *Proceedings of the European Space Power Conference*, Florence, Italy, 2-6 September, ESA SP-320.

Louganski, P Konstantin.1999. Modelling and analysis of a dc power distribution system in 21st century airlifters. master's thesis, Virginia Polytechnic Institute and State University.

La Salle, J P and Lefschetz, S. 1961.*Stability by Lyapunov's Direct Method with Applications*. New York: Academic Press.

Letov, A M .1961. *Stability in Non-Linear Control Systems.*, Princeton, N.J: Princeton University Press.

Lasalle, J P. 1960. Some Extensions of Liapunov's Second Method. *IRE Trans.*, CT-7, p.520 December .

Macklin, W. J., Jarvis, C.R., Neat, R.J and Thakur, V.V. 1998.The development of lithium ion polymer battery for space power. *Proceeding of the fifth European space power conference,* Terragona, Spain, 21-25 September, ESA SP 416.

Maldonado, M. L., Shah, N. M., Cleek, K. J., Walia, P. S., Korba, G. 1996. Power Management and Distribution System for a More Electric Aircraft (MADMEL) – Program Status. *Proceedings of the 31st Intersociety Energy Conversion Engineering Conference*, 148-153.

Markvart, Tomas. 1994. *Solar Electricity,* John Wiley & Sons.

Mashiko, K. Susan. 2009. DOD Space Experiments Review Board. *Memorandum.*

Medley, A.1996. Artificial Intelligence for spacecraft fault diagnosis. M.Sc. Thesis, Cranfield University, Collage of Aeronautics, Aerospace Science.

Messenger, Roger, Ventre, Jerry. 2003. *Photovoltaic Systems Engineering.* New York: CRC Press.

Middlebrook, R. D. 1976. Input Filter Considerations in Design and Application of Switching Regulators. *IEEE Industry Applications Society Annual Meeting Proceedings*, 366-382.

Middlebrook, R. D and Ćuk, S. M, 1976. A General Unified Approach to Modelling Switching Converter Power Stages. *Proc. IEEE Power Electronics Specialists Conference*, 1976 Record

Mohan N., Undeland M. T., & Robbins P.W. *Power Electronics: Converters Applications, and Design*, 3rd edition.

Mohammed, I.H., Ahmed, N.H., Eliwa, E.A, Sabry, W., Mostafa, R. 1999. Innovative Design of a cubesattellite power distribution and control subsystem. *Online journal Electronic and Electrical Engineering*, 1:67-68, July.

Moshre, T. 1999. Conceptual Spacecraft Design Using a Genetic Algorithm Trade Selection Process. *Journal of Aircraft* , 200–208, January.

Mosher, T. 1998. Spacecraft Design Using a Genetic Algorithm Optimization Approach. *Proceedings of IEEE Aerospace Conference.*

Munteanu, Catalin Alexandadru. 2008-2009. *nanosat/cubesat constallation concept*, Master's Thesis, Lulea University of Technology.

NASA site, *http://www.jsc.nasa.gov/bu2/about.html,* [Augest, 2011].

NASA site, *http://nmp-techval-reports.jpl.nasa.gov/, [December* 2010].

NASA site, *http://www.jpl.nasa.gov/basics/bsf15-1.html,* [June, 2010].

NASA site, *http://space-power.grc.nasa.gov/ppo/publications/index.html*, [February, 2010].

NASA site, *http://wwwaig.jpl.nasa.gov/public/mls/onboard/onboard_home.html,* [April 2010]

NASA document, *http://is.arc.nasa.gov/AR/ASEA/ASEA.html*,[June 2010].

NASA document, http://science.nasa.gov/headlines/y2001/ast13nov_1sidebar.htm, [August 2010].

Nobel,Lynn Michael. 1990. Preliminary design of the Pansat electrical power system. Masters thesis, naval post graduate school, Monterey, California ,[June 2010].

Nugent, Ryan, Munakata, Riki, Chin, Alexandra, Coelho, Roland jr., Puig-Suari, Jordi. 2008. The picosatellite standard for research and Education. *AIAA document*, Aerospace Engineering Department California Polytechnic State University.

Obland, Michael, Klumpar, M. David, Kim, S ean, Hunyadi, George, Jepsen, Steve, Larsen, Brian. 2002. Power subsystem design for the Montana Earth orbiting pico-explorer(MEROPE) Cubesat-class satellite. *IEEEAC paper No.197.*

Ocean Server Technology, Inc. 2008. http://www.ocean-server.com/aboutus.html,[September 2010.]

Olsson, Dan. 1998. The 100 volts power bus-more than a higher voltage. *Proceedings of the fifth European space power conferenc*e, Tarragona, Spain, 21-25 September, ESA SP-146.

Olsson, Dan. 1993. A Power System Design for a Microsatellite. ESA/ESTEC, *European Space Power Conference,* Graz, Austria, 23-27 August, pp351-356.

Ortiona, Christopher J. 2009. Systems Level Engineering of Advanced Experimental Nanosatellites. Master's Thesis, Naval Postgraduate School, Monterey.[February 2010].

Orr, N. 2007. Development and testing of the power and software subsystems for the Canadian advanced nanospace experiment. Master's thesis, University of Toronto, [August 2010].

O'Sullivan, D & Weinberg, A. 1977. The Sequential Switching Shunt Regulator (S^3R). *Proc. Spacecraft Power Conditioning Seminar*, ESA SP- 126.

O'Sullivan, D., Spruyt, H & Crausaz, A. 1988. PWM Conductance Control. *Proc. 1EEE Power Electronics Specialist Conference.*

O'Sullivan, D.1994. Space Power Electronics Design Drivers. *Power and* energy *Conversion Division*, ESTEC, Noordwijk, The Netherlands.

Polaschegg, Mario. 2005. Study of a Cube-Sat Mission. Master's Thesis, www./physik.unigraz.at/spacesciences/files/ULG_II_Master_Thesis_Polaschegg.pdf [Feburary, 2010] .

Pradhan, D. K. 1996. *Fault-Tolerant Computer Syste Design*. Englewood Cliffs, NJ: Prentice Hall.

Ramamurthy, Anand. 2009. Flexible Digital Electrical Power System Design and Modeling for Small Satellites, Master's thesis, online, http://classic.wolfware.ncsu.edu/courses/ece480/lec/001/CubeSatMS_Thesis.pdf [January 2010].

Ramamurthy, A., Bhattacharya, S. 2008. Optimized digital maximum power point tracking implementation for satellites. *In IEEE 30th international Telecommunications Energy Conference*, September 2008, 1-5.

Reyneri, M. Leonardo, Speretta, Stefano, Corso, Del Dante. 2009. Redundant Power bus for distributed power management for modular satellite. journal, international Astronautical federation.

Rossberg, Felix. 2008. Simulation of the Deployment and Orbit Operations of the NPS-SCAT CubeSat. Master's Thesis, Naval Postgraduate School, Monterey.

Sarafin, Thomas P.1995. *Spacecraft Structures and Mechanisms*. Boston: Kluwer Academic Publishers.

Sandia National Laboratory: http://photovoltaics.sandia.gov/docs/PVFSCGallium_Arsenide_Solar_Cells.htm

Sable, M. D, Cho, B. H and Lee, F. C.1992. Spacecraft Power System Compatibility and Stability for the NASA EOS Satellite. *Proceedings of the Intersociety Energy Conversion Engineering Conference*.

Sayani, M. P, Wanes, J. 2003. Analyzing and determining optimum on-board power architectures for 48V-inputsystems. *IEEE Applied Power Electronics Conference (APEC)*.

Shannon, Derek, Singh-Derewa, Chrishma, Jayaram, Sanjay. 1999. The Florida Space institute's photon satellite bus. *SSC99 technical paper No.4*, 19 June.

Sharps, P.R., Stan, M., Gray, A., Ley, V., Newman, F., Clevenger B., Hills J., Griego C., Doman J., Sandoval A., and Fatemi N. 2007. Reaching the 30% Efficiency Level for Multi-junction Space Solar Cells. *presented at the Space Power Workshop*, April. 2007.

Skvarenina, T. L., Pekarek, S., Wasynczuk, O., Krause, P. C. 1996. Simulation of a More-Electric Aircraft Power System Using an Automated State Model Approach. *Proceedings of the Intersociety Energy Conversion Engineering Conference*, 133-136.

Smith, R. A., Van Horn, H. J. 1997. The J/IST of Improving JSF. *Aerospace America*: 20-22, November.

Speretta, Stefano, Reyneri, M. Leonardo, Sanso´e, Claudio, Tranchero, Maurizio, Corso, Del Dante. 2007. modular architecture for satellites. *58th International Astronautical Congress*, Hyderabad, India, 24 - 28 September 2007.

Siri, Kasemsan, Conner A. Kenneth. 2004. Sequential controlled distributed solar-array power system with maximum power tracking. *IEEEAC paper* No.1001.

Spectrolab, Inc. 1984.*Solar Cell Design Data Handbook*. Los Angeles, CA.
Stanford site, *http://ssdl.stanford.edu/Emerald/docs.htm,* [June,2010].

Sullivan, O and Weinberg, A. 1917. dispositif de Regulation du Courant a Partir de Plusiers Sources d'energie. Belgian Patent No. *0/176327,* 31 March.

Sullivan, D.O. 1989. Satellite power system topologies. *ESA Journal*, 13:77–88.

Sweeting, M. N.1992. Uosat microsatellite missions. *Electronics and Communication Engineering Journal*, pp 141 – 150.
Tabisz, W. A., Jovanovic, M. M., Lee F. C.1992. Present and Future of Distributed Power Systems. *Proceedings of the Applied Power Electronics Conference*, 11-18.

Tan, L. B., Tseng, K. J. 2003. Intelligent and Reliable Power Supply System for Small Satellites. Nanyang Technological University Blk S2, Nanyang Avenue, Singapore 639798, Republic of Singapore.

Temple, C. 1998. Avoiding the Babbling-Idiot Failure in a Time- Triggered Communication System. In *FTCS '98: Proceedings of The Twenty-Eighth Annual International Symposium on Fault-Tolerant Computing*, Washington DC, USA: IEEE Computer Society, p. 218.

Thwaite, Carl Pearson and Russel, Nick. 2005. Small Cell Lithium-Ion Batteries: The Responsive Solution for Space Energy Storage. Chris, ABSL, *3rd Responsive Space Conference*, April 25–28, Los Angeles, CA.

Trevor, Sorensen, Glenn, Prescott, Marco, Villa. 2005. KUTESAT-2: A student satellite mission for testing rapid-response small satellite technologies in low earth orbit. *3rd responsive space conference*, AIAA, April 25-28.

Tokyo university. 2005. Electrical power systems, www.space.t.u-tokyo.ac.jp/cubesat/mission/dev/pow/doc-e.html,[April 2010].

Tuthill, Jason. 2009. TINYSCOPE ADCS, Master's Thesis, Naval Postgraduate School, Monterey.

Underhill, B., Friedman, A., Wong, J., Reed,H., Hansen, E., Colaprete, A., Rodier, D., Horan, S. and Anderson, B. 1999. Three Corner Sat Constellation – Arizona State University: Management; Electrical Power System; Structures, Mechanisms, Thermal, and Radiation; Attitude / Orbit Determination and Control; ASU Micropropulsion Experiment; and Integration. *13th Annual AIAA/USU Conference on Small Satellites.*

Walker, G. 2001. Evaluating MPPT converter topologies using a MATLAB PV model. J. Elect. Electron, Eng, Australia, 21: 49-56.

Waydo, Stephen, Henry Daniel, Campbell Mark. 2002. CubeSat Design for Leo-Based Earth Science Missions. *IEEEAC paper* No.248.

Weinberg, A and O'Sullivan, D. 1977. LC^3 : Application to Voltage Regulation. *Proc. Spacecraft Power-Conditioning Seminar*, ESA SP-126.

Weimer, J. A. 1995. Power Management and Distribution for the More Electric Aircraft. *Proceedings of the 30th Intersociety Energy Conversion Engineering Conference*,273-277.

Whitehead, N R Dugal and Johnson, Y B. 1993.Results of an electrical fault study, *(CDDF Final Report No. N06)*, 3413, NASA Publication, September.

Wijesinghe, Pushpa. 2003. Tandem solar cells. December.

Zahran, M., Tawfik, S. and Dyakov, Gennady. 2006. L.E.O. Satellite Power Subsystem Reliability Analysis. *Journal of Power Electronics*, 6(2):106-110, April.

Zhifei, wu, Zheng, You, Salvignol, Jerome. 2000. Tsinghua-1 Micro-satellite Power System Architecture and Design. Space Center: Tsinghua University, Beijng, China.

Ziegler, J. F., Curtis, H. W., Muhlfeld, H. P., Montrose, C. J., Chin, B., Nicewicz, M., Russell, C. A., Wang, W. Y., Freeman, L. B., Hosier, P., LaFave, L. E., Walsh, J. L., Orro J. M., Unger, G. J., Ross, J.M., O'Gorman, T. J., Messina, B., Sullivan ,T. D., Sykes, A. J., Yourke, H., Enger, T. A., Tolat, V., Scott, T. S., Taber, A. H., Sussman, R. J., Klein, W. A., and Wahausand, C. W. 1996. IBM experiments in soft fails in computer electronics. *IBM Journal of Research and Development*, 40(1), January.

Zhao, Lingyin.2006. Implementations of Battery Charger and Power-Path Management System Using bq2410x/11x/12x. *Texas instrument Application Report*, SLUA376–June.

9 APPENDIX A

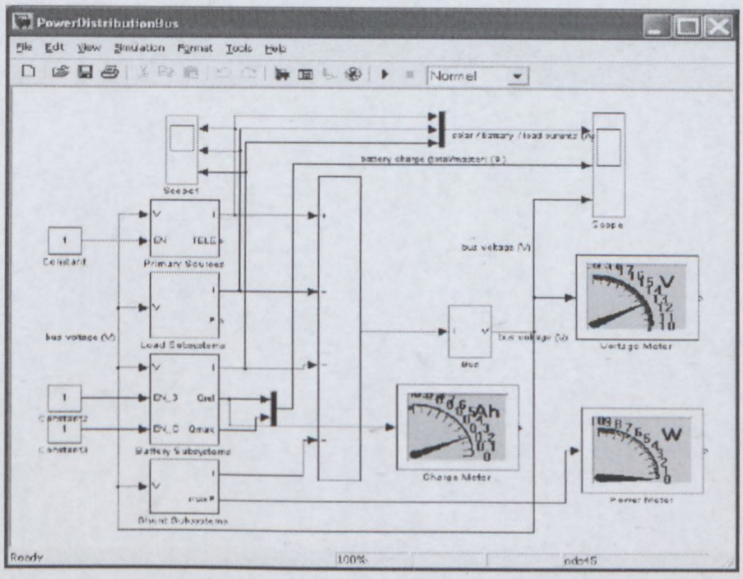

Figure A.1 Power bus simulink model

Combine parallel and series connection of solar cell are obtained from the simple equivalent circuit shown below, which also represents the modelling technique of the power source.

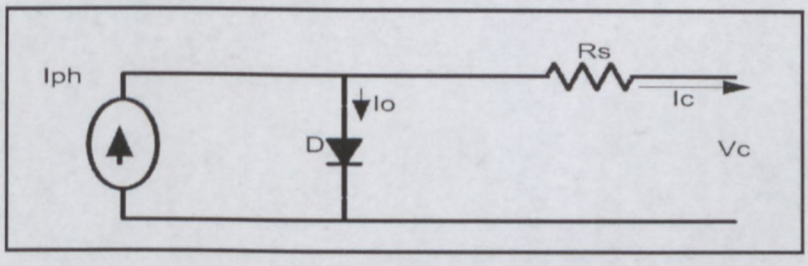

Figure A.2 equivalent circuit of photovoltaic cells

The over voltage is usually the function of photocurrent mainly determined by load current depending on the solar irradiation level during the operation.

$$V_C = \frac{AkT_C}{e}\ln\left(\frac{I_{PH} + I_O - I_C}{I_O}\right) - R_S I_C \qquad (1)$$

Where e is electron charge $(1.602 \times 10^{-19} C)$

K: is Boltzmann constant ($1.38\times10^{-23} J/^{o}K$)

I_C : is cell output current, A

I_{PH} : photocurrent, function of irradiation level and junction temperature (2A)

I_o :reverse saturation current of diode(0.0002A)

R_S : series resistance of cell(0.001Ω)

T_C: Reference cell operating temperature(20 ^{o} C)

V_C : cell output voltage, V

Both T_C and k should have the same temperature unit in Kelvin or Celsius. The factor is used to adjust I-V characteristics of the cell obtained from equation 1 to the actual characteristic obtained by testing. I_C is obtained by dividing the array current by the number of cells connected in parallel before being used in equation 1, which is valid for certain cell operating temperature T_C. Effects of temperature changes and solar irradiation levels have been included in the design. The solar cell operating temperature varies as a function of solar irradiation level and ambient temperature. The variable ambient temperature T_a affects the cell output voltage and cell photocurrent. These effects are represented in the model by the temperature coefficients C_{TV} and C_{TI} for cell output voltage and cell photocurrent, respectively, as:

$$C_{TV} = 1 + \beta_T (T_a - T_x) \qquad (2)$$

$$C_{TI} = 1 + \frac{\gamma_T}{S_C}(T_a - T_x) \qquad (3)$$

Where $\beta_T = 0.004$, $\gamma_T = 0.06$ for cells used while $T_a = 20^{o}C$ is the ambient temperature when testing the cells . Another cell ambient temperature is T_x. When operating temperature and photo current increases, the representation is

$$C_{SV} = 1 + \beta_T \alpha_S (S_x - S_C) \qquad (4)$$

$$C_{SI} = 1 + \frac{1}{S_C}(S_x - S_C) \qquad (5)$$

Where S_C is the solar irradiation level during cell testing and S_x is the new level irradiation level. Change in temperature is $\Delta T_C = \alpha_S (S_x - S_C)$ (6).

The following Figure in A.2 and A.3 are represent of conditions which will occur due to over-voltage of un-voltage activities on the bus when instability occur.

9.1 MODELLING POWER SYSTEM PERFORMANCE

Simulations can be carried out for spacecrafts in orbit around Earth. The orbits may be geo-synchronous, sun-synchronous or defined by their parameters (i, ω, Ω, perigee and apogee altitudes). Solar intensity, load levels, power collected, and battery state of charge are modelled with time.

The batteries number of cycles will be estimated in order to predict spacecraft power system lifetime:

$$\text{Number of cycles} = \frac{(Total[Cycle * capacity])}{capacitey - \exp ected - to - use} \qquad (1)$$

The angular velocity ω is given in the following equation:

$$w = \sqrt{\frac{MG}{r^3}} \qquad (2)$$

Where M is the mass of the earth, G is the gravitational constant, and r is the square of the distance between the orbiting body and the center of the earth. The angular radius of the spherical earth as seen from the spacecraft, ρ used in the determination of when the spacecraft is in direct sunlight, as see in Equation below

$$\sin \rho = \frac{RE}{RE + h} \qquad (3)$$

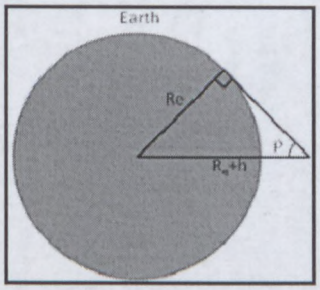

Figure A.3 Geometric relationship between earth and spacecraft

The constant, ρ is used in the determination of when the spacecraft is in direct sunlight. The angle β is critical to accurately predicting the varying length of eclipse periods for LEO satellites as they orbit the earth and as the earth orbits the sun. The beta angle is defined as the angle between the sun's solar rays and the spacecraft orbit plane.

$$\beta = SineCosiSinu + [\frac{Sin(1-Cose)Sin(u+v)}{2}] - [\frac{Sini(1+Cose)Sin(u-v)}{2} \quad (4)$$

Where *e* is the tilt axis of the earth, *i* is the satellite inclination, *u* is the right ascension of the sun in the ecliptic plane, and *V* is the right ascension of the ascending node of the satellite's orbit. The beta angle is illustrated below

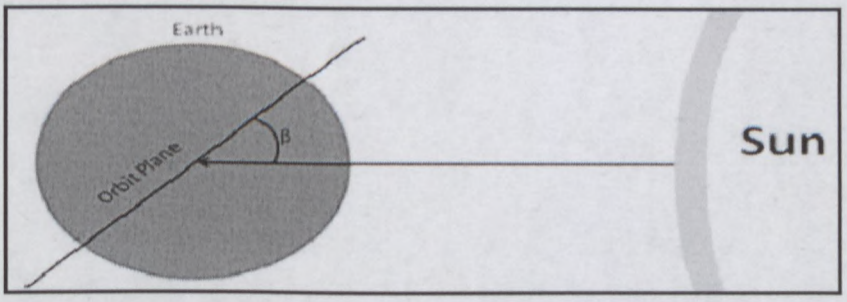

2Figure A.4 Illustration of Beta Angle

A prudent approach will be to choose a worst-case scenario based on the combination of beta angle, solar intensity, and solar cell adjusted efficiency. The simulation will be run for two cases to determine which is the worst case scenario by analyzing each case given solar intensity, beta angle and Solar cell efficiency.

A satellite is in eclipse if the following condition is true,

$$Cosv < -\frac{Cos\rho}{Cos\beta} \qquad (5)$$

To find the incidence angle of the sun on the solar panels, the attitude of the solar panel must be compared with the direction of the sun's rays. The components of the solar unit vector are given as,

$$S = -(Cos\beta Sinv)X_o - (Sin\beta)Y_o - (Cos\beta Cosv)Z_o \quad (6)$$

Where **S** is the unit solar vector and X_O, Y_O, and Z_O are perpendicular axes of the spacecraft body frame.

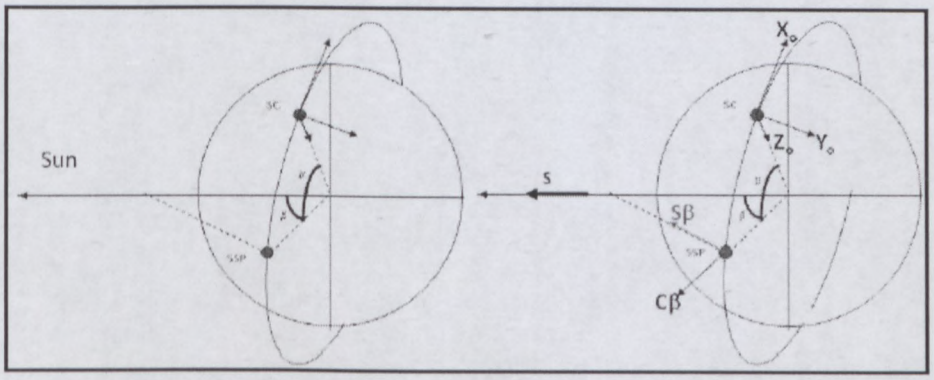

Figure A.5 Solar Unit Vector of the Spacecraft

The efficiencies must also be included in the load contents such as ADCS controller, Payload-frame, payload-camera and GPS. The loads and the power collected by the solar array as inputs of the battery charge regulator of power management and distribution (PMAD) to determine if the batteries are being charged or discharged. This can be stated mathematically as,

Charge if $\eta_S P_{Sa} > \frac{P_L}{\eta_P}$

Discharge if $\eta_S P_{Sa} < \frac{P_L}{\eta_P}$

During charge, the power from the solar array will be split between power going to the load (net of efficiencies) and power going to the batteries (also net of efficiencies). This is expressed mathematically as

$$P_{Sa} = \frac{P_L}{\eta_P \eta_S} + \frac{P_{BC}}{\eta_C \eta_i \eta_S} \quad (7)$$

During discharge, the power from the solar array is not sufficient to supply the required load power. Thus, the batteries must be used to partially or fully supply the load. In either case, no power is being delivered from the solar arrays to the batteries. The power required by the load is expressed as,

$$P_L = P_{Sa}\eta_S\eta_p + P_{BD}\eta_D\eta_2\eta_p \quad (8)$$

Note that if no power is being supplied by the solar array, as during eclipse or extreme slewing during sunlight, the second expression of the second term goes to zero. These equations contain the following test condition:

$$P_{Sa}\eta_s - \frac{P_L}{\eta_P}$$

9.2 MODEL OF SHUNT REGULATOR

The shunt regulator adopts the method of linear shunt system of a whole solar cell array, which was composed of control circuit and shunt adjustment circuit. The control circuits take charge of measuring the voltage of the bus and controlling the shunt adjustment circuit. The adjustment circuit which crossed access to the output of solar array shunt output current of the solar array according to the error of output of voltage. In that way, it maintains the output voltage of bus at the value we expected.

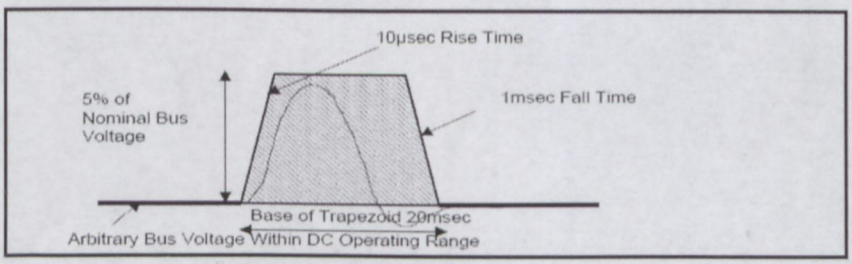

Figure A .6 Over surge voltage condition on the bus

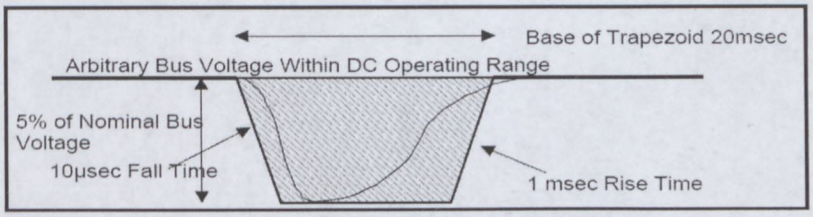

Figure A.7 Undershoot voltage on the bus

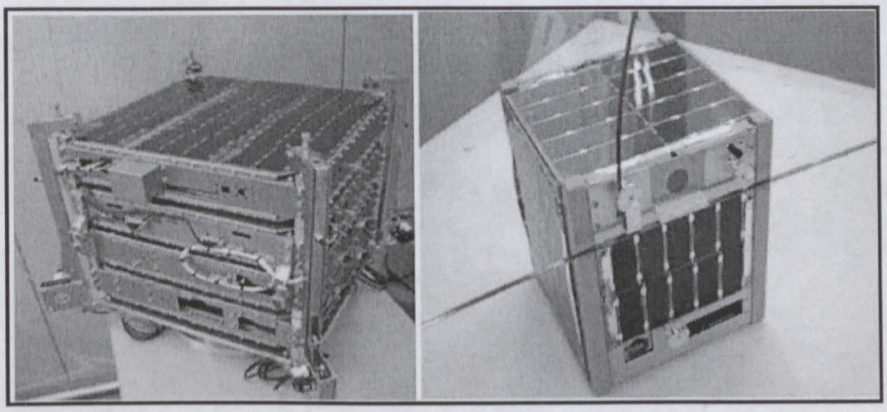

Figure A.8 SOHLA-2, University of Tokyo and 1U-Cubesat from Clyde space, Inc

10 APPENDIX B

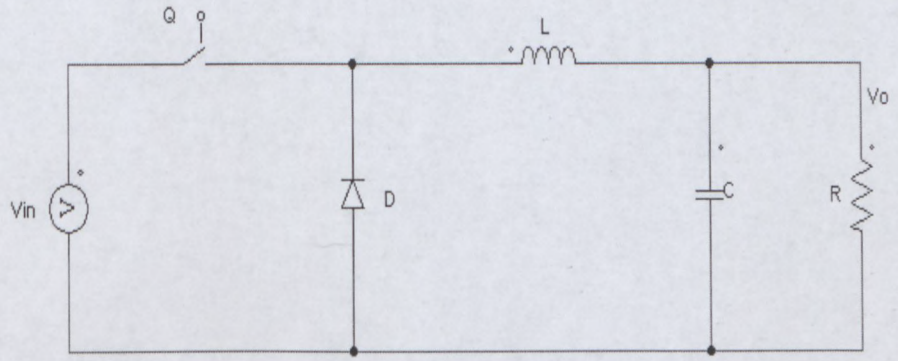

Figure B.1 Buck converter

In buck converter with the following value

$$V_s = 15V\ , V_o = 5V\ , R\ = 15V\ , f_s = 15V\ \Delta V = 50mV\ , i_{L(\max)} = 1.2A$$

by using the mathematical analysis below

$$D = \frac{V_o}{V_s}, \quad I_o = \frac{V_o}{R}\ , \quad L = \frac{DT_s(V_s - V_o)}{2(i_{L(\max)} - I_o)} \text{ and } \quad C = \frac{T_s^2\ (1-D)V_o}{8 \cdot \Delta V_o \cdot L}$$

Produces these values L=1.667mH, C= 200µF

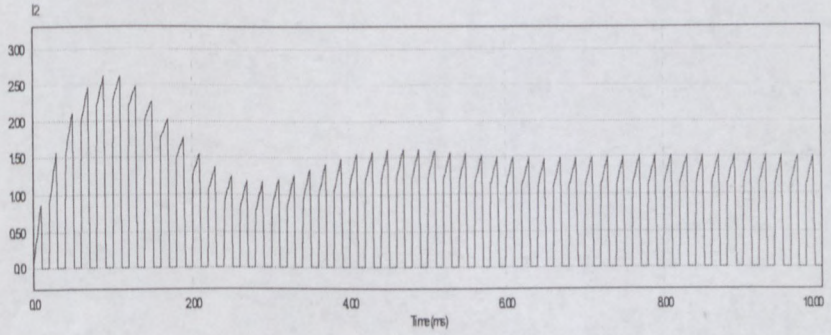

Figure B.2 Buck converter input waveform

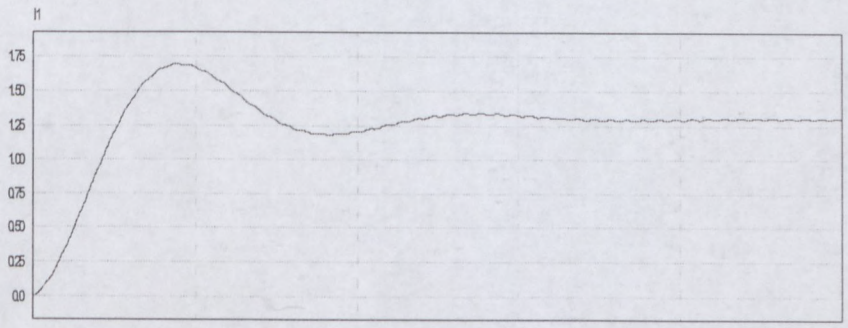

Figure B.3 Buck converter output waveform

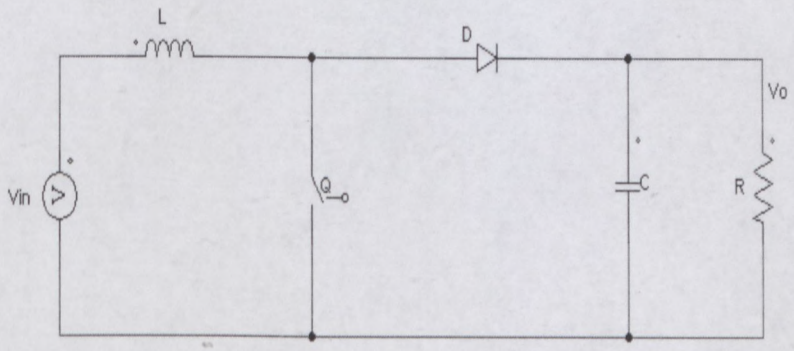

Figure B.4 Boost converter circuit

Given the following in boost converter ,

$V_S = 10 \quad V_o = 20 , R = 10 , f_S = 10kHz , \Delta i_L = 0.8$

$$\frac{V_o}{V_S} = \frac{1}{1-D}$$

$$D = 0.5$$

$$\Delta i_L = \frac{V_S}{L} DT_S$$

$$L = \frac{V_S}{\Delta i_L} DT_S = 625\mu H$$

$$\frac{\Delta V_o}{V_o} = \frac{DT_S}{RC}$$

$$C = \frac{DT_S V_o}{\Delta V_o R} = 1000\mu F$$

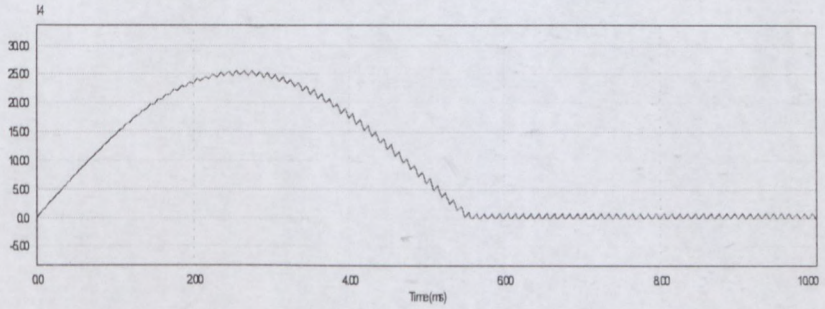

Figure B.5 Boost converter input waveform

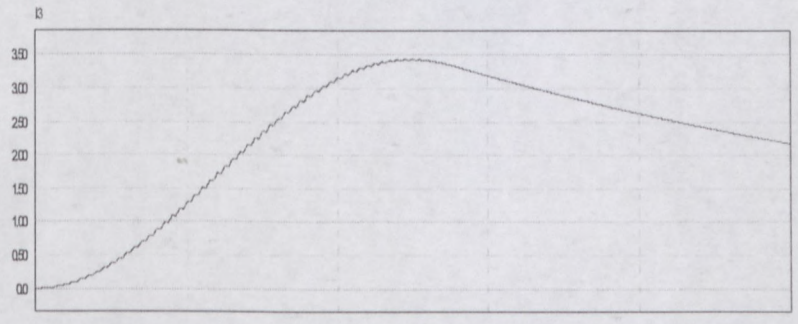

Figure B.6 Boost converter output waveform

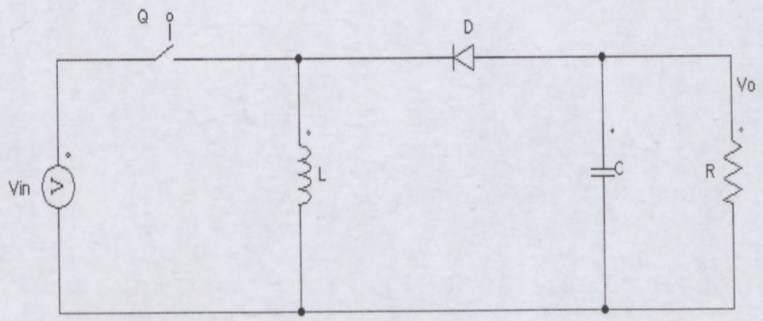

Figure B.7 Buck-boost converter

$$V_s DT_s + (-V_o)(1-D)T_s = 0$$

$$\frac{V_o}{V_s} = \frac{D}{1-D}$$

$$\frac{I_o}{I_s} = \frac{1-D}{D}$$

$$\Delta Q = I_o DT_S$$

$$\Delta V_o = \frac{\Delta Q}{C} = \frac{V_o DT_S}{RC}$$

$$I_{LB} = \frac{\Delta i_L}{2} = \frac{V_S DT_S}{2L}$$

$$V_o = \frac{DV_S}{1-D} \qquad L = \frac{D \cdot V_S}{f_S \cdot \Delta i_L} \quad and.....C = \frac{DT_S I_O}{\Delta V_O}$$

$$V_O = 20,\ V_S = 30,\ \Delta V = 0.4 \quad \Delta i_L = 0.195, \quad L = 615.4\mu H,\ I_o = 1.3A,\ and.....C = 130\mu F$$

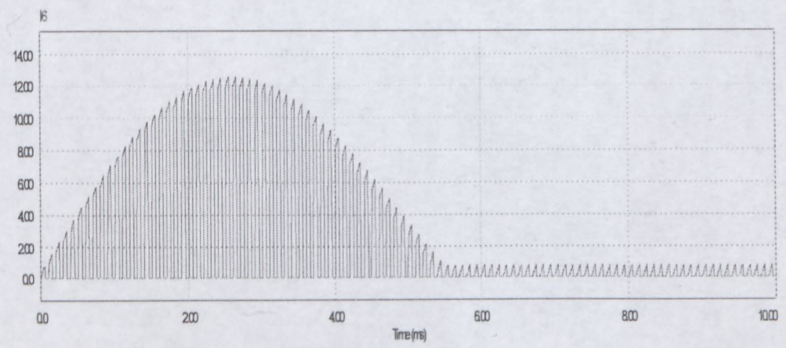

Figure B.8 Buck-boost converter input waveform

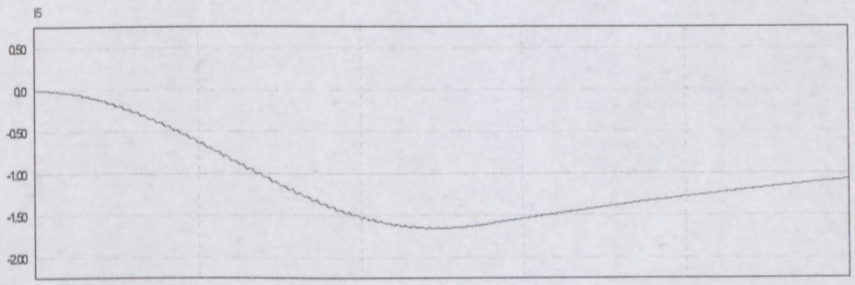

Figure B.9 Buck-boost converter output waveform

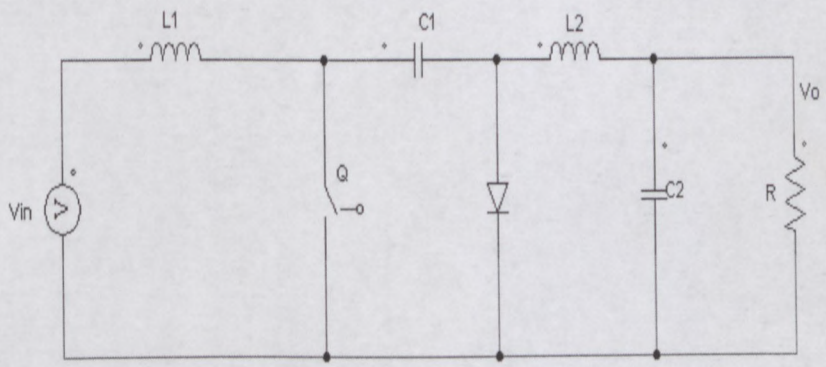

Figure B.10 CUK converter

Given that inductor 1 is L_1 and inductor 2 as L_2 then,

$$L_1 = V_S DT_S + (V_S - V_{C1})(1-D)T_s = 0$$

$$\therefore V_{C1} = \frac{1 \cdot V_S}{1-D} \qquad (2)$$

$$L_2 = (V_{C1} - V_o)DT_S + (-V_o)(1-D)T_S = 0$$

$$\therefore V_{C1} = \frac{1 \cdot V_o}{D} \qquad (3)$$

Equation 2 and 3 will lead to

$$i_{L1}(1-D)T_S = i_{L2}DT_S$$

$$\frac{i_{L1}}{i_{L2}} = \frac{I_o}{I_S} = \frac{1-D}{D}$$

$$\frac{V_o}{V_S} = \frac{D}{1-D}$$

$$V_o = \frac{DV_S}{1-D}$$

Given V_S=10, V_O=5 f_S=50kHz, C=5μF, 100μF, $L_1$200μH,L_2=1000μH

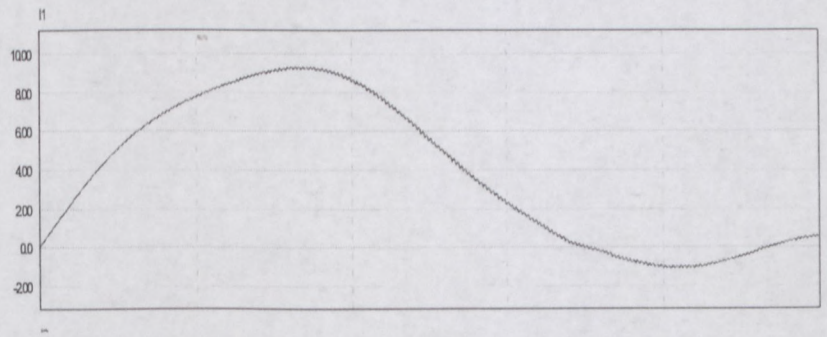

Figure B.11 CUK converter input waveform

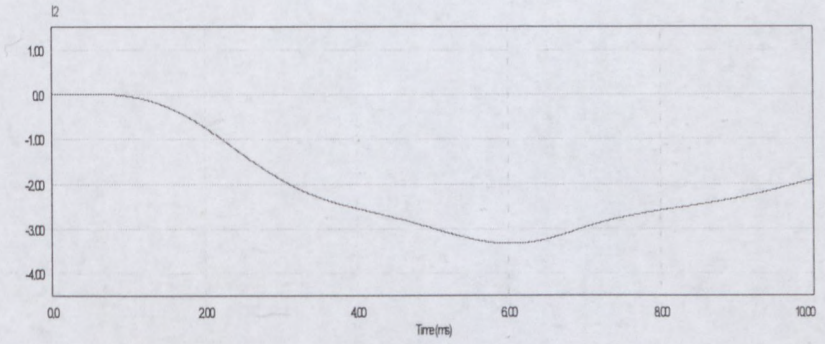

Figure B.12 CUK converter output waveform

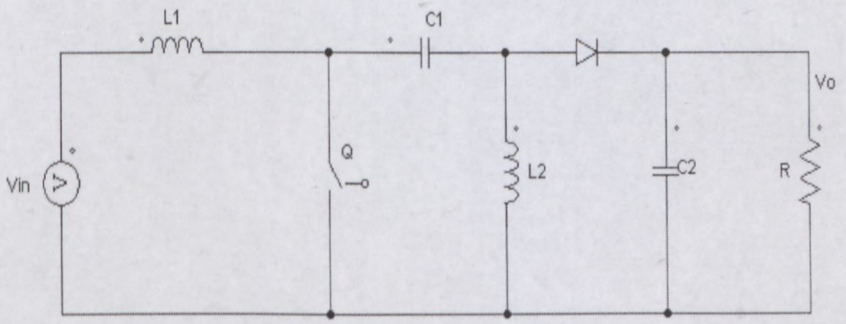

Figure B.13 SEPIC converter

$$D = \frac{V_O + V_D}{V_S + V_O + V_D}$$

$$V_o = \frac{DV_S}{1-D}$$

$$L = \frac{I}{2} \bullet \frac{V_S D}{\Delta I_L f_S}$$

$$C \frac{I_o D}{\Delta V f_S}$$

Since the CUK is different type of SEPIC we use this values again V_S=10, V_O=5 f_S=50kHz, C=5μF, 100μF, $L_1$200μH,L_2=1000μH

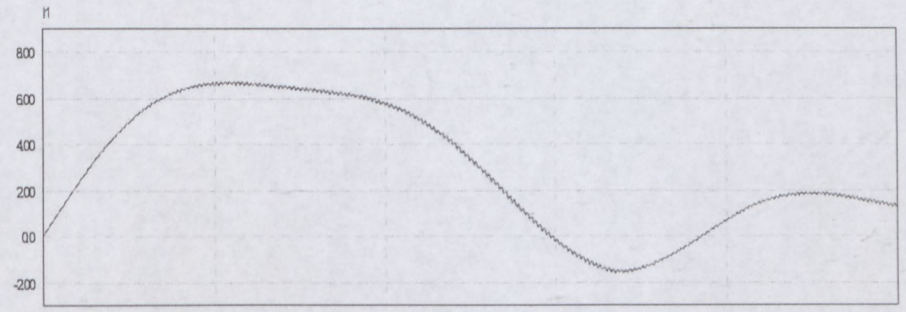

Figure B.14 SEPIC converter input waveform

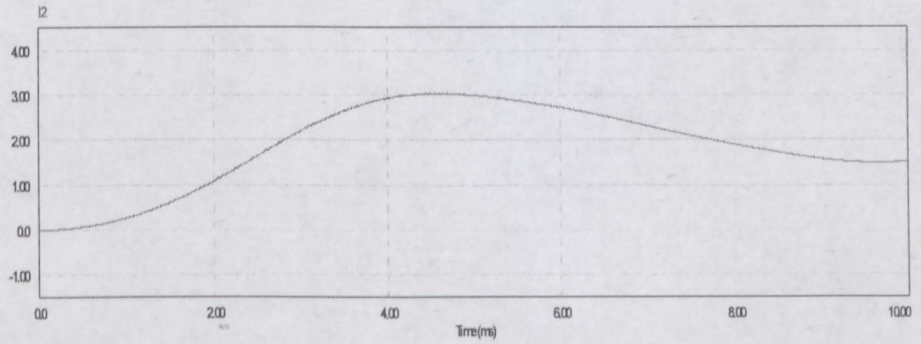

B.15 SEPIC converter output waveform

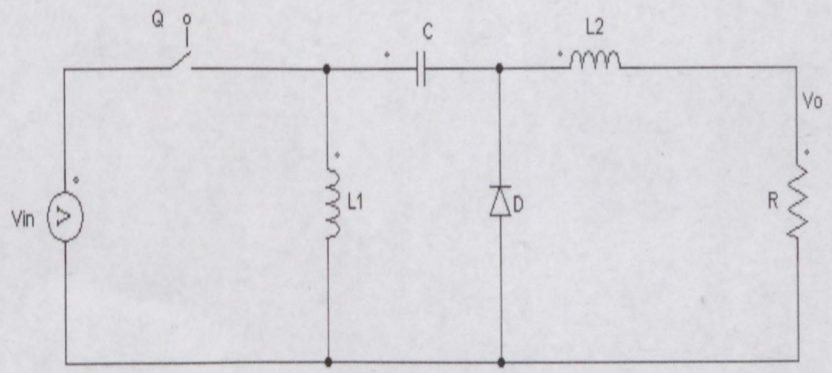

Figure B.16 Zeta converter

$$D = \frac{V_o}{V_s + V_o} \qquad (6)$$

$$\frac{D}{1-D} = \frac{I_s}{I_{out}} = \frac{V_o}{V_s} \qquad (7)$$

Where I_s and I_o are the input current and output current respectively.

$$L = \frac{1}{2} \cdot \frac{V_S D}{\Delta I_L f_S}$$

$$C = \frac{\Delta I \cdot V_S}{8 \Delta V f_S}$$

Using the values given below the simulation input and output waveforms are displayed.

$V_O = 10,\ V_S = 20,\ \Delta V = 0.4 \quad \Delta i_L = 0.19, \quad L = 600\mu H,\ I_o = 1.3A,\ and.....C = 100\mu F$

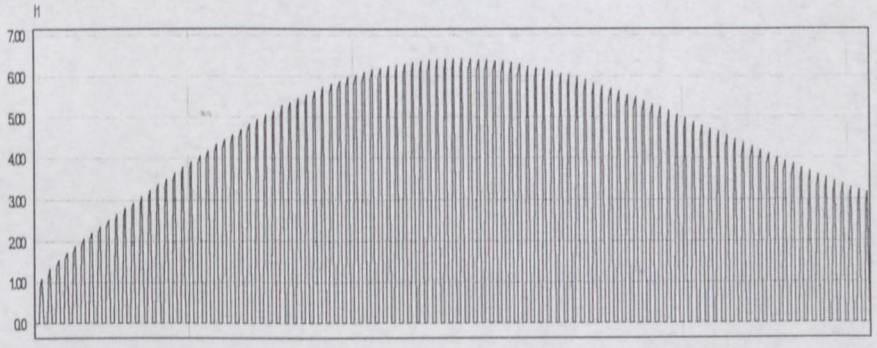

Figure B.17 Zeta converter input waveform

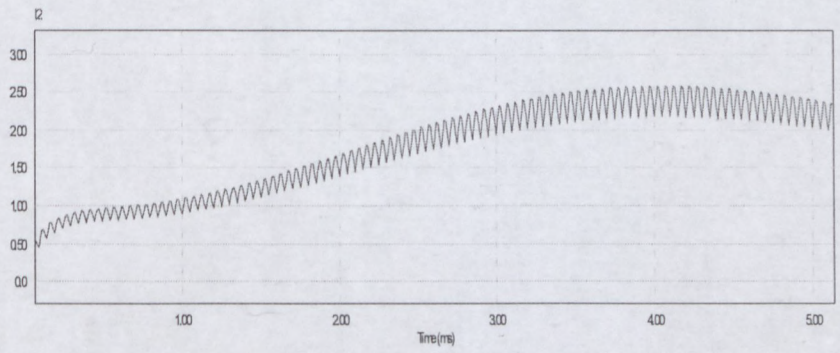

Figure B.18 Zeta converter output waveform